EVALUATING THE EFFECTIVENESS OF VIBRATION-MITIGATION DEVICES FOR STRUCTURAL SUPPORTS OF SIGNS, LUMINAIRES, AND TRAFFIC SIGNALS

FINAL REPORT

Prepared for
TRANSPORTATION RESEARCH BOARD
NATIONAL COOPERATIVE HIGHWAY RESEARCH PROGRAM

of

The National Academies of Sciences, Engineering and Medicine

TRANSPORTATION RESEARCH BOARD OF THE NATIONAL ACADEMIES OF SCIENCES, ENGINEERING AND MEDICINE

PRIVILEGED DOCUMENT

This document, not released for publication, is furnished only for review to members of or participants in the work of CRP. This document is to be regard as fully privileged, and dissemination of the information included herein must be approved by CRP.

Prepared By
Richard Christenson and Pablo Agüero-Barrantes
University of Connecticut, Storrs, CT

Delong Zuo
Texas Tech University, Lubbock, TX

Andrew Adams, Maria Lopez and Thomas Murphy
Modjeski and Masters, Inc., Mechanicsburg, PA

June 2023

ACKNOWLEDGMENT OF SPONSORSHIP

This work was sponsored by one or more of the following as noted:

☒ American Association of State Highway and Transportation Officials, in cooperation with the Federal Highway Administration, and was conducted in the **National Cooperative Highway Research Program**,

☐ Federal Transit Administration and was conducted in the **Transit Cooperative Research Program**,

☐ Federal Aviation Administration and was conducted in the **Airport Cooperative Research Program**,

☐ The National Highway Safety Administration and was conducted in the **Behavioral Traffic Safety Cooperative Research Program**,

which is administered by the Transportation Research Board of the National Academies of Sciences, Engineering, and Medicine.

DISCLAIMER

CONTENTS

AUTHOR ACKNOWLEDGEMENT

The research reported herein was performed under NCHRP Project 12-111 by the Department of Civil & Environmental Engineering at the University of Connecticut (UConn), Texas Tech University (TTU), Modjeski & Masters, Inc. and the US Army Corp of Engineers Engineer Research and Development Center (ERDC). UConn was the contractor for this study.

The authors of this report are Richard Christenson, Professor, and Pablo Agüero-Barrantes, Ph.D. candidate at UConn, Delong Zuo, Professor, at Texas Tech University, and Andrew Adams, Maria Lopez and Thomas Murphy at Modjeski and Masters with significant input in the early stages of the project from the US Army Corp of Engineers ERDC – Matthew Smith, Quincy Alexander, Vincent Chiarito and Charles Ellison. The authors acknowledge Mr. Jeff Livingston, Assistant Director of Technical Operations at National Wind Institute at Texas Tech University and Mr. Lee Wilkis, a senior technician at the same Institute, for implementing the full-scale instrumentation of the traffic signal support structures and assisting with experimental setups for the wind tunnel testing.

ABSTRACT

This report documents a test procedure for evaluating the effectiveness of vibration-mitigation devices for structural supports of signs, luminaires, and traffic signals and proposes a procedure for considering the effectiveness of these devices in the design process of the structural supports. An effective vibration-mitigation device can be accounted for in the design process by reducing the fatigue demand through use of a response modification factor (R, or R-factor). In this way, the complex behaviors of the interaction between the structure and the vibration-mitigation device can be accounted for in a simple manner when designing sign, luminaire, and traffic signal structures. The use of an R-factor to reduce fatigue demands in Section 11 of the AASHTO LRFD Specifications for Structural Supports for Signs, Luminaries, and Traffic Signals (AASHTO LRFD SLTS Specifications) requires that suitable testing and modeling of the device is performed and documented. The research developed a six-step process for evaluating the effectiveness of mechanical vibration-mitigation devices for structural supports of signs, luminaires, and traffic signals. This research also proposed a procedure, consistent with the AASHTO LRFD SLTS Specifications, for considering the effectiveness of these devices in the design process of the structural supports.

SUMMARY

The current AASHTO LRFD Specifications for Structural Supports for Signs, Luminaries, and Traffic Signals (AASHTO LRFD SLTS Specifications) addresses potential failure due to wind vibrations by requiring members and connections to have nominal strengths in excess of the expected loadings by a sufficient margin to reduce risk of failure to an acceptable amount (AASHTO, 2013). The AASHTO LRFD SLTS Specifications indicate that in lieu of designing to resist periodic galloping forces, effective vibration-mitigation devices can be implemented, however there is no guidance how to quantify the effect of a device on the structure's behavior. This research developed a test procedure for evaluating the effectiveness of vibration-mitigation devices for structural supports of signs, luminaires, and traffic signals and proposes a procedure for considering the effectiveness of these devices in the design process of the structural supports. The evaluation of effectiveness of vibration mitigation devices is primarily intended to reduce fatigue loads specified in AASHTO LRFD SLTS Specifications but can also be applied for excessive vertical deflections resulting from galloping wind loads. These procedures were developed to be appropriate for potential incorporation into the AASHTO LRFD SLTS Specifications.

An effective vibration-mitigation device can be accounted for in the design process by reducing the fatigue demand through use of a response modification factor (R, or R-factor). In this way, the complex behaviors of the interaction between the structure and the vibration-mitigation device can be accounted for in a simple manner when designing sign, luminaire, and traffic signal structures. The use of an R-factor to reduce fatigue demands in Section 11 requires that suitable testing and modeling of the device has been performed and documented by the device manufacturer (or other entity). The generalized steps required to apply the "R-factor" method are presented in this report. It is the responsibility of the entity performing the testing and developing the model to ensure that the testing and modeling are sufficient to suitably capture the effect of the vibration-mitigation device on structures; indicate the range of properties of structures to which the device and developed model are applicable; and provide the required information to the owner to account for device influence on behavior as utilized. Owner approval would be required for the use of these devices, similarly to the current provisions in Section 11 of the AASHTO LRFD SLTS Specifications.

Because of the complexities associated with the general behavior of vibration-mitigation devices and potential difficulties in generating models which are fully consistent with the actual behavior, two approaches are proposed to develop the R-factors: 1) use of a validated model or 2) direct use of test data. The selected approach may influence the number of test data points required. The first approach involves validating a model and using that for development of the R-factors over the range of structure input parameters. Recognizing that modeling of vibration-mitigation devices with sufficient accuracy over a range of structure properties can be challenging for some devices, a second approach is available wherein the results of the physical testing are directly used to estimate the effect of the vibration-mitigation device on a range of structures. In the testing approach, damping values between test data points can be found using interpolation provided that the test points are spaced sufficiently close such that linear interpolation is an appropriate, or at least conservative, estimate of actual behavior. It is the responsibility of the entity performing the testing and documenting the results to indicate the range over which the use the provided data is applicable, and to ensure the provided data adequately captures the behavior over that range.

This research has developed a test procedure for evaluating the effectiveness of mechanical vibration-mitigation devices for structural supports of signs, luminaires, and traffic signals. The evaluation of aeroelastic dampers is outside of the scope of this study and will require further extensive study before they should be used to provide fatigue protection. The six-step process would be carried out and documented by the device manufacturer (or other entity) and the design structure designer, as described below.

This first four steps are carried out by the device manufacturer (or other entity).

Step 1 – Document Device Information: For each device, information is provided including (but not limited to) a description of the device's geometric and mass characteristics, the manner in which it provides damping, history of development, intended applications, typical usage (including attachment and placement details), device sensitivities, its suitability for use in mitigating vibrations caused by fatigue wind loading, the types of wind loading and directions of motion it is intended to mitigate against, the structure archetype(s) and range of characteristic properties for which the work is being developed, expected required maintenance over the lifetime of the device, and the anticipated test matrix and test protocols.

Step 2 – Characterize Behavior: The vibration-mitigation device is tested to determine its effect on the desired dynamic range of properties of target structures (e.g., typically various combinations of frequency and dynamic weight). Ranges of frequency and dynamic weight for different archetypes can be found in Chapter 3 of this report. The number of tests necessary to perform will depend on several factors, including the accuracy of any developed model and the behavior of the determined damping over the range of input parameters.

Step 3 – Develop and Validate Model: Models may be as simple or as complex as necessary to effectively capture the effect of the mitigation device on the structure archetype being examined. Once the model is developed and refined, the resulting damping values of the tested structure with mitigation device are compared with those found from the analytical model. When the magnitude of the difference between the model- and test-determined damping is greater than +/-20%, it is suggested that the model be reworked to better approximate the effect of the vibration-mitigation device on the structure's behavior. The percent difference values for damping between the test and model are to be provided in the documentation.

If consistency between the model and test data cannot be effectively accomplished, then the approach of directly using test values (with sufficient test data such that interpolation between data points is appropriate) is recommended. Additional test points may be necessary to ensure the behaviors are suitably captured over the range of properties for which the mitigation device is intended for use on.

Step 4 – Document Model: Once a model is validated it can be made available such that a design engineer can use it to determine the damping ratio for that mitigation device utilized on their particular structure. Alternatively, the damping ratio values found from the model or testing can be provided as a matrix of values for the input parameters. It is the responsibility of the entity performing the testing and developing the model to ensure that the model or results values are appropriate over the range of input properties specified.

The remaining two steps in the process are carried out by the designer.

> **Step 5 – Determine Dynamic Properties:** Typically, the structural dynamic properties needed are the frequency and dynamic weight (note: dynamic weight is different, and less, than the total weight of the structure and is described in Section 3.4.1). These properties are developed for the in-plane and/or out-of-plane behavior depending on the fatigue wind load being mitigated against.
>
> **Step 6 – Determine Damping Ratio:** Using the provided model or a table of damping ratios for a specific device, the designer determines a damping ratio for the properties of their structure. The effect of potential changes to the structure over its lifetime (e.g., adding or removing of signs, signals, etc.) are incorporated at this stage, by determining the minimum damping ratio within a range of input parameters centered on the values determined in Step 5. For the typical case of utilizing frequency and dynamic weight, it is recommended that the ranges of frequencies and dynamic weights examined are Frequency: +/- 10%; Dynamic Weight: +/- 20%.

This research also proposes a procedure, consistent with the AASHTO LRFD SLTS Specifications, for considering the effectiveness of these devices in the design process of the structural supports. This procedure for the design of new structures is a simplified approach which accounts for the complex dynamic behaviors of the interaction of the structure and the vibration-mitigation device using the damping ratio determined in Step 6.

For vibration-mitigation devices used to reduce fatigue demands of new structures (as described in Section 11 of the AASHTO LRFD SLTS Specifications), the manufacturer (or entity which has performed the necessary testing) shall provide the information required to account for their influence on behavior as utilized in the specifications. If approved by the owner, the use of a mitigation device to reduce fatigue demands of new structures can be included in the design. This is done through revising equations 11.5-1, 11.8.2-1 and C.3-1 in the AASHTO LRFD SLTS Specifications to include a response modification factor, R, to account for the effect of a vibration-mitigation device for a specific wind loading, defined in Article 11.8 of the AASHTO LRFD SLTS Specifications. A vibration-mitigation device can be used to reduce demand (on the left-hand side of equations 11.5-1 and 11.8.2-1) as an alternative to modifying the structural details to provide increased resistance (on the right-hand side of equations 11.5-1, 11.8.2-1 and C.3-1) in cases where the fatigue demand exceeds the fatigue resistance.

When a vibration-mitigation device approved for design of new structures by the owner is present, the response modification factor, R, shall be determined by the designer for truck gust (TrG), natural wind gust (NWG), combined wind on high-mast towers (HMT), and galloping induced vibration (GVW) in a proposed equation 11.8.2-1 in the AASHTO LRFD SLTS Specifications:

$$R = \begin{cases} \gamma_R \frac{\zeta_c}{\zeta_u} & for\ R > \Psi_R \\ 1 & otherwise \end{cases} \qquad \text{(11.8.2-1, } \textit{AASHTO LRFD SLTS Specifications}\text{)}$$

where: γ_R is a multiplier to account for the uncertainty in the prediction of the vibration-mitigation device performance, ζ_c is the damping ratio of the structure including the vibration-mitigation device determined as described in the product documentation identified in the test procedure for evaluating the effectiveness of vibration-mitigation devices; and ζ_u is the damping ratio of the structure without the vibration-mitigation device (equal to 0.2% unless published experimentally determined values for the specific structure type being examined are available). The minimum required value Ψ_R accounts for further uncertainty in the process. For each device, testing is required that either directly provides ζ_c values for a range of properties of the intended structural

system or provides an analytical model which the designer can utilize to determine ζ_c for their specific structure. When R, in equation 11.8.2-1 of the AASHTO LRFD SLTS Specifications, falls below Ψ_R, a value of 1.0 shall be used for R instead. If no vibration-mitigation device is utilized a value of 1.0 shall be used for R. As a result of this research, the multiplier γ_R is set to $\gamma_R = 0.6$, and the minimum required value Ψ_R is set to $\Psi_R = 3.0$. These values are determined based on engineering judgment of the team, considering the variability of data, and the need for a non-marginal effect of the mitigation device.

1 BACKGROUND

Traffic signs, luminaires, and traffic signals are typically supported by flexible structural elements with low damping that are prone to wind-induced vibration and susceptible to fatigue and failure. These structures are located adjacent to or directly over roadways whereby maintenance, repair or replacement is costly in terms of both time and money and failure can compromise the safety of the traveling public. The current AASHTO LRFD Specifications for Structural Supports for Signs, Luminaries, and Traffic Signals (AASHTO LRFD SLTS Specifications) addresses potential failure due to wind vibrations by requiring members and connections to have nominal strengths in excess of the expected loadings by a sufficient margin to reduce risk of failure to an acceptable amount (AASHTO, 2013). This can result in inefficient structural designs, using large members and cumbersome connections, and be a poor use of resources. The AASHTO LRFD SLTS Specifications indicate that in lieu of designing to resist periodic galloping forces, effective vibration-mitigation devices can be used for cantilever sign and traffic signal structures, based on historical or research verification of its vibration damping characteristics and as approved by the Owner. However, the AASHTO specification makes no reference for the allowance of vibration-mitigation devices for other fatigue loading cases such as vortex-induced vibration and truck or natural wind gusts, or applications to high mast or other luminaires.

Vibration-mitigation devices for sign, luminaire and traffic signal structures can reduce these structures' susceptibility to wind-induced vibration, thereby increasing safety, enhancing performance, reducing material costs, and resulting in more efficient designs and less maintenance of the structures. The NCHRP Report 796 reported that about 76% of the 36 agencies in the AASHTO member states that responded have used vibration-mitigation devices. However, owners often do not consider the regular use of mitigation devices because it is difficult to quantify the effectiveness of a vibration-mitigation device. The AASHTO LRFD SLTS Specifications gives no guidance on how to qualify an effective vibration-mitigation device, and it is known that the performance of vibration-mitigation devices can be highly complex and dependent on various factors including the type and strength of the wind excitation, the structural and aerodynamic properties of the structure and the location of the device on the structure, as well as with the variability of each of these factors. Determining the performance of and/or designing structures using vibration-mitigation devices was beyond the scope of the previous NCHRP study and the resulting AASHTO LRFD SLTS Specifications do not specifically address using these devices.

NCHRP Project 12-111 has developed a test procedure for evaluating the effectiveness of mechanical vibration-mitigation devices for structural supports of signs, luminaires, and traffic signals; and proposes a procedure, consistent with the AASHTO LRFD SLTS Specifications, for considering the effectiveness of these devices in the design process of the structural supports. The recommendation to facilitate the research findings/products to be used in practice is to adopt the proposed revisions and additions to the LRFD Specifications for Structural Supports for Highway Signs, Luminaires, and Traffic Signals.

2 RESEARCH APPROACH

This section provides a review of relevant literature, research and information regarding structural dynamics and aerodynamic and vibration absorber approaches to reduce unwanted vibration in support structures. A review of specifications for seismic isolation devices is provided to serve as staring point for the proposed method to evaluate the effectiveness of vibration-mitigation devices and to incorporate the devices into the design procedure of STLS support structures.

Next, various criteria to measure the effectiveness of a vibration-mitigation device are provided and discussed. The damping ratio provides a good balance between ease of measurement and overall performance indicator and is adopted within this report to evaluate effectiveness of vibration-mitigation devices. Various test procedures are identified to determine the various criteria proposed, including field testing, free and forced vibration testing in a laboratory, and wind tunnel testing.

The response modification factor, R, is introduced, which is central to the research approach and the proposed design process incorporating effective vibration-mitigation devices into the AASHTO LRFD SLTS Specifications. The R-factor reduces the demand, as an effective damper will reduce the structure's response to a wind load.

2.1 Review of Relevant Literature, Research and Information

Various approaches have been considered to reduce excessive wind-induced vibrations in sign, luminaire and traffic signal structures. This section provides a review of the two main classifications of vibration-mitigation devices proposed for sign, luminaire and traffic signal structures, namely aerodynamic modifications and vibration absorbers. Following a literature review of these mitigation devices, an overview of existing specifications and the qualification process and means for characterizing performance for seismic isolation devices is provided to identify how a similar engineering discipline specifies and ensures performance in protective devices. The section concludes with a summary of a survey distributed to the AASHTO Committee on Bridges and Structures (COBS) on the use of vibration-mitigation devices by States throughout the country and a description of resources available to identify standard archetype test specimens.

2.1.1 Structural Dynamics Overview.

A structural system can be defined in terms of mass, stiffness and damping. The dynamics of the structural system is described using Newton's second law of motion where the equation of motion (ensuring equilibrium of the system) is determined (Chopra, 2017). In particular for a single-degree-of-freedom mass-spring-damper system, as shown in Figure 2.1, the equation of motion can be written as

$$\ddot{x}(t) + 2\zeta\omega_n\dot{x}(t) + \omega_n^2 x(t) = \frac{1}{m}f(t) \tag{2.1}$$

where $x(t), \dot{x}(t), \ddot{x}(t)$ are the displacement, velocity and acceleration of the system, ζ is the damping ratio, $\omega_n = \sqrt{k/m}$ is the fundamental natural frequency, f is the applied load (external force), m is the mass and k is the stiffness.

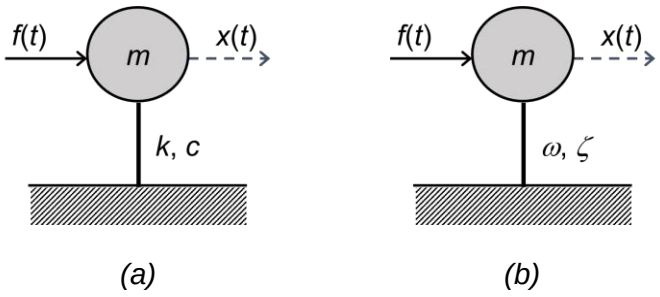

Figure 2.1: Single-degree-of-freedom mass-spring-damper dynamic system: (a) mass, stiffness, damping coefficient; and (b) mass, frequency and damping ratio.

The mass, m, is associated with the weight of the structure and is calculated as the product of the volume of material and the mass density of the material (e.g., steel or aluminum) used. The stiffness, k, is defined as the extent to which the structure resists deformation to an applied load. Stiffness is a function of the cross-sectional properties, length and supports of the structural members and the material properties. Both mass and stiffness can be calculated fairly accurately for a given structural design. The damping is defined as reduction in the response over time. Damping, unlike mass and stiffness is much more difficult to estimate from a structural design and can be a highly complex phenomenon. Often it is a practical assumption to assume the damping is a linear function of the velocity, called linear viscous damping. The viscous damping can be described by a damping ratio, ζ. The amount of damping in sign, luminaire and traffic signal structures, referred to as the inherent damping, can be very small, often not exceeding 0.2% (0.002).

The steady state response (such as due to galloping) of the single-degree-of-freedom system at resonance (when the system is excited at the natural frequency of the structure), X_{res}, can be shown to be

$$X_{res} = (1/2\zeta)X_{st} \tag{2.2}$$

where X_{st} is the static displacement of the system. From this equation, it can be observed that as the damping ratio decreases the amplitude of the response at resonance increases. Alternatively, an increase in damping will decrease the amplitude of the response. As an example, increasing the damping ratio by a factor of 10, from 0.2% (0.002) to 2% (0.02), will result in a decrease in the steady state response by a factor of 10, to 10% (1/10) of the response or a 90% reduction.

The peak response due to impulsive loads (such as truck or natural gusts) is also reduced with an increase in damping, albeit less dramatically. This can be observed from shock spectra for systems with viscous damping. For example, the shock spectra for a half-cycle sine pulse with a pulse duration equal to the natural period ($T_n = 2\pi/\omega_n$) provides for a response reduction from a damping ratio of 1% (0.01) to 10% (0.1) to 80%, or a 20% reduction. Additional benefit from a fatigue standpoint is achieved if the number of cycles above the CAFT is reduced with the added damping.

The free vibration response for equation 2.1 (where $f(t)=0$) can be written as

$$x(t) = e^{-\zeta\omega_n t}(A\cos\omega_D t + B\sin\omega_D t) \tag{2.3}$$

where *A* and *B* are constants that can be determined from the initial conditions of the system (the displacement and velocity at time *t*=0). The response is attenuated in time by the first term on the right-hand side of the equation. The logarithmic decrement, δ, can be approximated for lightly damped systems as $\delta \cong 2\pi\zeta$. Again, it is observed that the reduction in the response is directly proportional to the damping ratio. It can also be shown that the number of cycles it takes for a 50% reduction in the displacement amplitude is approximately equal to 0.11/ ζ . For example, if a system is excited by some impulse such that the resulting stress is twice that of the level CAFT (Constant Amplitude Fatigue Threshold) and it is left to free vibration, increasing the damping ratio by a factor of 10, from 0.2% (0.002) to 2% (0.02), will result in a decrease in the number of cycles above the CAFT by a factor of 10, from 55 cycles to 5 cycles.

It is also observed from equation 2.3 that a negative damping ratio and positive natural frequency, ω_n, will result in an exponentially increasing response in time. This behavior due to negative damping (i.e., a damping ratio that is less than zero) is unstable. In certain wind conditions, the interaction of the wind on the structure results in negative damping added to the positive damping of the structure. In such cases, when the negative damping exceeds the small amount of inherent damping in the structure, then the overall damping of the system is negative, and the response will be unstable (grows exponentially).

2.1.2 Aerodynamic Modifications.

Aerodynamic modifications work by changing the physical characteristics of the structure to reduce the magnitude of the effect of the wind loading that is seen by the structure, effectively by reducing the amount of negative damping present in the system. Figure 2.2 shows a schematic of examples of aerodynamic modifications. Research has considered aerodynamic modifications such as damping plates, strakes, etc., to reduce the effect of the wind on structures, with varying results.

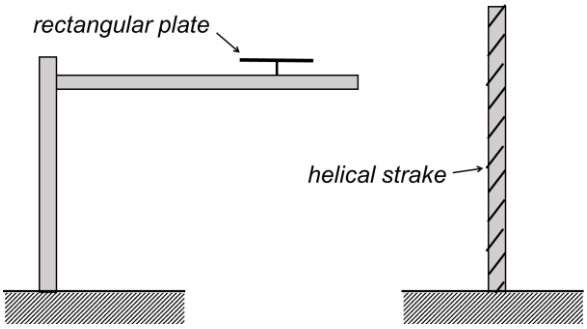

Figure 2.2: Examples of aerodynamic modifications: (a) rectangular plate on a traffic signal support structure mast arm disrupts the flow of wind over the mast arm; and (b) helical strakes on a luminaire structure disrupt the formation of vortices over the height of the pole.

To suppress wind-induced vibration of traffic signal support structures, rectangular plates (a.k.a. rectangular wings, or plate airfoils) have often been mounted on a section of the bare arm away from the signal lights to act as an aerodynamic damping plate. In recognition of the observed ineffectiveness of such devices installed on traffic signal support structures in Texas, McDonald,

et al. (1995) conducted a field experiment to evaluate the performance of a plate that is much larger than those used in practice and mounted directly above of a traffic signal cluster instead of away from it. Over a period of 18 hours, the test structure was rotated so that the mean wind direction was always approximately perpendicular to the mast arm, and the strain on the pole of the structure was monitored with and without the damping plate installed. It was observed that at moderate wind speeds of 10-15 mph (4.5-7 m/s), the 5-minute root mean square (RMS) values of the strain were much lower when the plate was present than when it was not. Based on this observation, the study concluded that rectangular plates can effectively mitigate wind-induced vibrations of traffic signal support structures provided that the plate is sufficiently large and that it is mounted directly above the signal light with a separation of at least 3 in. (8 cm). It should be noted that rectangular plates will increase the area subjected to truck-induced wind gust.

In a related study, Pulipaka, et al. (1998) assessed the performance of two plate-like damping devices in suppressing wind-induced vibrations of traffic signal support structures. One of the devices was a simple flat rectangular plate, while the other was a flat rectangular plate with two small tubes added to the two longer edges (referred to as a flat plate with rounded edges). Instead of a direct comparison between the responses of full-scale structures to wind excitation with and without the plate dampers, this study evaluated the total (i.e., mechanical + aerodynamic) damping of the structure with and without the damping plates based on wind tunnel tests of section models at a length scale of 1 to 4. In the tests, the section models of the mast arm with and without the plates mounted above the signal light model were elastically supported in an open-circuit wind tunnel and released from initial displacements at various wind speeds. The recorded free vibrations were used as a basis to evaluate the dependence of the flutter derivatives of the models on the velocities of the wind, which were further used as a basis to assess the aerodynamic damping added to the models at various wind speeds. The outcomes of the study suggested that both types of damping plate are effective in suppressing wind-induced vibration of traffic signal support structures. The unmitigated structure was unstable when the wind speed was above approximately 20 mph (9 m/s) because the negative aerodynamic damping at these wind speeds was larger than the positive mechanical damping of the structure. By contrast, the structure with either type of damping plate was stable because the total damping of the system remained positive at all the test wind speeds. The study did note that the wind speed at which the unmitigated model became unstable was higher than the wind speed at which full-scale traffic signal support structures were observed to exhibit large-amplitude vibrations. The different results between the model-scale and full-scale studies were attributed to the differences between the scaled model and the full-scale structure, as well as the fact that wind tunnel tests were conducted in smooth flow while full-scale wind is turbulent.

In addition to rectangular damping plates, helical strakes have also been used to suppress wind-induced vibrations of slender structures such as sign, luminaire and traffic signal support structures. Connor et al. (2012) conducted field experiments to evaluate the effectiveness of helical wires in mitigating vortex-induced vibrations of high-mast lighting towers. In this study, helical wires of various sizes and configurations (in terms of the number and pitch of the wires as well as the length of the tower covered by the wires) were mounted on three high-mast lighting towers (two in Wyoming and one in Iowa) that were instrumented for long-term monitoring. The wind-induced stresses on the towers were used as an indicator to assess the performances of the helical-wire systems. The data from the experiments suggested that double helical wires of 1 in. in diameter and 5 ft or 4 ft pitch (for each wire) were effective in eliminating vortex-induced vibration whether the wires covered the total length of the tower or only the top 1/3 of the tower. It was also observed that while a single helical wire was able to reduce the stresses caused by vortex-induced vibration, this wire configuration was not able to completely suppress such vibrations.

2.1.3 Vibration Absorbers.

Vibration absorbers work by dissipating the energy of the wind loading applied to the structure, resulting in less energy being input to cause vibration of the structure. Figure 2.3. presents two examples of vibrations absorbers. Previous research has considered various types of vibration absorbers, including tuned mass dampers, tuned liquid dampers, friction dampers, impact dampers, elastomeric pads, etc., to dissipate energy with varying results.

Lengel and Sharp (1969) first examined the performance of Stockbridge type tuned mass dampers to reduce the wind induced vibration of overhead sign structures. They employed strain gages located near the splicing flanges to determine the peak stresses for forced vibration cases and then observed that no vibration of the sign structure was observed when the damper was installed near the mid-span of the sign structure.

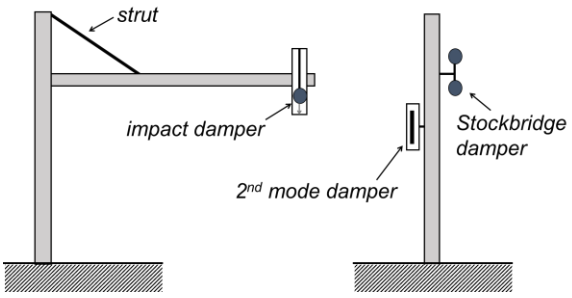

Figure 2.3: Examples of vibration absorbers: (a) strut to provide added stiffness or in-line with a shock absorber to dampen vibration and an impact damper where the mass impacts the bottom of the tube it is housed within, both on a traffic signal support structure mast arm; and (b) Stockbridge damper that behaves as a tuned mass damper and a second mode damper which behaves as a horizontal impact damper, both on a luminaire structure.

Jo et al. (1989) considered an impact ball damper to reduce vortex-induced vibration in highway light poles. Free vibration tests were conducted, where the mast arm was manually excited in the first in-plane or first out-of-plane mode and then released and allowed to freely vibrate. Acceleration measurements on the lamp, tip of arm, top of pole and side of pole as well as stress (measured from strain gages) at the bottom of the pole were used to determine the damping of the pole structure under forced vibration loads applied at the top of the pole structure and at the base at the various frequency modes of the structure. Wind tunnel tests were also conducted in a large wind tunnel and the displacement and acceleration amplitudes were measured with and without the damper for a range of wind speeds.

Hamilton et al. (2000) conducted extensive studies of several different types of vibration absorbers attached to a traffic signal structure with a 50 ft mast arm. Including:

- An elastomeric pad was placed between the mast arm baseplate and the baseplate of the box connection.
- A strut, or diagonal brace, with an automobile shock absorber (with adjustable settings) in line was attached between the mast arm and pole.

- An Alcoa dumbbell damper (a.k.a. Stockbridge damper), one realization of a tuned mass damper, was tested.
- Various impact dampers were also tested including a Hapco second mode impact damper; a flat-bar impact damper; strand impact damper; and a shot-put impact damper.

Free vibration tests were conducted, where the mast arm was manually excited in the first in-plane or first out-of-plane mode and then released and allowed to freely vibrate. Acceleration measurements at the tip of the mast arm were used to determine the damping coefficient of the traffic signal structure for the in-plane and out-of-plane motions.

Kalajian (1998) and Cook et al. (2001) examined different types of vibration absorbers attached to traffic signal structures. They examined damping of the mast-arm to pole connection using Belleville disc springs and neoprene pads placed between the mast arm and pole connection plates. Tuned mass dampers were also examined, employing a Stockbridge damper as well as a device built from a weight and spring, and a liquid tuned damper. Also examined were friction dampers and impact dampers. Free vibration tests on a mast arm in the laboratory as well as four mast arms in the field were conducted for these mitigation devices. In each test, the mast arm was manually excited in the first in-plane mode and then released and allowed to freely vibrate. Acceleration measurements at the tip of the mast arm were used to determine the damping coefficient of the traffic signal structure in the in-plane mode.

Cook et al. (2000) examined impact dampers attached to traffic signal structures. Free vibration tests were conducted, where the mast arm was manually excited in the first in-plane or first out-of-plane mode and then released and allowed to freely vibrate. Acceleration measurements at the tip of the mast arm were used to determine the damping coefficient of the traffic signal structure for the in-plane and out-of-plane motions. Additionally, sinusoidal forced vibration tests were conducted with an eccentric mass shaker. The acceleration measurements were used to estimate mast arm tip displacements during the first 35 seconds as the response measurements were increased to a steady state value.

McManus et al. (2003) conducted extensive studies of a number of different types of vibration absorbers attached to a traffic signal structure with a 50 ft mast arm. An elastomeric pad was placed between the pole base plate and the foundation. Various struts were attached between the mast arm and pole, and different impact dampers were tested. Sinusoidal forced vibration tests were conducted at several different frequencies using an eccentric mass shaker mounted at the top of the mast arm. Acceleration measurements at the tip of the mast arm as well as strain measurements in the mast arm near the pole connection were used to determine the peak in-plane amplitude response of the traffic signal structure over a range of frequencies. In one instance, different oscillating masses were used to examine the linearity of the impact damper performance.

Rice and Foutch (2006) and Rice et al (2017) considered the application of Stockbridge dampers to reduce wind and truck gust excitation of overhead sign structures. Field tests were conducted to manually excite the horizontal direction, measure the free vibration acceleration response of the structure and determine the damping coefficient from the free vibration response.

Caracoglia and Jones (2004 and 2007) considered impact dampers in the form of a canister damper and a chain damper for an aluminum tapered pole. Laboratory test measurements included accelerometers in and out-of-plane at the top and near the mid-height of the pole. Free

vibration tests, where the pole was pulled back using an actuator and then released were used to estimate the percent of critical damping.

Hoque and Christenson (2011) and Christenson (2011) conducted laboratory tests of a signal head vibration absorber tuned mass damper to reduce wind-excited vibration of a traffic signal structure. Free vibration tests on a mast arm in the laboratory were conducted for the mitigation device. The mast arm was manually excited in the first in-plane mode and then released and allowed to freely vibrate. Acceleration measurements at the tip of the mast arm were used to determine the critical damping ratio of the traffic signal structure in the in-plane mode for the controlled and uncontrolled cases. Christenson et al. (2014) then went on to test the signal head vibration absorber on traffic signal structures in the field. In the field tests a tri-axial accelerometer and anemometer are used to measure in and out-of-plane vibrations and wind speed and direction. Measurements were recorded over periods of months and 1-minute responses were transformed using the Hilbert transform to estimate the modal amplitude and frequency of the vibration for cases with and without the vibration damper.

Li et al. (2015) considered the use of a pounding tuned mass damper to reduce wind induced vibration in a small-scale traffic signal pole model consisting of an L-shaped beam. Free vibration tests were conducted, and accelerations were measured to determine the damping ratio. These tests were then followed by testing using an eccentric mass shaker to observe the reduction in the magnitude of the steady state acceleration response. The paper does not identify the frequencies used to excite the structure with and without the mass damper.

Dubbs (2018) conducted field testing of first and second mode dampers on light poles mounted on a bridge deck, hypothesized to be subjected to vortex shedding. Three methods of testing were conducted including: force vibration testing using a hammer to excite the light pole where frequency and damping ratio were determined from power spectral density functions of the acceleration response; pluck tests for free vibration where the damping ratio was computed using the logarithmic decrement technique; and ambient vibration monitoring to compare acceleration magnitudes over the time period for undamped and damped poles. Accelerations were measured using two wireless accelerometers, one on the arm and the second two-thirds along the height of the main pole. Wind speeds were also measured. The author noted that the hammer impact tests provided the best quality data, however, the poles were not excited sufficiently to obtain realistic damping estimates. The free vibration tests provided better excitation; however, the signal quality was difficult to produce in a repeatable and reliable manner. Lastly, the author notes that the ambient tests were collected during a period where the poles were not sufficiently excited, which resulted in questionable reliability of the ambient test results. This study identified the benefits and challenges with different methods of field testing.

Further, relevant to the research of this project is the work conducted by Fernandez et al. (2009) for an isolator for a camera mounted at the top of a traffic camera poles. While the vibration of the pole itself was not the focus of the research, nor was the application of a vibration absorber, the paper does describe field testing of a passive mechanical isolation device to reduce the response of the camera itself. The acceleration at the top of the pole and on the camera were determined by field tests under actual wind conditions and time history and spectral response were developed and the amplitudes compared.

Research has been conducted for vibration absorber types of vibration-mitigation devices as applied to wind-excited sign, luminaire and traffic signal structures. These research studies have considered free vibration tests, forced vibration tests, wind tunnel tests and field tests to evaluate the performance of the vibration absorber. Both acceleration and strain gage measurements have

been used to evaluate performance. The performance was quantified as changes between the measured damping or time or frequency domain measurements of the structure with and without the vibration absorber.

2.2 Existing Specifications and Test Procedures.

The specifications for seismic isolation devices, in particular the qualification process and means for characterizing performance, were examined to identify how similar disciplines specify performance in protective devices. In particular, the use of a damping coefficient, β_L, for seismic isolation devices should be noted. This factor accounts for the damping provided by the isolation bearings and is used to reduce the force applied to the structure to allow for a simplified static analysis to be easily modified in lieu of conducting more detailed analysis of the complex dynamic system. Further, the process to test and qualify new damping devices should be noted. A similar process could be utilized for vibration-mitigation devices.

The NEHRP (National Earthquake Hazards Reduction Program) Recommended Seismic Provisions for New Buildings and Other Structures, called FEMA P-1050 (2015), was developed by the Building Seismic Safety Council of the National Institute of Building Science for the Federal Emergency Management Agency (FEMA) to aid the process of translating seismic research into practice. FEMA P-1050 was written as a series of recommended changes and modifications to the seismic code provisions adopted in ASCE/SEI 7-10, and it documents a process for using simplified and idealized models to design protection systems for more complex actual buildings and other structures subjected to seismic events. The process is based on using correction factors that relate the ideal system response to the expected response of the actual system. In such a fashion, the response of the structure is modified for the effects of damping in the system.

Very similar to the AASHTO LRFD SLTS Specifications, static elastic analysis procedures are used in the design process for the seismic code. As such, the nonlinear inelastic response resulting from structural damage or damping mechanisms are not directly accounted for. For seismic design of buildings, a response modification factor, R-factor, is used to account for the nonlinear (more complex) response of the structural system resisting seismic loads. The R-factor reduces the load (demand) on the structure to account for the benefits of damping systems and allowable damage not accounted for in a simplified elastic static analysis and takes the general form, as first proposed in the ATC-3-06 (ATC 1978) as

$$V_b = V_e / R \tag{2.4}$$

where V_b is the design base shear, and V_e is the base shear calculated by static elastic analysis, a simplified analysis). The values of R range from 1 to 8. The R-factor and other coefficients necessary are generally obtained from tables in ASCE/SEI 7 standard. As such, widespread use of new seismic configurations requires the ASCE committee to incorporate new coefficients into ASCE/SEI 7. The FEMA P-1050 committee recognized the need to rapidly qualify new seismic systems and sponsored the development of Quantification of Building Seismic Performance Factors (FEMA P-695) with the goal of developing a procedure to establish consistent, rational, building performance response parameters. FEMA P-695 was released in 2009, and in 2015 FEMA P-1050 formally adopted FEMA P-695 for “qualification of new systems and components; evaluation of performance objectives for seismic design and re-evaluation of seismic design categories.”

FEMA P-695 (2009) supports FEMA P-1050 by recommending a methodology for obtaining and quantifying critical “seismic performance factors”, including the response modification factor (R-

factor), System Overstrength Factor (Ω_0), Deflection Amplification Factor (C_d), The FEMA P-695 methodology addresses the development of detailed system design information and probabilistic assessment of collapse risk while utilizing nonlinear analysis techniques, and explicitly considers uncertainties in ground motion, modeling, design, and test data. The focus is primarily on estimating "strength and deformation demands on systems that are designed using linear methods of analysis but are responding in the nonlinear range."

The FEMA P-695 qualification process, shown in Figure 2.4, begins with identifying a seismic structural system concept and obtaining required information. The structural behavior is then characterized through the use of structural system archetypes, or typical examples. Archetypes provide a method of addressing significant features of the proposed system and defining permissible configurations. Six building characteristics are considered critical to defining structural system archetypes: building height; fundamental period; structural framing configuration; framing bay sizes or wall lengths; magnitude of gravity loads; and member and connection design and detailing requirements.

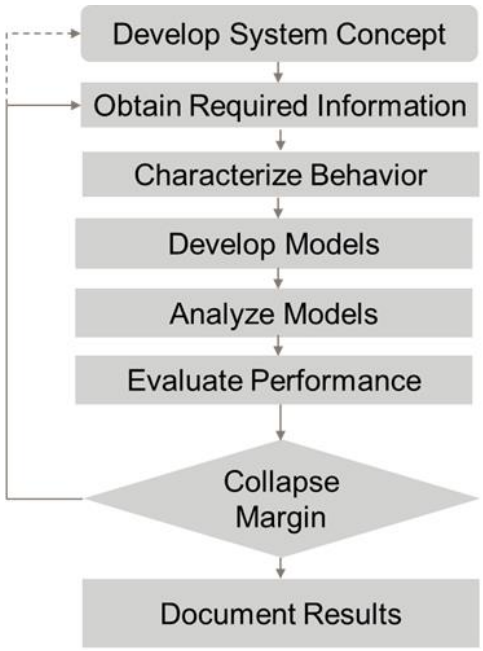

Figure 2.4: Qualification process for seismic isolation devices.

Archetypes are further broken down into performance groups which reflect major changes in behavior within the archetype that require separate analysis. Once archetypes are defined, a series of nonlinear collapse models are developed to represent the range of intended configurations and applications. As much as possible, the models attempt to explicitly address all potential failure mechanisms, and the methodology includes procedures for assessing the effects of behavior not explicitly modeled. The models are calibrated using material, component, or assembly test data and other evidence to verify their ability to simulate expected behavior.

Detailed dynamic analysis is performed using a set of 50 standard ground motions (i.e, actual loads not the code provided design loads). Assuming the model survives the initial loading, the ground motions are increased until failure/collapse is established. Finally, with collapse

established in these detailed models, the simplified models are evaluated using trial values of the seismic performance factors and using the code provided design loads. A collapse margin ratio is then calculated and compared to acceptable values. FEMA P-695 includes modeling and design uncertainties in the process for determining acceptability of the collapse margin ratio with a 10% probability serving as an average baseline value.

For eventual use in design and construction, FEMA P-695 requires that the entire design process be thoroughly documented for review by an independent peer review panel, an approving authority having jurisdiction. FEMA P-1050 also provides a similar simplified design process for addressing damping in seismically isolated structures. In this process, system damping is associated with a displacement correction factor through a table relating percent critical damping to the appropriate correction factor.

2.3 Identify Criteria and Potential Test Procedures

Vibration-mitigation devices affect the dynamic response of support structures for signs, luminaires, and traffic signals. The dynamic interaction between the mitigation device and the structure can have a significant effect on the overall performance of the vibration-mitigation device. Criteria to identify the effectiveness of various mitigation devices in previous work was specific to the types of wind-induced vibration they intended to address and to the type of structure which they were applied. As a result, test procedures for evaluating the effectiveness of vibration-mitigation devices for various structural supports of signs, luminaires, and traffic signals under different types of wind loading (including galloping, gust, truck and vortex) may be different. It is in the best interest of the Specifications to have a simplified and uniform set of criteria for test methods to evaluate the effectiveness of vibration-mitigation devices. In this task, general criteria and potential test procedures are identified for evaluating the effectiveness of vibration-mitigation devices for sign, luminaire, and traffic signal structures for the various types of wind loading.

When considering specific criteria and test procedures to quantify performance, it is important to recognize the different excitation mechanisms which develop from various wind conditions (i.e., the steady state response of galloping and vortex induced vibration; versus the impulsive loading and transient response to natural wind and truck gust). Stationary buffeting oscillation and the transient response from impulse wind gusts are each proportionally reduced by increases in the structural damping, and increased system damping using a vibration-mitigation device can attenuate the amplitude of buffeting oscillation to achieve infinite fatigue life of the structure. However, for the large-amplitude vibrations due to vortex shedding or galloping caused by negative aerodynamic damping, it is best to completely eliminate the onset of these types of vibrations by providing sufficient supplemental damping to the system to overcome the negative aerodynamic damping. Otherwise, galloping oscillations can reach excessively large or even divergent amplitudes, and vortex-induced vibration, although being a limit-cycle type (i.e., the amplitude of the vibration cannot exceed certain thresholds), can cause rapid accumulation of fatigue stress cycles due to their occurrence at low to moderate wind speeds over broad ranges of wind directions. The fatigue limits in the SLTS Specifications are for high-cycle fatigue (section C1.5.2.3 in the SLTS Specifications) and thus conditions of low-cycle fatigue should be avoided. For some wind conditions, a minimum required level of performance of a vibration-mitigation device is warranted to insure the high-cycle fatigue responses are not initiated. This minimum level of performance was considered as part of this research.

Furthermore, when considering specific criteria and test procedures to quantify performance, it is important to recognize the performance of the damping device can be highly dependent on the physical and dynamic characteristics of the structure itself. Additionally, some wind conditions

occur in a certain frequency range, such that some structures may inherently not be susceptible to these wind conditions. As such, the criteria used to measure performance needs to include measures of the damping, mass and natural frequency of the structure. A range of typical frequencies and sizes/masses should be defined for each of the sign, luminaire and traffic signal support structure types.

2.3.1 Criteria to Quantify Dynamic Response.

Various criteria have been used in previous research to quantify the response of sign, luminaire and traffic signal structures. Common criteria include damping ratio, peak or root mean square (RMS) response, force coefficients, power spectral density functions (PSDs) and frequency response functions (FRFs). The criteria are defined by the specific response (and in some cases both the excitation and response) analyzed and the vibration characteristic being estimated with that response.

The vibration responses that can be measured on sign, luminaire and traffic signal structures with minimal effort and cost include strain, acceleration, and potentially displacement. Strain sensors and accelerometers provide reliable and relatively inexpensive means to measure dynamic response when coupled to a data acquisition system. Displacements can be measured from string potentiometers or lasers and may also be available as measurements, however, these measurements typically require a relatively small stand-off distance, such that a fixed reference point needs to be within a few inches of the point of the structure being measured. These different responses will typically be proportional to each other, within the elastic range, and can be used interchangeably to quantify the performance criteria.

The excitation, whether it be wind or an applied force, can be measured from anemometer, pressure sensors, load cell, or inferred from a given mass moving/rotating at a specified velocity. A measurement of the excitation, synchronized with the response, can be helpful in quantifying the response as a function of the excitation.

The damping ratio (Chopra, 2017) can be measured from the response measurement in a free vibration test. Assuming linear viscous damping, the attenuation of the response is exponential and described by

$$u(t) = A \exp(-\zeta \omega_n t) \tag{2.5}$$

where $u(t)$ is the attenuation of the response as a function of time, t, A is the initial amplitude (at time t=0), ζ is the damping ratio to be measured, and ω_n is the natural frequency (rad/sec). The natural frequency can also be measured from the free vibration test as $\omega_n = 2\pi(n/t_n)$, where n is the number of cycles/oscillations observed over t_n seconds. The damping ratio is a function of the structural system (structure and any mitigation devices). Assuming the structure remains in the linear elastic range, the damping ratio is not a function of the different wind conditions.

The Scruton number (Marra, et al., 2015), a critical parameter in predicting vortex induced vibration, is proportional to the structural damping and mass of the structure.

Considering the random nature of wind-induced responses, the statistics of steady state response, including peak response amplitude and root mean square (RMS) (a measure of the standard deviation, or square root of the variance), are useful in characterizing the response (Bendat and Piersol, 2010). The RMS assumes the response measured over the period of excitation is both stationary and ergodic, and that the response is Gaussian in nature. Peak or

RMS response is a direct measurement of the response, and it may be difficult to extrapolate peak or RMS results to different wind conditions.

Not present in literature for vibration-mitigation devices applied to SLTS support structures is the Frequency Response Function (FRF) (Bendat and Piersol, 2010). The FRF is a standard measure in the area of experimental structural dynamics. The FRF is a measure for linear systems. While the structures to be considered are operating within a linear range, the vibration-mitigation devices may not be linear. FRFs taken at various operating points can help to quantify the non-linear effects of the vibration-mitigation devices. One challenge of using FRFs is that the experimental determination of a transfer function requires measurement of both input force and output response. The input force measurement may not be available in the field but may be available in the laboratory.

2.3.2 Test Procedures to Identify Dynamic Properties.

To evaluate each of the proposed evaluation criteria, different test procedures can be utilized. In the literature for vibration-mitigation devices applied to STLS support structures, tests are typically conducted on one particular structure, although there are studies that have considered two or more variations of the structure. Types of testing includes field testing, laboratory testing, and wind tunnel testing.

Field testing utilizes actual structures either in-service or out-of-service and utilize actual wind conditions for the excitation. The testing can be conducted on a single day but relies on certain wind conditions being present that day or done over an extended period where the response (and excitation, if available) is periodically measured.

Free vibration tests involve the structure being manually excited in the mode of interest and then released and allowed to vibrate freely. This can be done with structures in a laboratory or out in the field and can even be done on structures in a wind tunnel.

Forced vibration tests are where the structure is excited in a manner to simulate a specific wind excitation. The excitation can be with an eccentric mass shaker or a linear shaker to provide a constant or varying (sweeping) frequency sinusoidal excitation, or with an impact hammer to provide an impulsive load. Varying levels of input force can be obtained by increasing the oscillating mass in the shakers or using a larger impact hammer or larger swing.

Wind tunnel testing uses scaled models and can use free vibration tests to evaluate the level of damping of the system. Wind tunnel and field testing of vibration-mitigation devices that eliminate or reduce negative aerodynamic damping will need to require the measurement of the damping in the system as a performance measure either during the events in the field, or in a more controlled environment in a wind tunnel. .

Table 2.1 provides a mapping of the above-mentioned criteria to the test procedures used to identify them and the associated benefits and concerns.

Table 2.1. Benefits and concerns for evaluation criteria and test procedures.

Criteria	Test Procedure	Benefits & Concerns
Damping coefficient	Free vibration (pluck test) - *lab or field*	Simple to collect amplitude dependent system damping, Difficult to excite only the mode of interest
Peak or RMS response	Forced vibration (linear or eccentric mass shaker) - *lab or field*	Difficult to excite highly damped structure at low frequency with limited stroke/mass, Difficult to find resonant frequency of lightly damped systems
Force coefficients of structural sections (e.g., Hua and Zuo, 2013)	Stationary wind tunnel tests – *wind tunnel*	Difficult in the assessment of end effects, Not useful for assessment of negative damping in vortex-induced vibration.
Aerodynamic damping of structural sections	Dynamic tests of elastic wind tunnel models – *wind tunnel*	Challenge in physical configuration of model supporting system and assessment of end effects
Peak or RMS response	Full-scale monitoring (accelerometers, anemometers) - *field*	Long durations (months) and experiments not controllable
Frequency response function	Impulse test (impact hammer) - *lab*	Not feasible to collect amplitude dependent data, Often excite higher modes of vibration
Frequency response function (FRF)	Forced vibration (linear shaker, white noise) - *lab*	Difficult to excite highly damped structure at resonance with limited stroke/mass of shaker
Frequency response function (FRF)	Force vibration (eccentric mass shaker, sine sweep) - *lab*	Time consuming to collect steady state response of lightly damped system & sweep over frequency range of interest at fine resolution (minutes)

2.4 LRFD Philosophy for Fatigue Resistance and Vibration-mitigation Devices

A design philosophy to incorporate the use of vibration-mitigation devices would be based on the Load and Resistance Factor Design (LRFD) with appropriate load and resistance factors utilized. The load factors, calibrated to provide approximate reliability indices, are identified in Table 3.4-1 of the AASHTO LRFD SLTS Specifications for fatigue loads including truck gust (TrG), natural

wind gust (NWG), vortex-induced vibration (VVW), combined wind on high-level towers, and galloping induced vibration (GVW). Proposed modifications to the LRFD Specifications for Structural Supports for Highway Signs, Luminaires, and Traffic Signals could incorporate a response modification factor, R, to account for the reduction in response due to the vibration-mitigation device.

To incorporate the response modification factor into the design process, the response of the structure to the applied loading would be determined using the typically employed methods, and then the response would be reduced to account for the effects of the vibration-mitigation device. Dividing the nominal response by the factor R allows for a simplified linear static analysis of the system to consider effects of the vibration-mitigation device, in lieu of conducting detailed analysis of the more complex dynamic system.

2.4.1 Quantifying Performance of Vibration-Mitigation Devices.

Critical to understanding the effectiveness of a vibration-mitigation device is establishing a well-defined measure of the dynamic performance of the device as applied to the structural system. A robust system qualification method is necessary to properly classify vibration-mitigation devices for their performance. The developed method must also be sufficiently flexible to accommodate a wide range of vibration-mitigation devices and simple enough to encourage advancements in mitigation device technologies. The method could be based on conducting a finite set of experimental tests (e.g., field tests, laboratory tests, wind tunnel tests) to characterize the vibration-mitigation device performance over a range of structures, types of wind loadings and amplitudes of response, and then developing a numerical model to analyze and evaluate the mitigation device performance for a specific structure design.

Since the vibration of sign, luminaire and traffic signal support structures is typically dominated by a single mode of vibration, the dynamic behavior of the structure can be represented (numerically and physically) as a single mass oscillating on a spring in the elastic range at a particular frequency. While high mast light poles have been observed to vibrate in the first few modes of vibration, these modes are well spaced and can be examined independently as series of single mass oscillators. A range of typical frequencies and dynamic masses can be defined for each of the sign, luminaire and traffic signal support structures and a grid of these can be identified such that manufacturers will be able to physically test their devices and validate corresponding models for various dynamic mass (or dynamic weight) and frequency combinations of interest.

2.4.2 Calculating Response Modification Factors.

Given a quantifiable measured performance of the vibration-mitigation device identified from validated models of the structure with the device in place, a corresponding response modification factor (R) can be determined for each load case considered. The response modification factor would consider the characteristics of the dynamic loading for the different wind loads and the corresponding response (i.e., steady state vibration of galloping versus impulsive response from truck-induced gusts and wind gusts). Structural dynamics theory and accompanying simulations would be used to determine an equivalent response modification factor, R, considering the reduction in the amplitude of the response and number of cycles for a given increase in damping for each load case. Use of the response modification factor in design would need to include conservatism to account for the confidence in the design, testing and characterization of the mitigation device and the overall structural response. The implementation of the R-factor would aim to ensure that a minimum acceptable level of structural reliability in line with the intent of the full AASHTO LRFD SLTS Specifications is maintained.

The structure's response to galloping is a steady state response at the resonance of the structure. The amplitude of the response of a steady state response for the undamped (only inherent damping in the structure), a_u, and controlled (mechanical vibration-mitigation device present), a_c, excited at the resonant frequency is related to the damping ratio (Chopra, 2017) as:

$$a_u = \frac{1}{2\zeta_u} \tag{2.6}$$

$$a_c = \frac{1}{2\zeta_c} \tag{2.7}$$

The decrease in the displacement is the ratio of the inherent to damped damping ratio, obtained by dividing (2.7) by (2.6) such that:

$$\frac{a_c}{a_u} = \frac{\zeta_u}{\zeta_c} \tag{2.8}$$

The decreased response will reduce the wind-induced nominal stress range and is accounted for in the design process through a response modification factor, R, used to reduce the demand proportional to the reduced response (more specifically, $\frac{1}{R}\gamma(\Delta f)_n$).

For luminaire, sign and traffic signal support structures, if no damping ratio has been experimentally determined for the specific structure, a default value of $\zeta_u = 0.002$ (0.2%) is to be used.

A multiplier, γ_R, is employed to account for the uncertainty in the prediction of the vibration-mitigation device performance, accounting for both the uncertainty in predicting the damping of the structure with a vibration-mitigation device (ζ_c) and the uncertainty in the inherent damping of the uncontrolled structure (ζ_u). Accordingly, the ratio of the response reduction is reduced by this factor γ_R. The response modification factor, R, for galloping load is calculated as:

$$R = \gamma_R \frac{\zeta_c}{\zeta_u} \tag{2.9}$$

Further, to provide a conservative nature in the process, a minimum value for the R-factor is specified to be greater than Ψ_R. This accounts for uncertainty of possible changes in the structure and the structure's dynamic properties over the life of the structure and provides for protection against uncertainty in the overall reliable nature of a vibration-mitigation device and serves to ensure that incremental improvements and only marginally improved performance is not accepted. The R-factor for steady-state type wind loads is determine from equation 2.9 as:

$$R = \begin{cases} \gamma_R \frac{\zeta_c}{\zeta_u} & for\ R > \Psi_R \\ 1 & otherwise \end{cases} \tag{2.10}$$

Next consider response modification factor for natural wind gust and truck-induced gust. Truck-induced gust loading, as identified in the measured dynamic loads of Cook, et al. (1996) can be approximated with a triangular load with a 0.125 sec. rise time, a 0.375 sec. total duration, and 18.8 psf pressure. From impulse response charts in Chopra (2017), the dynamic response amplification over the static response is a function of the duration of the impulse, t_d, divided by the vibration period of the structure, T (which is the inverse of the natural frequency). For structures with frequencies between 0.6 Hz and 3 Hz, t_d/T ranges from 0.22 to 1.25 and assuming vibration-mitigation devices may likely increase damping for truck gust impulse loading only on

the order to 0.01 (1%), the change in the response amplification is negligible. A vibration-mitigation device, even an effective one, may not significantly reduce the maximum amplitude of the response, but it may quite significantly reduce the number of cycles. The free vibration, $x(t)$, of an underdamped system can be written as

$$x(t) = \quad A_o e^{-\zeta \omega_n t} \cos(\omega_d t) \tag{2.11}$$

where A_o is the original amplitude of the displacement, and $\omega_d = \omega_n \sqrt{1-\zeta^2}$ is the damped natural frequency. For lightly damped systems, $\omega_d \cong \omega_n$ and considering peak amplitudes at the *n*th period (T) of oscillation, denoted x_n, where $t = nT = n/2\pi\omega_n$ then (2.11) can be written as

$$x_n = \quad A_o e^{-\zeta \omega_n n/2\pi\omega_n} \tag{2.12}$$

So, considering the undamped and damped systems, given the same initial displacement, A_o, the number of cycles needed to get below an infinite fatigue life amplitude for x_n is determined from (2.12) for uncontrolled and controlled systems with associated damping levels as

$$\ln\left(\frac{x_n}{A_o}\right) = \quad -\zeta_u \, n_u/2\pi = -\zeta_c \, n_c/2\pi \tag{2.13}$$

which can be rearranged such that

$$\frac{n_c}{n_u} = \quad \frac{\zeta_u}{\zeta_c} \tag{2.14}$$

The decreased number of cycles for impulsive-type wind loads can be accounted for in the design process through the response modification factor, R, used to reduce the number of wind load induced stress cycles (more specifically, $n_c = \frac{1}{R} n_u$ for finite fatigue). From the above, it can be shown that the R for truck-induced vibration is the same R as for galloping, as determined from the damping ratio, written again here for convenience.

$$R = \quad \begin{cases} \gamma_R \frac{\zeta_c}{\zeta_u} & for\ R > \Psi_R \\ 1 & otherwise \end{cases} \tag{2.10}$$

Given that the galloping, natural wind gust and truck-induced gust all rely on equation (2.10) to calculate R, the combined wind effect for high mast lighting towers fatigue also uses equation (2.10).

2.4.3 Design of Support Structures.

To provide designers a method for considering damping devices in the fatigue design of sign, luminaire and traffic signal support structures, a simplified design procedure is advantageous. The design procedure would consist of applying the response modification factor to modify the demand, such that support structures shall be designed for fatigue to resist wind-induced stresses, as provided in a modified version of Equations 11.5-1, 11.5.1-1, 11.9.3-1 and C.3-1 in the AASHTO LRFD SLTS Specifications 11.9.3-1:

$$\gamma\left(\frac{\Delta f}{R}\right) \leq \phi(\Delta F) \qquad \text{(11.5-1, AASHTO LRFD SLTS Specifications)}$$

$$\gamma\frac{(\Delta f)_n}{R} \leq \phi(\Delta F)_n \qquad \text{(11.5.1-1, AASHTO LRFD SLTS Specifications)}$$

$$\gamma\frac{(\Delta f)_n}{R} \leq \phi(\Delta F)_n \qquad \text{(11.9.3-1, AASHTO LRFD SLTS Specifications)}$$

$$\frac{(\Delta f)_l}{R} \leq (\Delta F)_l \qquad \text{(C.3-1, AASHTO LRFD SLTS Specifications)}$$

where γ is the load factor defined in Table 3.4-1, $(\Delta f)_n$ is the wind-induced nominal stress range defined in Article 11.9.2, $(\Delta F)_n$ is the nominal fatigue resistance as specified Article 11.9.3, φ is the resistance factor and is equal to 1.0 for fatigue loading, and R is the response modification factor as suggested in this project. When there is no effective vibration-mitigation device used, R is equal to 1.0.

3 FINDINGS AND APPLICATIONS

A survey was distributed to the AASHTO Committee on Bridges and Structures (COBS) on the use of vibration-mitigation devices by States throughout the country. The survey was completed November 2018. A total of 25 State Departments of Transportation identified themselves, including: Arizona, Arkansas (2), Colorado, Connecticut, Delaware, Florida, Illinois, Iowa, Kansas, Maryland, Montana, Missouri, Minnesota, North Dakota, New Jersey, New York, Ohio, Oklahoma, Oregon, South Dakota, Texas, Utah, Virginia, Washington and Wyoming. A total of 26 responses were recorded for the 25 states (Arkansas had two respondents). This section first provides a review of these results.

The archetypes subsection of 3.2 is a result of structural designs of luminaires, sign and traffic signal support structures provided as a part of the NCHRP 12-111 survey. This subsection identifies and defines the term dynamic weight that is used in this report, along with natural frequency and damping ratio, to identify the dynamic properties of a structural system. The various structural designs provided were numerically modeled in SAP2000 (CSI, 2021) to identify numerically the natural frequency and dynamic weight. This section shows examples of some typical STLS support structures and identifies the dynamic space that these various structures span.

Next, test procedures to evaluate the effectiveness of a vibration-mitigation device were carried out. The test procedure was refined over the course of this project through application to various vibration-mitigation device examples. This work is summarized in Appendix I: Examples.

Finally, in this section, the proposed structural design process is presented. These two sections, 3.3 and 3.4, constitute the main body of this research project.

3.1 NCHRP 12-111 Survey Results

The survey indicates, as shown in Figure 3.1, that for sign structures, 35.71% of the States are using the AASHTO LRFD SLTS Specifications, 28.57% are using the 2015 6th edition (AASHTO, 2015b), 17.86% the 3rd edition (AASHTO, 1994), 10.71% the 4th edition (AASHTO, 2006) and 7.14% the 2013 6th edition (AASHTO, 2013). No States are using the 5th edition of the Specifications (AASHTO, 2011) for sign structures. For luminaire structures, 39.29% of the States are using the 2015 6th edition of the Specifications, 28.57% are using the LRFD Specifications, 21.43% the 4th edition, 28.57% are using the 2015 6th edition, 7.14% the 3rd edition and 3.57% the 2013 6th edition. No States are using the 5th edition of the Specifications for luminaire structures. For traffic signal structures, 34.48% of the States are using the 2015 6th edition of the Specifications, 27.59% are using the LRFD Specifications, 20.69% the 4th edition, 28.57% are using the 2015 6th edition, and 17.24% the 3rd edition. No States are using the 2013 6th edition or the 5th edition of the Specifications for traffic signal structures.

As shown in Figure 3.2, vibration-mitigation devices are being used on all types of traffic structures. Six responses were recorded for organizations using vibration-mitigation devices for sign structures, 4 for luminaires, and 14 for traffic signal structures. Nine of the respondents indicated they used no vibration-mitigation devices for any structures in their organization. The other responses (6 total) provided specifics on vibration-mitigation devices, including sign blanks, Stockbridge dampers and second mode canister light pole dampers, used on various structures. As such, 64% of the responding States have used vibration-mitigation devices, less than but consistent with the 76% reported in NCHRP Report 796.

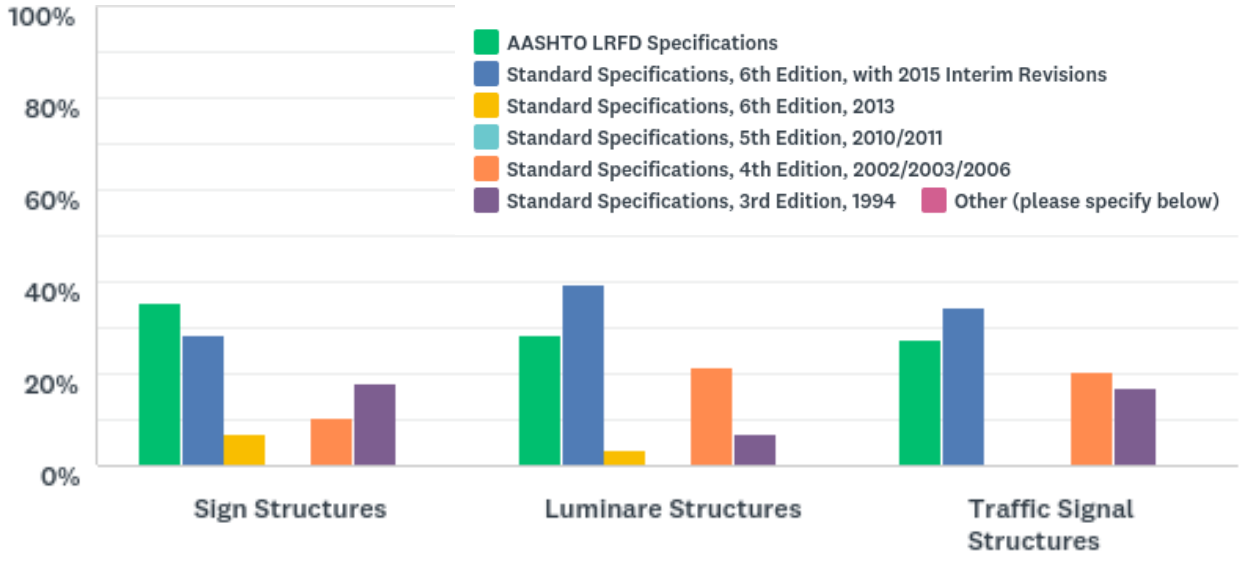

Figure 3.1: Survey response to "Which Specifications is your organization currently using for sign, luminare and traffic signal structures?"

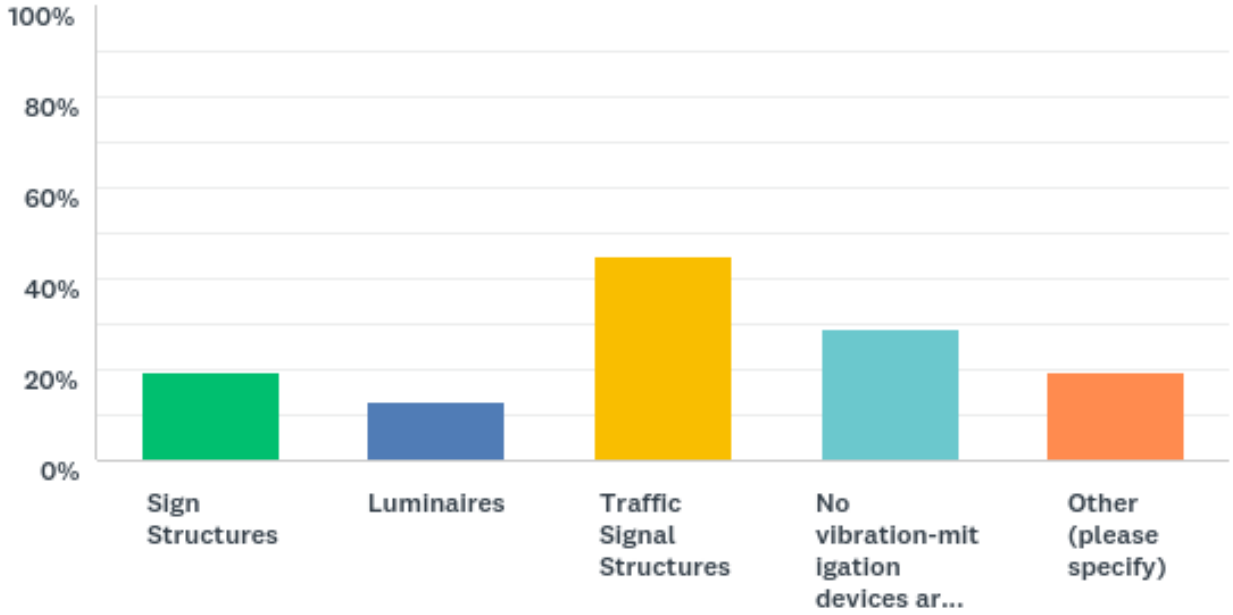

Figure 3.2: Survey response to "Does your organization use vibration-mitigation devices for any of the following support structures?"

The survey identified that 75.86% of the respondent's organizations follow the fatigue importance criteria provided in the commentary of the Specifications.

The Specifications identify different wind loads for different structures. For traffic signal structures, 43.33% of the respondent's organizations design for galloping and 53.33% include truck induced gust for the design. Those that do not design for these loads indicate mitigation devices are installed if galloping is observed.

Respondents identified specific types of vibration-mitigation devices for the different traffic structures. Stockbridge dampers were identified for use on sign structures. For luminaires, internal dampers (likely second mode dampers) and chain dampers (hung inside the pole) were identified. On traffic signal structures, respondents identified using sign blanks, Stockbridge dampers, Valmont TR-1, Pelco Triton SP-7004, Frey Corp. 63DM, and various impact dampers developed by Cook, et. al (2000).

The vibration-mitigation devices for sign structures target galloping but all wind types are identified (galloping, natural wind gusts and vortex induced vibration). The vibration-mitigation devices for luminaires targeted second mode vibration with galloping and natural gusts identified. For traffic signal structures, galloping was identified, as well as natural gusts.

With regard to the experience with the vibration-mitigation devices, respondents identified that vibration-mitigation devices are effective or adequate because observed vibrations are not observed after installation. Some respondents have no anecdotal or measured evidence. The measured evidence was reported from pole manufactures and universities, but a general lack of monitoring for performance was noted. Sign blanks were noted to work in some instances, however, to not always be effective. Additionally, a respondent identified a traffic signal pole failure with a Stockbridge damper installed.

To approve the use of vibration-mitigation devices historical verification or research verification is specified. To satisfy this, respondents noted the use of NCHRP Report 412 (Kaczinski, 1998) and NCHRP Report 469 (Dexter and Ricker, 2002), historical performance observed by the organization, or pole manufacture research and field experience. It was identified in the survey that in general organizations do not have any current methods for measuring or evaluating the effectiveness of vibration-mitigation devices, outside of video to record events.

When asked what type of devices and what level of performance respondents would like to see from vibration-mitigation devices, respondents indicated they are interested in vibration-mitigation devices that are simple and effective. If a simple device can provide effective performance this would be desired. But there is a consensus that effective devices are desired.

3.2 Structural Support Dynamic Archetypes

The AASHTO LRFD SLTS Specifications describes a number of typical structure types in Section 1.4 of the specifications. Based on designs provided by States that responded to the NCHRP 12-111 survey, this report develops archetypes and identifies the associated range of frequencies and dynamic weights. The information developed in this report will be used to identify typical dynamic properties for STLS support structures for which vibration-mitigation devices should be designed and evaluated.

3.2.1 Dynamic Properties of Interest

The dynamics of a structural system is described mathematically through force equilibrium as a second order ordinary differential equation, called the equation of motion (EOM). For a single-degree-of-freedom system the EOM can be written as:

$$m\ddot{x}(t) + c\dot{x}(t) + kx(t) = f(t) \tag{3.1}$$

where *m* is the mass, *c* is the damping coefficient, *k* is the stiffness, *x(t)* is the displacement, *f(t)* the excitation force and [•] denotes a derivative with respect to time. The natural frequency ω_n and damping ratio ζ are defined as $\omega_n^2 = k/m$ and $\zeta = c/(2\omega_n m)$ (Chopra, 2017). The natural frequency in Hz (cycles per second) is defined as $f_n = \omega_n/2\pi$ f_n. By dividing equation (3.1) by *m* the EOM can be written as:

$$\ddot{x}(t) + 2\zeta\omega_n\dot{x}(t) + \omega_n^2 x(t) = \frac{1}{m}f(t) \tag{3.2}$$

From equation (3.2), it is observed that the dynamics of the system can be fully described by the natural frequency, damping ratio and mass. The mass and stiffness (and thus natural frequency) are determined from the structural properties. The damping cannot be determined from structural properties and should be assumed based on observed behavior of similar structures.

For a system with multiple degrees-of-freedom (i.e. a finite element model) with *n* degrees-of-freedom, the EOM takes the matrix form where

$$M\ddot{X}(t) + C\dot{X}(t) + KX(t) = \Gamma f(t) \tag{3.3}$$

where *M* is the *n*x*n* mass matrix, *C* is the damping matrix, *K* the stiffness matrix, *X(t)* is the nx1 displacement vector, and Γ is the nx1 loading vector for the excitation force *f(t)*. From the eigenvalue problem of the undamped system, the natural mode Φ_n and corresponding natural frequency ω_n of the *n*th mode can be written as a modal matrix $\boldsymbol{\Phi}$ and spectral matrix $\boldsymbol{\Omega}$. As a result of the orthogonality properties of the natural modes, the modal mass matrix ($\bar{M} = \boldsymbol{\Phi}^{\boldsymbol{T}} M \boldsymbol{\Phi}$) and modal stiffness matrix ($\bar{K} = \boldsymbol{\Phi}^{\boldsymbol{T}} K \boldsymbol{\Phi}$) are diagonalized. For certain assumed forms of damping, the modal damping matrix ($\bar{C}$) can also be diagonalized. It is often convenient to write the *n* coupled EOMs in equation (3.3) as *n* decoupled EOMs in modal form:

$$\bar{M}\ddot{Q}(t) + \bar{C}\dot{Q}(t) + \bar{K}Q(t) = \bar{\Gamma}f(t) \tag{3.4}$$

where $\bar{\Gamma} = \boldsymbol{\Phi}^{\boldsymbol{T}}\Gamma$.

Transportation structure vibration problems can typically be considered as behaving in a single mode of vibration. For a specific dynamic mode of vibration, the *j*th mode, the system can be simplified to be defined by a single-degree-of-freedom EOM:

$$\bar{M}_j\ddot{q}_j(t) + \bar{C}_j\dot{q}_j(t) + \bar{K}_j q_j(t) = \bar{\Gamma}_j f(t) \tag{3.5}$$

For a displacement at the *j*th DOF, x_j, and an applied force at that same DOF, f_n, the modal mass of the *n*th mode can be normalized to the *j*th DOF of the *n*th natural mode as $\bar{m}_n = \bar{M}_n/\Phi_{jn}^2$ such that the modal equation of motion of the *n*th mode can be written in terms of the actual physical displacement at the *j*th DOF as (Premount & Seto, 2008):

$$\bar{m}_n\ddot{x}_j(t) + \bar{c}_n\dot{x}_j(t) + \bar{k}_n x_j(t) = f_n(t) \tag{3.6}$$

Similar to the rearranging of (7.1) into (7.2), for (7.6) the dynamics of the *n*th mode can be written:

$$\ddot{x}_j(t) + 2\zeta\omega_n\dot{x}_j(t) + \omega_n^2 x_j(t) = \frac{1}{\bar{m}_n}f_n(t) \tag{3.7}$$

with a single dynamic mass, $\bar{m}_n$, a natural frequency, ω_n, and a damping ratio, ζ, for the *j*th DOF of the *n*th mode. The natural frequency, ω_n, is determined from an eigenvalue analysis of the mass and stiffness matrices in equation (3.3). As mentioned above, the damping must be assumed, as it cannot be determined from structural properties. In lieu of an alternative value, it is assumed to be 0.2% herein as an approximate upper bound. The modal mass is proposed to be presented as a modal weight (as weight is more intuitive than mass) and to clarify that this is associated with the dynamic representation and not a physical quantity, it is referred to in this report as *dynamic weight,* $W_n = \bar{m}_n g$, where g is the acceleration due to gravity. The dynamic weight is determined from the model mass of the *n*th mode ($\bar{M}_n$) and the *j*th degree-of-freedom of the mode shape of the corresponding *n*th mode (Φ_{jn}) as

$$W_n = g\bar{M}_n/\Phi_{jn}^2 \tag{3.8}$$

The equation of motion is then written as:

$$\ddot{x}_j(t) + 2\zeta\omega_n\dot{x}_j(t) + \omega_n^2 x_j(t) = (g/W_n)f(t) \tag{3.9}$$

The dynamic weight and natural frequency are determined for different types of STLS support structures from the structural properties provided by States responding to the NCHRP survey for each of the different types of STLS support structures.

3.2.2 Sign Structures

A total of 147 sign structure designs from Colorado, Delaware, Illinois, Iowa, Minnesota, New York, and Oregon were available to model. These can be subdivided into bridge type (span) structures and cantilevered structures. The dynamic properties for each structure has been determined by finite element analysis. The dynamic modes of interest are the first mode in-plane mode of vibration (vertical motion of the structure) and the first mode out-of-plane vibration.

From the information provided in response to the survey, 147 full 3D finite element models of steel sign support structures were built with the SAP2000 code (CSI, 2021). Gravitational loads of the signs and attachments were taken from the structure blueprints. The type of structures modelled were overhead cantilevers and overhead bridge sign structures and include both monotube and truss types. Models of the various structure types are shown in Figures 3.3-3.9.

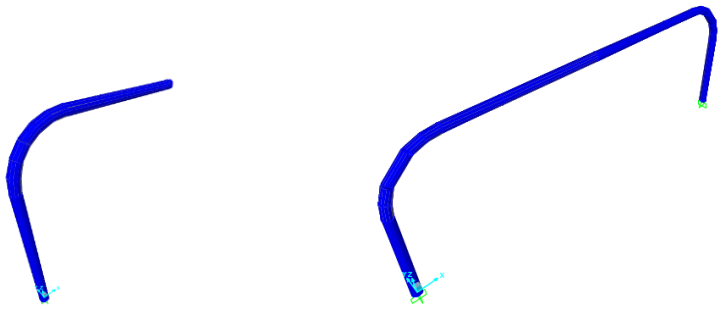

(a) (b)

Figure 3.3 State of Colorado sign structure models: (a) cantilevered; and (b) bridge-type examples.

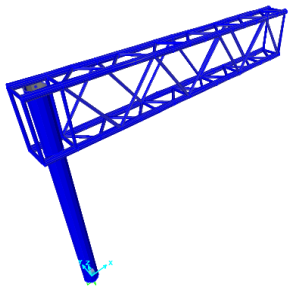

Figure 3.4 State of Illinois sign structure models: cantilevered example

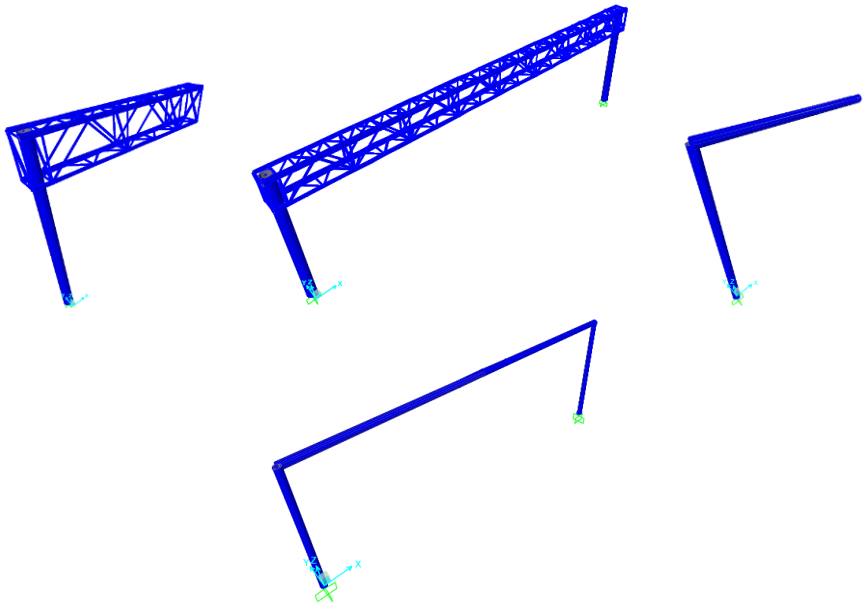

(a) (b) (c) (d)

Figure 3.5 State of Minnesota sign structure models: (a) cantilevered truss; (b) bridge truss-type; (c) cantilevered monotube; (d) bridge-type monotube examples.

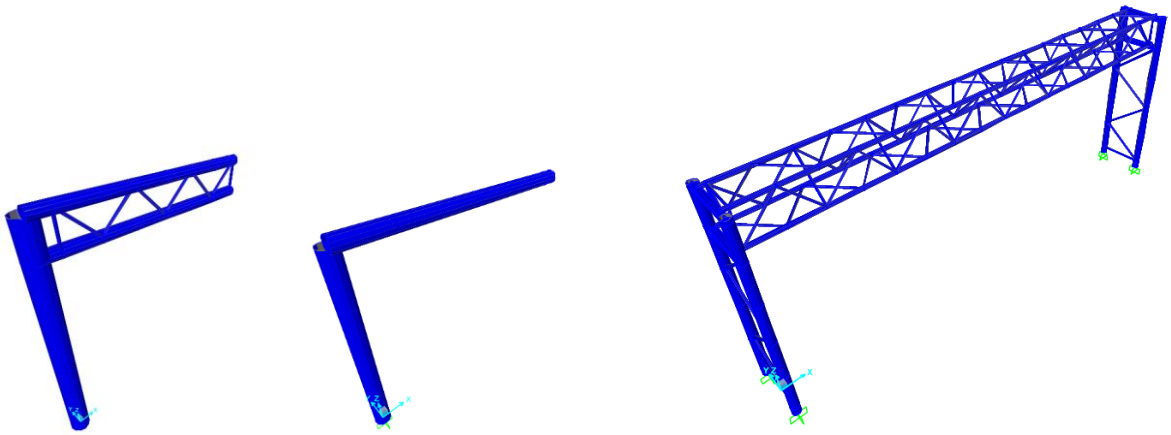

(a) (b) (c)

Figure 3.6 New York State sign structure models: (a) cantilevered truss; (b) cantilevered monotube; (c) bridge truss-type.

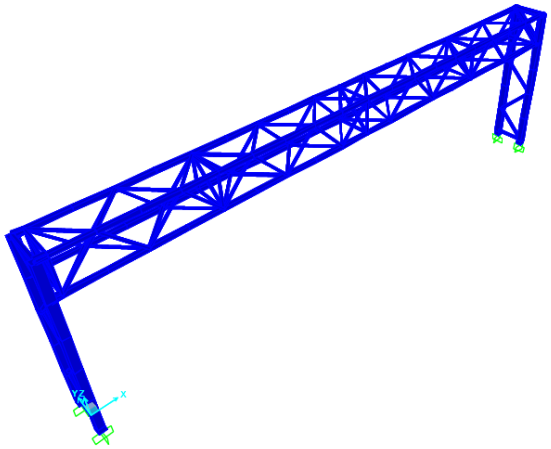

Figure 3.7 State of Oregon sign structure models: bridge-type example

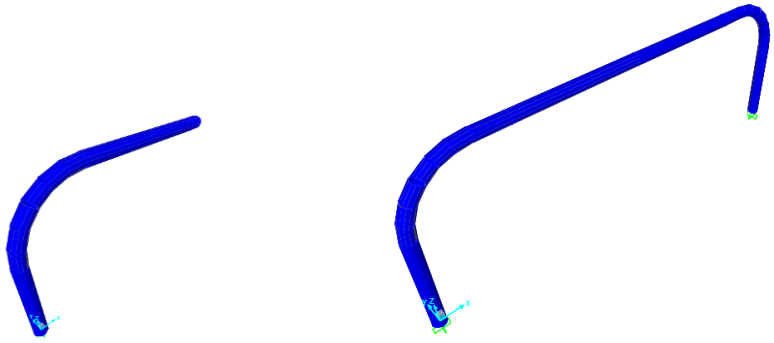

(a) (b)

Figure 3.8 State of Delaware sign structure models: (a) cantilevered; and (b) bridge-type examples.

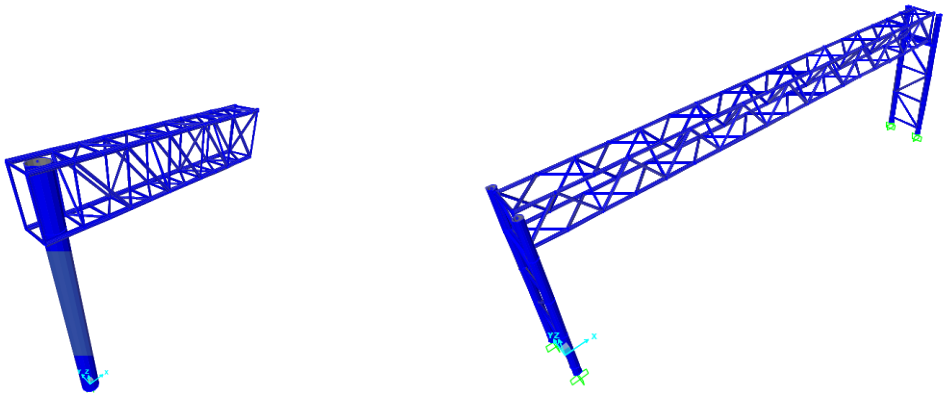

(a) (b)

Figure 3.9 State of Iowa sign structure models: (a) cantilevered; and (b) bridge-type examples

The natural frequency and mode shape were output from the SAP2000 dynamic analysis. The dynamic weight is defined here as the product of the modal mass and gravity, determined using the approach outlined in Section 3.4.1 of this report. The location of a vibration-mitigation device, as used in the calculation of the dynamic weight, for bridge-type structures is placed in the center of the span and for cantilevers is placed 2 to 3 ft. from the free end at the nearest node (Foutch, et al, 2006).

In-Plane Dynamic Properties. The in-plane dynamic results are distinctly different in terms of frequency range and dynamic weight range between the cantilevered and bridge-type structures.

For the analyzed cantilevered sign structures with span lengths from 13 to 52 ft, the dynamic weight ranges from 1300 lbs to 6000 lbs, as shown in Figure 3.10, In general, as span length increases the frequency decreases and the dynamic weight increases. The frequency versus dynamic weight, as shown in Figure 3.11, follows a trend that provide for archetype sign structure dynamic properties to be identified.

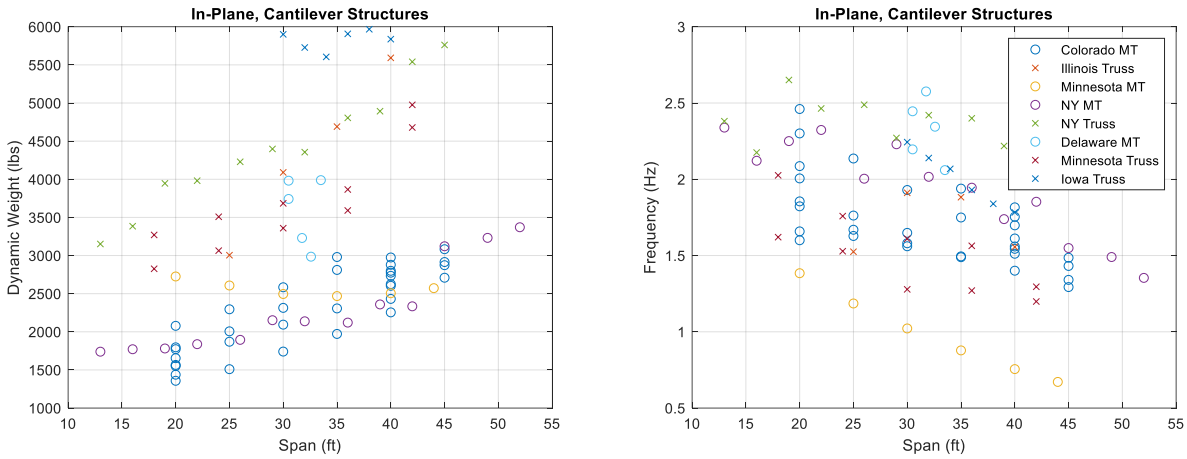

Figure 3.10 Cantilevered sign structure in-plane dynamic properties: (a) span length versus dynamic weight; and (b) span length versus natural frequency

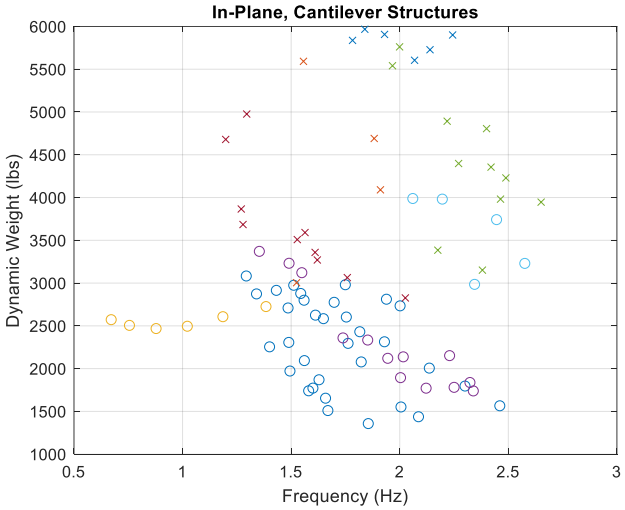

Figure 3.11 Cantilevered sign structure in-plane natural frequency versus dynamic weight

For the analyzed bridge-type sign structures with span lengths from 49 to 163 ft, the dynamic weight ranges from 2,500 lbs to 25,000 lbs, as shown in Figure 3.12a, while the natural frequency ranges from 1.6 Hz to 13 Hz, as shown in Figure 3.12b. In general, as span length increases the frequency decreases and the dynamic weight increases. The frequency versus dynamic weight, as shown in Figure 3.13, follows a trend that provide for archetype sign structure dynamic properties to be identified.

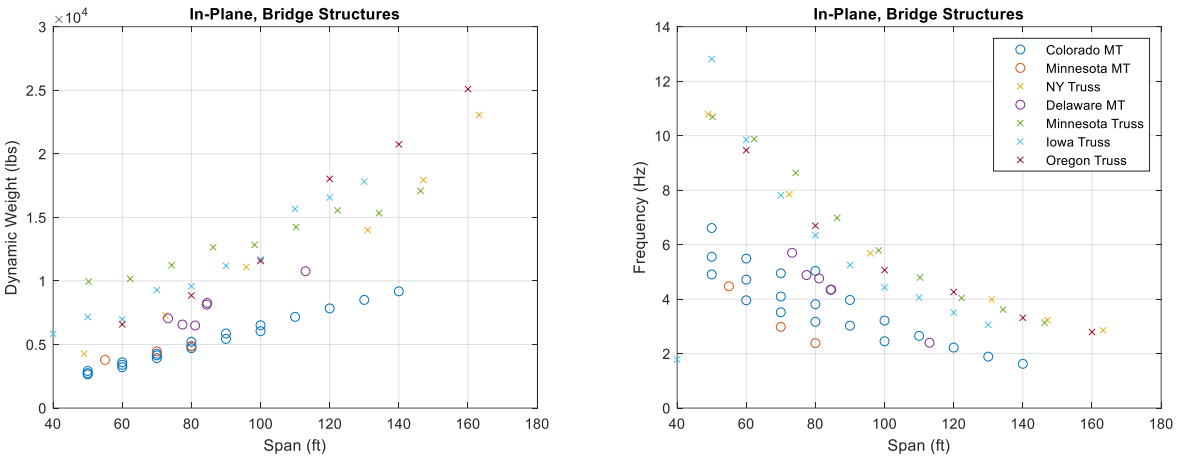

Figure 3.12 Bridge-type sign structure in-plane dynamic properties: (a) span length versus dynamic weight; and (b) span length versus natural frequency

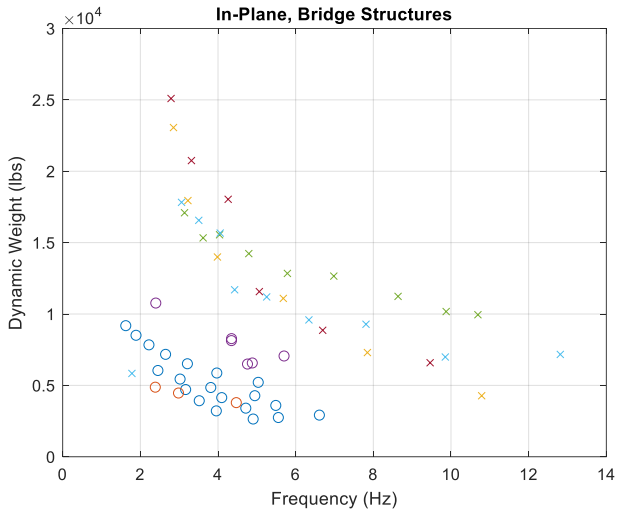

Figure 3.13 Bridge-type sign structure in-plane natural frequency versus dynamic weight

Out-of-Plane Dynamic Properties. Similar to the findings for in-plane dynamic behavior, the out-of-plane dynamic results are distinctly different between the cantilevered and bridge-type structures.

For the analyzed cantilevered sign structures with span lengths from 13 to 52 ft, the dynamic weight ranges from 1200 lbs to 5200 lbs, as shown in Figure 3.14a, while the natural frequency ranges from 0.6 Hz to 2.6 Hz, as shown in Figure 3.14b. In general, as span length increases the frequency decreases and the dynamic weight increases. The frequency versus dynamic weight, as shown in Figure 3.15, follows a trend that provide for archetype sign structure dynamic properties to be identified.

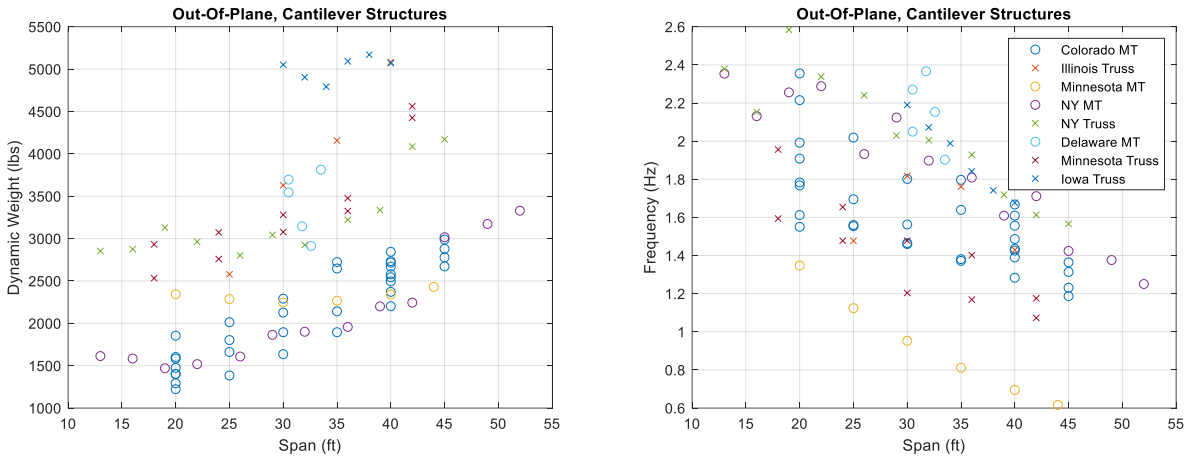

Figure 3.14 Cantilevered sign structure out-of-plane dynamic properties: (a) span length versus dynamic weight; and (b) span length versus natural frequency

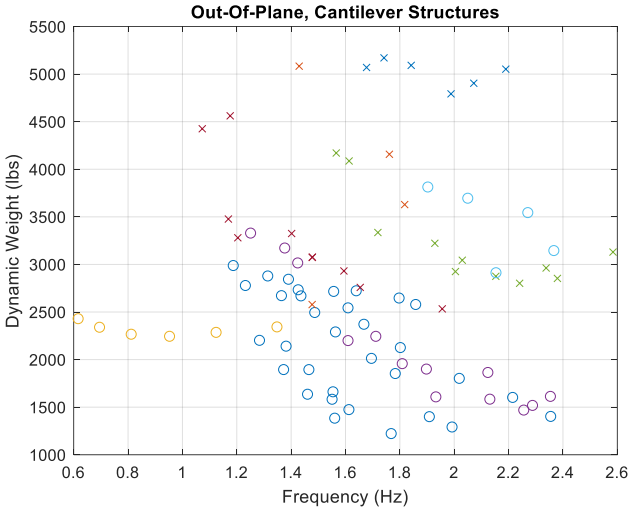

Figure 3.15 Cantilevered sign structure out-of-plane natural frequency versus dynamic weight

For the analyzed bridge-type sign structures with span lengths from 49 to 163 ft, the dynamic weight ranges from 4,600 lbs to 27,000 lbs, as shown in Figure 3.16a, while the natural frequency ranges from 1 Hz to 8 Hz, as shown in Figure 3.16b. In general, as the span length increases, the frequency decreases and the dynamic weight increases. The frequency versus dynamic weight, as shown in Figure 3.17, follows a trend that provide for archetype sign structure dynamic properties to be identified.

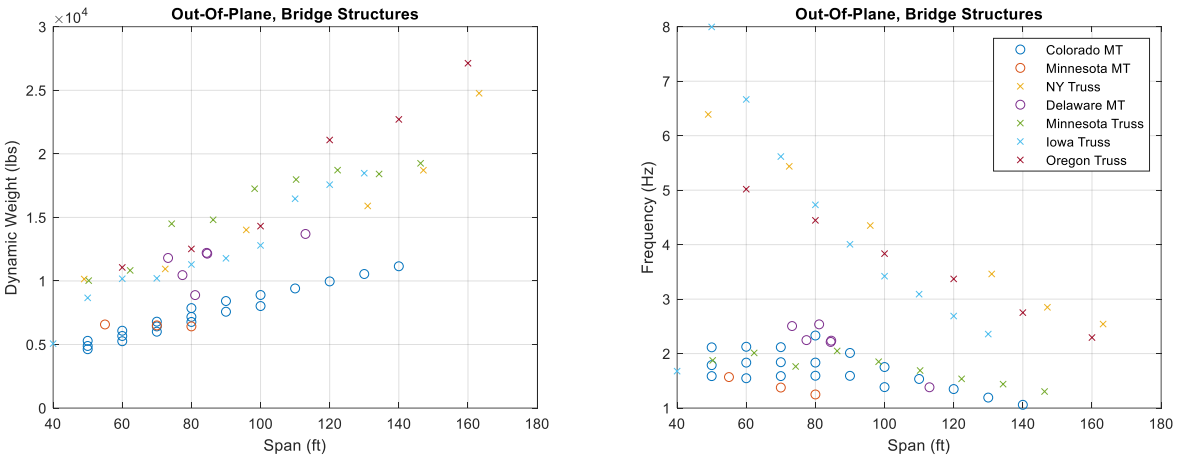

Figure 3.16 Bridge-type sign structure out-of-plane dynamic properties: (a) span length versus dynamic weight; and (b) span length versus natural frequency

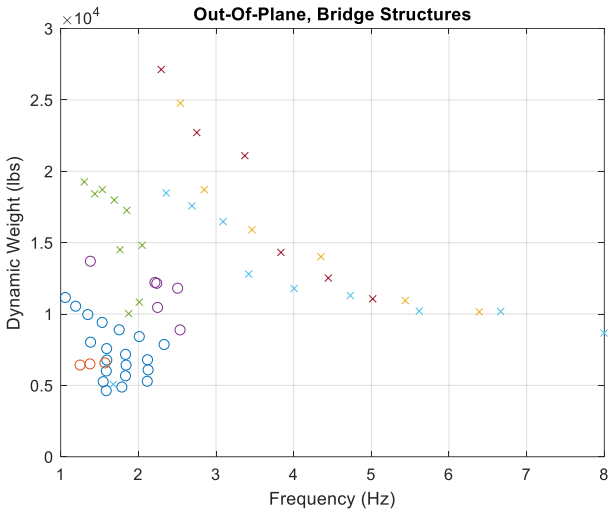

Figure 3.17 Bridge-type sign structure out-of-plane natural frequency versus dynamic weight

Sign Structure Archetypes. From Figures 3.11, 3.13, 3.15 and 3.17, it is observed that the natural frequencies and dynamic weights cover different ranges for the in-plane and out-of-plane modes for each cantilevered and bridge-type structures. To allow for a more specific range of these dynamic properties, four different types of motion and structures were identified and with each of these types three representative structures were specifically identified. For the in-plane motion, the sample space considered for cantilever sign structures was comprised of natural frequencies from 0.5 Hz to 3 Hz and dynamic weights from 1000 lbs to 6000 lbs. For bridge structures, the sample space considered was comprised of natural frequencies from 1.5 Hz to 13 Hz and dynamic weights from 2,500 lbs to 25,000 lbs. Three typical dynamic properties for in-plane vibration of traffic signal support structures are identified in Table 3.1.

Table 3.1: Sign Structure Archetypes for In-Plane Vibration.

	Cantilevered		Bridge-type	
Descriptor	Dynamic Weight (lbs)	Frequency (Hz)	Dynamic Weight (lbs)	Frequency (Hz)
Short Span Sign Structure	2,000	2.5	5,000	8.0
Mid-Range Span Sign Structure	3,500	1.5	10,000	4.0
Long Span Sign Structure	5,000	1.2	20,000	3.0

For the out-of-plane motion, the sample space considered for cantilever sign structures was comprised of natural frequencies from roughly 0.5 Hz to 3 Hz and dynamic weights from 1000 lbs to 6000 lbs. For bridge structures, the sample space considered was comprised of natural frequencies from 1.0 Hz to 7 Hz and dynamic weights from 5,000 lbs to 25,000 lbs. Three typical dynamic properties for out-of-plane vibration of traffic signal support structures are identified in Table 3.2.

Table 3.2: Sign Structure Archetypes for Out-of-Plane Vibration.

	Cantilevered		Bridge-type	
Descriptor	Dynamic Weight (lbs)	Frequency (Hz)	Dynamic Weight (lbs)	Frequency (Hz)
Short Span Sign Structure	2,000	2.0	5,000	2.0
Mid-Range Span Sign Structure	3,000	1.6	15,000	2.0
Long Span Sign Structure	3,500	1.2	20,000	3.0

3.2.3 Luminaires

A total of 22 luminaire structure designs from Delaware, Iowa, Minnesota and Washington were available to model and analyze to determine their dynamic properties. The pole heights of these designs range from 25 ft to 45 ft. The dynamic modes of interest are the first and second modes of vibration.

From the information provided in response to the survey, 22 full 3D finite element models of steel sign support structures were built with the SAP2000 code. The type of structures modelled are: typical pole with luminaire mounted at the top of the pole and typical pole with luminaire arms. The Delaware poles have the luminaire mounted at the top of the pole. The Iowa and Washington poles have balanced luminaire arms. The Minnesota poles have a bent monotube luminaire arm. The Delaware, Iowa and Washington poles are steel, while the Minnesota poles are aluminum. Typical structure models are shown in Figure 3.18.

The natural frequency and mode shape were output from the SAP2000 dynamic analysis. For first mode, the damper device was assumed to be placed at the top (free end) of the pole. For second mode vibration, the damping device was assumed to be placed 2/3 of the height of the pole from the base.

(a) *(b)*

Figure 3.18 Typical Pole with Luminaire Mounted at Pole Top, 37 ft height: (a) Delaware; (b) Iowa

First Mode Dynamic Properties. For the first mode dynamics, the typical poles with heights from 25 to 45 ft were found to have dynamic weights ranging from 20 lbs to 70 lbs, as shown in Figure 3.19a, and natural frequency ranging from 4 Hz to 1 Hz, as shown in Figure 3.19b. The Delaware poles are much heavier than the more typical poles and have dynamic weights from 420 to 530 lbs with natural frequencies roughly between 3 and 6 Hz. For all poles, as the height increases the frequency decreases and the dynamic weight increases. The frequency versus dynamic weight, as shown in Figure 3.20, follows a trend that provide for two archetype luminaire structure dynamic properties to be identified.

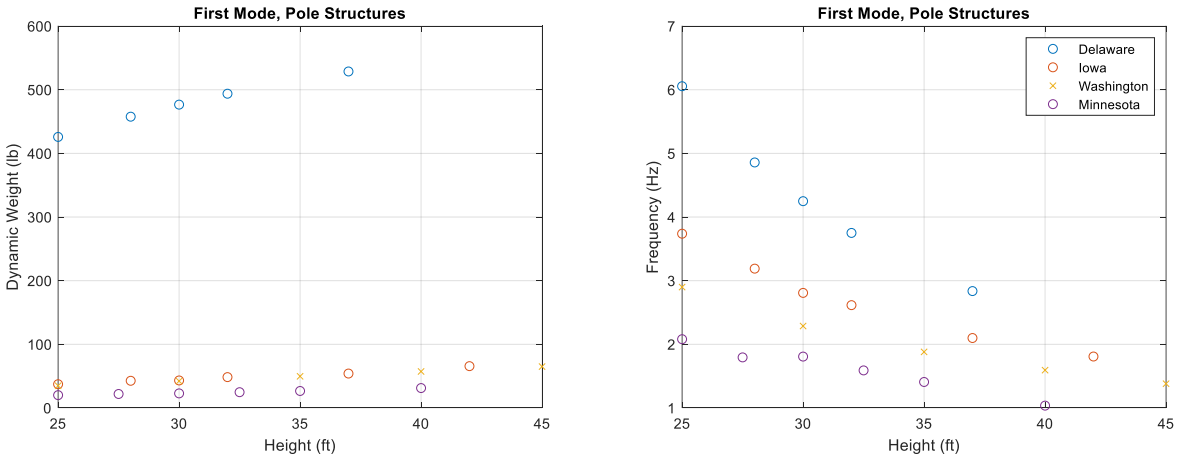

Figure 3.19 Luminaire first mode dynamic properties: (a) pole height versus dynamic weight; and (b) pole height versus natural frequency

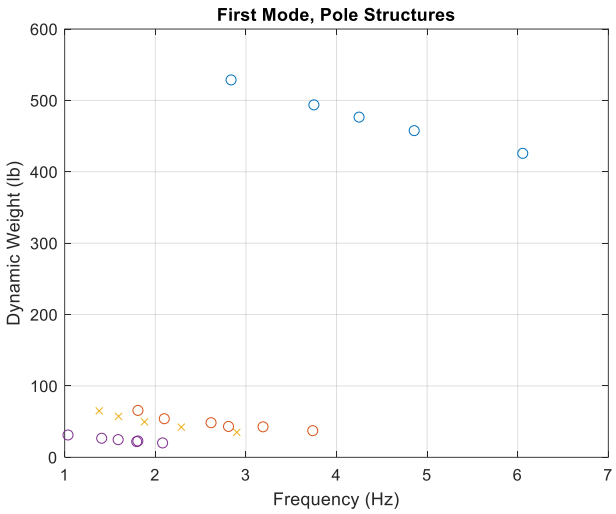

Figure 3.20 Luminaire first mode natural frequency versus dynamic weight

Second Mode Dynamic Properties. For the second mode dynamics, the typical poles with heights from 25 to 45 ft were found to have dynamic weights ranging from 20 lbs to 55 lbs, as shown in Figure 3.21a, and natural frequency ranging from between roughly 4 and 18 Hz, as shown in Figure 3.21b. The Delaware poles are much heavier than the more typical poles and have dynamic weights from 410 to 480 lbs with natural frequencies roughly between 14 and 33 Hz. For all poles, as the heights increase the frequency decreases and the dynamic weight increases. The frequency versus dynamic weight, as shown in Figure 3.22, follows a trend that provide for an archetype luminaire structure for second mode dynamics to be identified. Since the Delaware poles have second mode frequencies above 20 Hz, they may not be susceptible to second mode wind induced vibration.

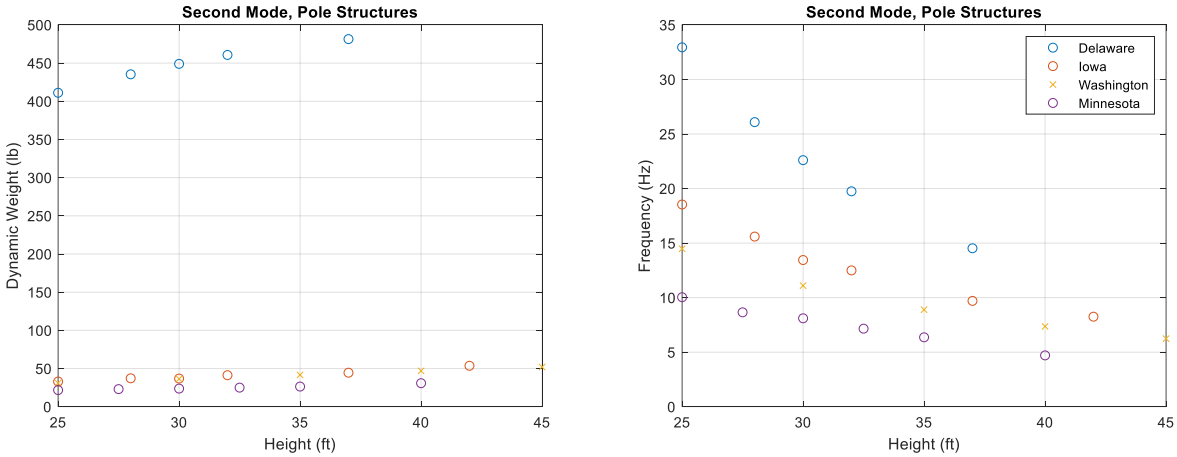

Figure 3.21 Luminaire second mode pole dynamic properties: (a) pole height versus dynamic weight; and (b) pole height versus natural frequency

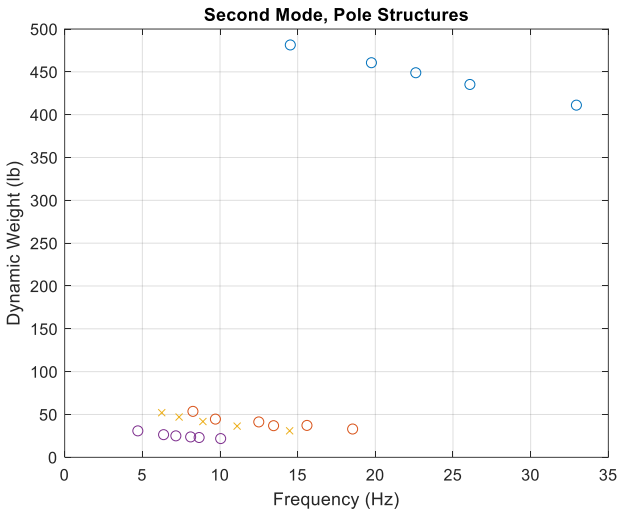

Figure 3.22 Luminaire second mode pole natural frequency versus dynamic weight

Luminaire Pole Archetypes. From Figures 3.20 and 3.22, it is observed that the natural frequencies and dynamic weights cover different ranges for the first mode and second mode vibration and two types of structures, shorter and taller, are identified as representative structures for each. The dynamic properties of the Delaware poles are not considered for archetype dynamic properties, due to the dramatically different properties these luminaires are observed to have. For the first mode vibration, the sample space considered was comprised of natural frequencies from 1 to 4 Hz and dynamic weights from 20 lbs to 70 lbs. Two typical dynamic properties for first mode luminaire structures are identified in Table 3.3.

Table 3.3: Luminaire Archetypes for First Mode Vibration.

Descriptor	Dynamic Weight (lbs)	Frequency (Hz)
Shorter Luminaire	30	4.0
Taller Luminaire	60	1.5

For the second mode vibration, the sample space considered was comprised of natural frequencies from 4 to 20 Hz and dynamic weights from 10 lbs to 50 lbs. Two typical dynamic properties for second mode luminaire structures are identified in Table 3.4.

Table 3.4: Luminaire Archetypes for Second Mode Vibration.

Descriptor	Dynamic Weight (lbs)	Frequency (Hz)
Shorter Luminaire	30	18.0
Taller Luminaire	50	6.0

3.2.4 Traffic Signal Support Structures

A total of 19 traffic signal support structure designs from Colorado, Illinois, Iowa and Washington were available to model and analyze to determine their dynamic properties. The mast arm lengths of these designs range from 25 ft to 75 ft. The dynamic modes of interest are the first mode in-plane mode of vibration (vertical motion of the mast arm) as well as the first mode out of plane vibration (horizontal motion of the mast arm).

From the information provided in response to the survey, 27 traffic signal support structures from Colorado, Illinois, Iowa and Washington with mast arm lengths ranging from 25ft to 75ft have been modeled with the SAP2000 code. Typical structure models are shown in Figure 3.23.

The natural frequency and mode shape were output from the SAP2000 dynamic analysis. For first mode in-plane and out-of-plane, the damper device is assumed to be placed at the free end of the mast arm.

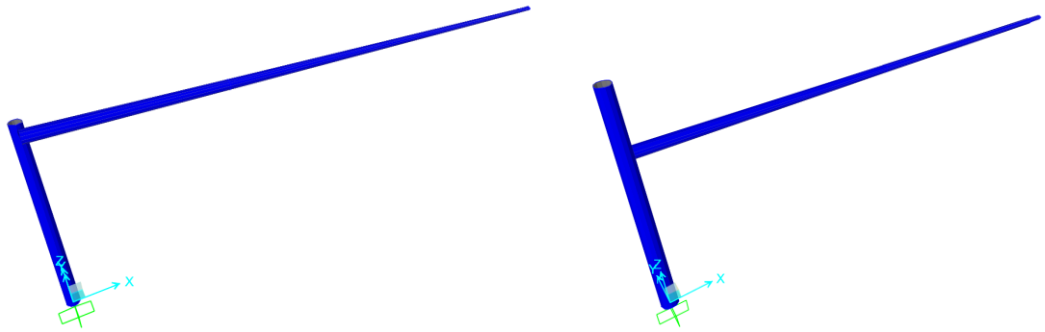

(a) *(b)*

Figure 3.23 Typical Traffic Signal Support Structure Models: (a) 65 ft. Washington Mast Arm; (b) 50 ft. Colorado Mast Arm

In-Plane Dynamic Properties. As shown in Figures 3.24-3.25, for the analyzed signal support structures with mast arm lengths from 25 to 75 ft, the dynamic weight ranges from 250 lbs to over 500 lbs while the natural frequency ranges from 1.8 Hz to 0.8 Hz.

Out-of-Plane Dynamic Properties. The results in Figures 3.26-3.27 show that as the mast arm length increases from 25 to 75 ft, the dynamic weight increases from 250 lbs to 650 lbs while the natural frequency decreases from 1.7 Hz to 0.75 Hz.

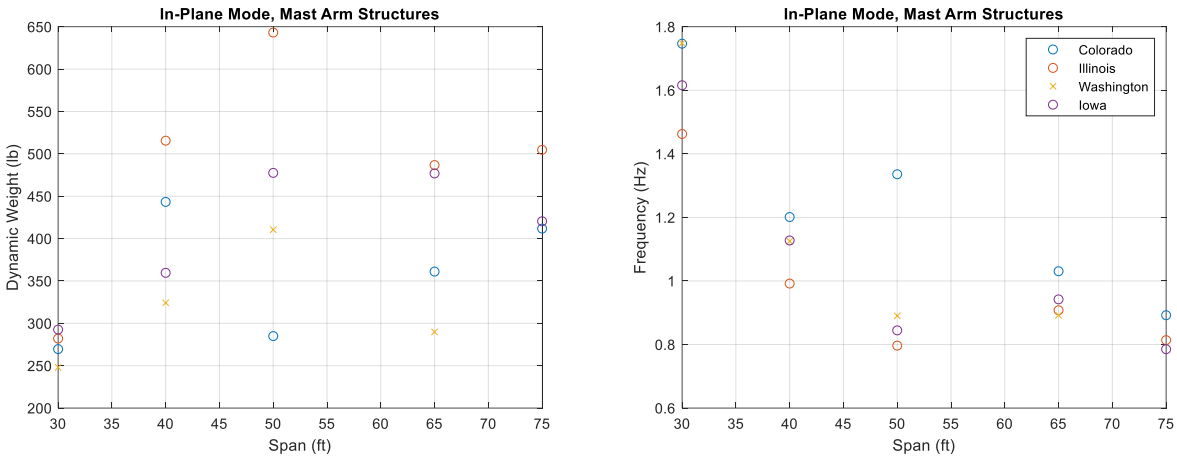

Figure 3.24 Traffic signal support structure in-plane dynamic properties: (a) mast arm length versus dynamic weight; and (b) mast arm length versus natural frequency

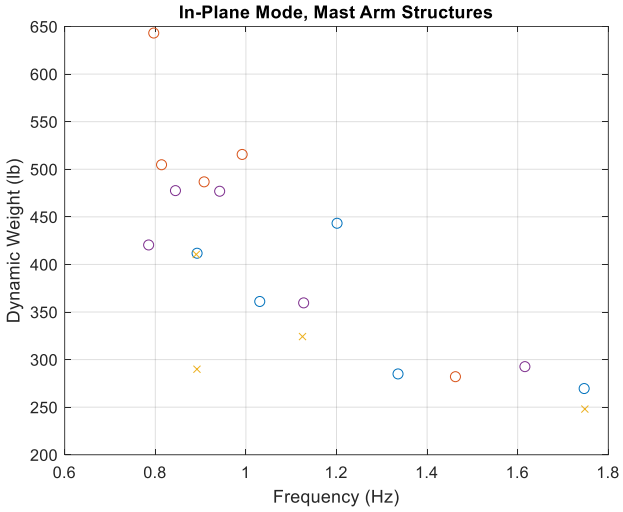

Figure 3.25 Traffic signal support structure in-plane natural frequency versus dynamic weight

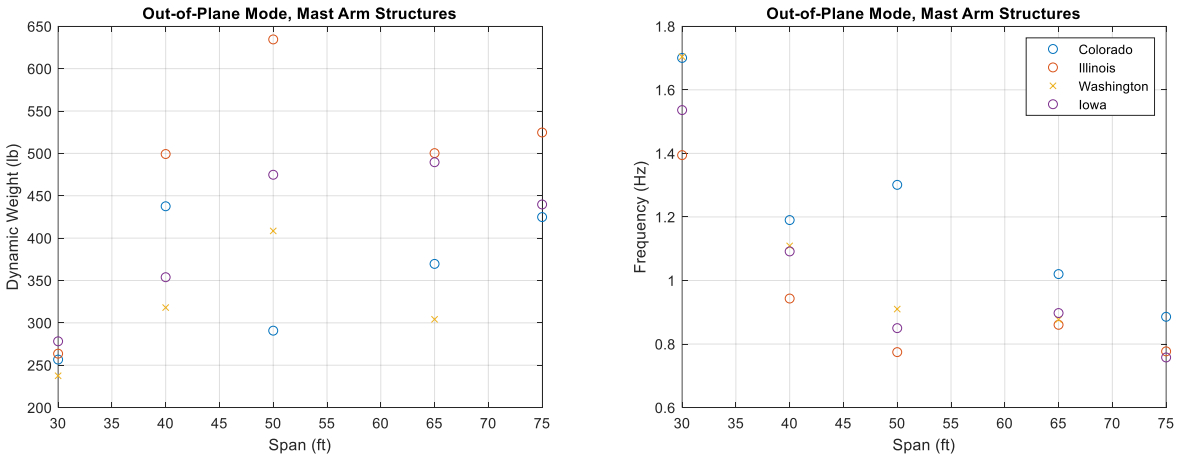

Figure 3.26 Traffic signal support structure out-of-plane dynamic properties: (a) mast arm length versus dynamic weight; and (b) mast arm length versus natural frequency

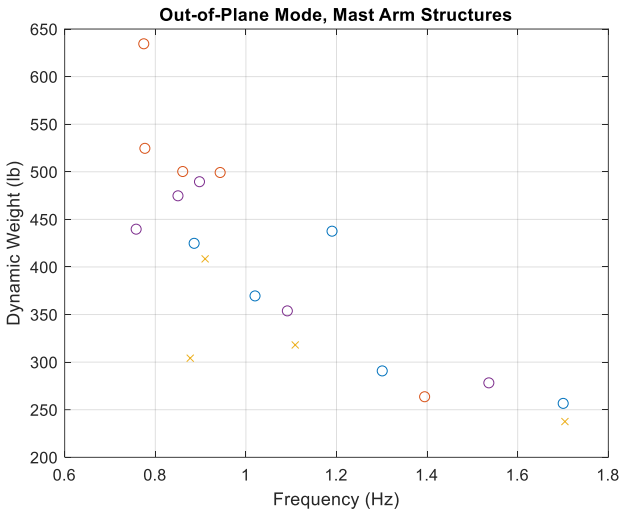

Figure 3.27 Traffic signal support structure out-of-plane natural frequency versus dynamic weight

Traffic Signal Support Structures Archetypes. Both in-plane and out-of-plane motion were characterized for short, mid and long mast arm traffic signal support structures. For the in-plane motion, the sample space considered was for natural frequencies from 0.8 Hz to 1.75 Hz and dynamic weights from 200 lbs to 650 lbs. Three typical dynamic properties for in-plane vibration of traffic signal support structures are identified in Table 3.5.

Table 3.5: Traffic Signal Support Structure Archetypes for In-Plane Vibration.

Descriptor	Dynamic Weight (lbs)	Frequency (Hz)
Short Mast Arm	300	1.4
Mid-Range Mast Arm (40’)	400	1.0
Long Mast Arm	600	0.8

For the out-of-plane motion, the sample space to be considered is for natural frequencies from 0.75 Hz to 1.75 Hz and dynamic weights from 200 lbs to 650 lbs. Three typical dynamic properties for out-of-plane vibration of traffic signal support structures, which happen to be the same as in-plane, are identified in Table 3.6.

Table 3.6: Traffic Signal Support Structure Archetypes for Out-of-Plane Vibration.

Descriptor	Dynamic Weight (lbs)	Frequency (Hz)
Short Mast Arm	300	1.4
Mid-Range Mast Arm (40’)	400	1.0
Long Mast Arm	600	0.8

3.3 Proposed Specific Criteria and Test Procedures

An effective vibration-mitigation device can be accounted for in the design process by reducing the fatigue demand through use of a response modification factor (R, or R-factor). In the previous section, 3.2, typical dynamic ranges of specific structure types were identified while in this section specific criteria and test procedures are proposed to evaluate vibration-mitigation devices for these structures. In this way, the complex behaviors of the interaction between the structure and the vibration-mitigation device can be accounted for in a simple manner when designing sign, luminaire, and traffic signal structures. The use of an R-factor to reduce fatigue demands in Section 11 requires that suitable testing and modeling of the device has been performed and documented by the device manufacturer (or other entity). The generalized steps required to apply the "R-factor" method are presented in this report. It is the responsibility of the entity performing the testing and developing the model to ensure that the testing and modeling are sufficient to suitably capture the effect of the vibration-mitigation device on structures; indicate the range of properties of structures to which the device and developed model are applicable; and provide the required information to the owner to account for device influence on behavior as utilized. Owner approval is required for the use of these devices in accordance with Section 11 and the AASHTO LRFD SLTS Specifications.

Because of the complexities associated with the general behavior of vibration-mitigation devices and potential difficulties in generating models which are fully consistent with the actual behavior, two approaches are proposed to develop the R-factors: 1) use of a validated model or 2) direct use of test data. The selected approach may influence the number of test data points required. The first approach involves validating a model and using that for development of the R-factors over the range of structure input parameters. Recognizing that modeling of vibration-mitigation devices with sufficient accuracy over a range of structure properties can be challenging for some devices, a second approach is available wherein the results of the physical testing are directly used to estimate the effect of the vibration-mitigation device on a range of structures. In the testing approach, damping values between test data points can be found using interpolation provided that the test points are spaced sufficiently close such that linear interpolation is an appropriate, or at least conservative, estimate of actual behavior. It is the responsibility of the entity performing the testing and documenting the results to indicate the range over which the use the provided data is applicable, and to ensure the provided data adequately captures the behavior over that range.

This research has developed a test procedure for evaluating the effectiveness of mechanical vibration-mitigation devices for structural supports of signs, luminaires, and traffic signals. At this time, aerodynamic vibration-mitigation devices are not included in the proposed test procedures and should not be evaluated using the process outlined in this report. The six-step process, illustrated in Figure 3.28, should be carried out and documented by the device manufacturer (or other entity) and the design structure designer.

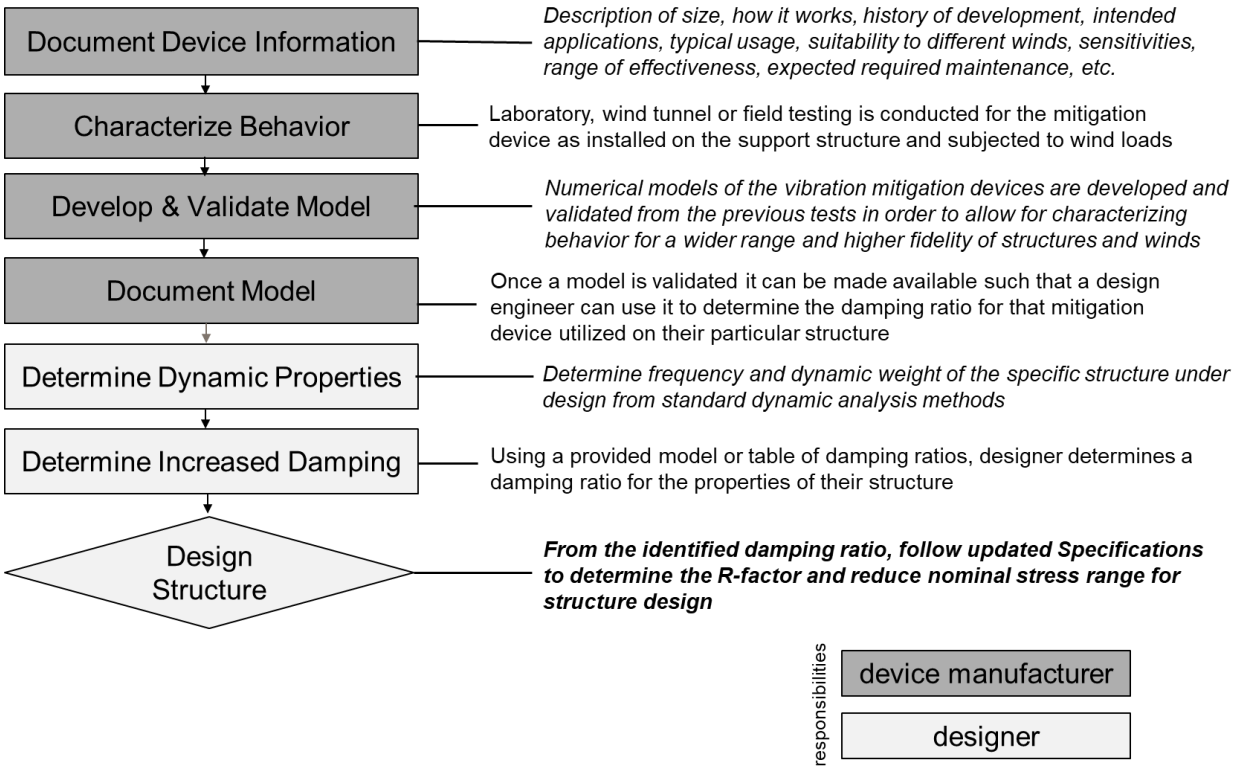

Figure 3.28: Proposed test procedure to evaluate effectiveness of vibration-mitigation devices.

The first four steps in this process should be carried out and documented by the device manufacturer (or other entity).

Step 1 – Document Device Information: The first step once a proposed vibration-mitigation device is identified is to gather information on the device critical to its performance in the field. For each device, information should be provided including (but not limited to) a description of the device's geometric and mass characteristics, the manner in which it provides damping, history of development, intended applications, typical usage (including attachment and placement details), device sensitivities, its suitability for use in mitigating vibrations caused by fatigue wind loading, the types of wind loading and directions of motion it is intended to mitigate against, the structure archetype(s) and range of characteristic properties for which the work is being developed, expected required maintenance over the lifetime of the device, and the anticipated test matrix and test protocols.

Device Description. The device information should include a device description consisting of the classification of the vibration-mitigation device as a vibration absorber or other; the physical characteristics of the device including size, materials and weight; and behavioral characteristics of the system including energy dissipation method(s); and attachment method(s). This description should also note any similarities to previously approved vibration-mitigation devices.

Intended Applications. The intended applications of the proposed vibration-mitigation device should be clearly identified, with regard to types of structures, as identified in

Section 1 of the AASHTO LRFD SLTS Specifications, and the wind load conditions, as identified in Section 3 of the AASHTO LRFD SLTS Specifications. Intended applications should be specific to types and sizes of structures, including specific types of Sign, Luminaire, Traffic Signal, and Combination Structures. Wind loading scenarios to be considered include Natural Wind Gust; Truck Induced Gust; Galloping; and Vortex Shedding. Any prior applications of the device to these or other structures and loads should be described with sufficient detail.

Design Requirements. It is anticipated that a class of vibration-mitigation devices will be provided as designs that owners can construct on their own. Alternatively, if a manufactured device is used then the design requirement information might be limited to a manufacturer and product number. In general, however, the design requirements will document the device components, including members and connections within the device, and the device properties that serve as reference values, and the criteria for determining and measuring these properties. The design requirements will describe the loading scenarios of the device (including multi-directional loading unless the combined effects are demonstrated to be unimportant), all expected device configurations, and any critical fatigue mechanisms of the device. The design requirements should document performance requirements of components of the device based on latest editions of applicable codes and standards, i.e., American Association of State Highway and Transportation Officials (AASHTO), American Institute of Steel Construction (AISC), American Society of Civil Engineers (ASCE), American Concrete Institute (ACI), etc.

Device Test Data. The device test data is any information pertaining to the device itself. This includes test data to validate material properties; document component behavior including strength and fatigue limits; establish performance acceptance criteria; or provide characteristics for calibrating the analysis models.

Step 2 – Characterize Behavior: The vibration-mitigation device is tested to determine the increased damping ratio of the structural system and the mitigation device's effect on the desired dynamic range of properties of target structures (e.g., various combinations of frequency and dynamic weight). Ranges of frequency and dynamic weight for different archetypes can be found in section 3.4 of this report. It is common and expected in structural dynamics that the increased damping a mitigation device can provide is highly dependent on the dynamic characteristics of the structure it is being attached to. In addition, amplitude of displacement is important for devices that result in nonlinear system behavior. Amplitudes of displacement should reflect displacements at which fatigue occur in critical structural elements or other maximum displacements as identified in the specifications, whichever is less.

The number of tests necessary to perform will depend on several factors, including the accuracy of any developed model and the behavior of the determined damping over the range of input parameters. The sensitivities of the device and archetypes the device may be applied to should be identified. While it is important to understand the behavior of the device itself, it is also critical to observe the behavior of the device as attached to the structure, so as to include any dynamic interaction between the two and verify performance. The device behavior should then be characterized using laboratory tests and/or field tests of the vibration-mitigation device as applied to a representative of the full structural system.

Device Sensitivities. Characterizing behavior includes identifying sensitivities of the device characteristics and its performance under various conditions, including wind or support types, velocity, displacement, or frequency, mass of the structure, location that the device is attached with respect to mode shapes, and coupled versus uncoupled response of the device to the wind and/or the structure.

Structural Archetypes. A key attribute to characterizing device behavior is identifying specific archetypes to which that behavior can be accurately characterized for. The archetypes might include sign, luminaire, traffic signal and combined structures. Sign structures include Overhead Balanced Cantilevers; Overhead Unbalanced Cantilevers; Overhead Cantilevers; Overhead Bridges; Overhead Bridges with Cantilever; Roadside Signs; and Sign Mounted on Grade Separation Structures. Luminaire support structures include Typical Poles with Luminaire Mounted at Pole Top; Typical Poles with Luminaire Arms - Balanced or Unbalanced; High-Level Luminaire Supports - Truss Type; and High-Level Luminaire Supports - Pole Type. Traffic signal support structures include Combination Cantilever Arm Mounted Luminaires and Traffic Signals; Cantilever Arm Mounted Traffic Signals (Balanced and Unbalanced); Pole Top-Mounted Traffic Signals; Bridge Mounted Traffic Signals; and Span Wire Mounted Traffic Signals.

Wind Loading. The wind loadings of interest can include Natural Wind Gust, Truck Induced Gust, Galloping, and Vortex Shedding.

Free Vibration Testing. The criterion to characterize behavior of the mechanical vibration-mitigation device from either laboratory or field testing for each of the wind loading conditions will be the measured damping ratio of the system. Further, the R-factor is determined in equation (2.10) from the damping ratio. The damping ratio is to be obtained from free vibration testing (a.k.a. pluck tests) using the classical logarithmic decrement method (Chopra, 2017), the energy dissipation per cycle method, or other methods rooted in structural dynamics theory. Following is a recommended procedure to conduct a free vibration test (both with and without the vibration-mitigation device) for luminaire, sign or traffic signal structures.

1. Instrument the structure with a sensor to measure the dynamic response (i.e., acceleration, strain or displacement) at a location that observes significant response (e.g., at the base for strain measurement; or at the free end or midspan for acceleration or displacement). This will ensure that the signal to noise ratio is sufficiently large to best observe the attenuation is the dynamic response. Do not let any cables hang off of the structure and they can add significant levels of damping, distorting the results. Sensor cables should be securely taped to the pole along the length until they can be transferred to the ground without any relative motion. Wireless sensors can alleviate this issue.
2. Collect data with an appropriate data acquisition system at a sufficiently large sampling rate to capture the dynamic response of the system (i.e., at sampling rates 10 to 100 times larger than the natural frequency of interest).
3. Excite the structure (i.e., by hand with an operator on a lift or in a bucket truck; or with an eccentric or linear mass shaker) at or near the natural frequency of interest and in the direction of motion to elicit a response in the structure near to the dynamic response of interest (i.e. first mode in-plane response of a sign or traffic signal support structure; first mode out-of-plane response of a sign or traffic signal support structure; or first or second mode response of a luminaire). Once the structure is moving at a sufficient amplitude, stop the forced excitation (i.e., remove one’s hands; or turn off the motion of the shaker).

4. Measure the response of the structure as it attenuates to a sufficiently small amplitude. Repeat tests 2-3 times to verify repeatability of the results.
5. In post-processing, use the classical logarithmic decrement method or the energy dissipation per cycle method to quantify the damping in the structure at the amplitudes of interest.

Step 3 – Develop and Validate Model: The intent is to not require experimental testing of all possible variations of structures, but to validate numerical models and use the numerical models to reliably predict the damping for design structures. Numerical models should be developed of the vibration-mitigation device as applied to specific archetypes and wind loading. Models may be as simple or as complex as necessary (e.g., dynamic or static, single or multi-degree-of-freedom, linear or nonlinear) to effectively capture the effect of the mitigation device on the structure archetype being examined.

Once the model is developed and refined, the resulting damping values of the tested structure with mitigation device are compared with those found from the analytical model. When the magnitude of the difference between the model- and test-determined damping is greater than +/-20%, it is suggested that the model be reworked to better approximate the effect of the vibration-mitigation device on the structure's behavior. The percent difference values for damping between the test and model are to be provided in the documentation.

If consistency between the model and test data cannot be effectively accomplished, then the approach of directly using test values (with sufficient test data such that interpolation between data points is appropriate) is recommended. Additional test points may be necessary to ensure the behaviors are suitably captured over the range of properties for which the mitigation device is intended for use on. It is critical if only test data is used that the test points be selected with fine enough resolution that decreased performance between points is ruled out and over a large enough range that results are interpolated and not extrapolated.

Step 4 – Document Model: Once a model is validated it can be made available such that a design engineer can use it to determine the damping ratio for that mitigation device utilized on their design structure. Alternatively, the damping ratio values found from the model or testing can be provided as a matrix of values for the input parameters. It is the responsibility of the entity performing the testing and developing the model to ensure that the model or results values are appropriate over the range of input properties specified.

The remaining two steps in the process are carried out by the designer. These steps will typically be carried out at a later date, at the time that a specific structure is to be designed – during the structural design process identified subsequently.

Step 5 – Determine Dynamic Properties of Design Structure: Typically, the structure dynamic properties needed are the frequency and dynamic weight (note: dynamic weight is different, and less, than the total weight of the structure, as identified subsequently in Section 3.3). These properties are developed for the in-plane and/or out-of-plane behavior depending on the fatigue wind load being mitigated against.

Step 6 – Determine Damping Ratio of Design Structure: Using the provided model or a table of damping ratios for a specific device as provided by the device manufacturer (or other entity), the designer determines a damping ratio for the properties of their structure. The effect of potential changes to the structure over its lifetime (e.g., adding or removing of signs, signals, etc.) are incorporated at this stage, by determining the minimum damping ratio within a range of input parameters centered on the values determined in Step 5. For the typical case of utilizing frequency and dynamic weight, the ranges examined are Frequency: +/-10%; Dynamic Weight: +/-20%.

The damping ratio of a single structure will potentially be different for the four different types of wind conditions (i.e., truck gust (TrG), natural wind gust (NWG), combined wind on high-mast towers (HMT) and galloping induced vibration (GVW)). Note that while vortex induced vibration (VVW) is listed in Table 3.4-1 of the Specifications, it is not considered in the LRFD Specifications outside of the combined loading on high mast towers (HMT). The type of wind condition will lead to a specific response and corresponding increased damping ratio. For example, TrG and GVW will result in the first mode in-plane response of sign and traffic signal support structures, while NWG will result in the first mode out-of-plane response of sign and traffic signal support structures. A device such as a Stockbridge damper may provide similar, but likely different, performance since the natural frequency and dynamic weight of the same structure in these two modes of vibration (in-plane and out-of-plane) will be different. A device such as the Valmont TR-1 damper will only provide damping in the in-plane mode of vibration and thus will have damping for TrG and GVW but zero effect (R=1) for NWG.

3.4 Proposed Structural Design Process

The proposed structural design process is consistent with the AASHTO LRFD SLTS Specifications, for considering the effectiveness of these devices in the design process of the structural supports. This procedure for the design of new structures is a simplified analysis which accounts for the complex dynamic behaviors of the interaction of the structure and the vibration-mitigation device. Much of the design will be similar to the current practice, with the proposed updated AASHTO LRFD SLTS Specifications for the vibration-mitigation devices. Currently when performing the fatigue checks, if the nominal wind-induced stress range is found to exceed the CAFT, the designer needs to modify the geometry or member thicknesses in order to reduce the nominal stress range. In lieu of this, the designer would now have the option of selecting a vibration-mitigation device to achieve an acceptable design. Once the design is complete, the other concerns of the owners can be considered, including cost maintenance, aesthetics, etc.

For vibration-mitigation devices used to reduce fatigue demands of new structures (as described in Section 11 of the AASHTO LRFD SLTS Specifications), the manufacturer (or entity which has performed the necessary testing) shall provide the information required to account for their influence on behavior as utilized in the specifications. If approved by the owner, the use of a mitigation device to reduce fatigue demands of new structures can be included in the design. This is done through revising equations 11.5-1, 11.5.1-1, 11.9.3-1 and C.3-1 in the AASHTO LRFD SLTS Specifications, and corresponding descriptions, to include a response modification factor, R, to account for the effect of a vibration-mitigation device for a specific wind loading, defined in Article 11.8 of the AASHTO LRFD SLTS Specifications.

$$\gamma\left(\frac{\Delta f}{R}\right) \leq \phi(\Delta F) \qquad \text{(11.5-1, AASHTO LRFD SLTS Specifications)}$$

$$\gamma\frac{(\Delta f)_n}{R} \leq \phi(\Delta F)_n \qquad \text{(11.5.1-1, AASHTO LRFD SLTS Specifications)}$$

$$\gamma\frac{(\Delta f)_n}{R} \leq \phi(\Delta F)_n \qquad \text{(11.9.3-1, AASHTO LRFD SLTS Specifications)}$$

$$\frac{(\Delta f)_l}{R} \leq (\Delta F)_l \qquad \text{(C.3-1, AASHTO LRFD SLTS Specifications)}$$

where γ is the load factor defined in Table 3.4-1, $(\Delta f)_n$ is the wind-induced nominal stress range defined in Article 11.9.2, $(\Delta F)_n$ is the nominal fatigue resistance as specified Article 11.9.3, φ is the resistance factor and is equal to 1.0 for fatigue loading, and R is the response modification factor, developed as suggested in this research. A vibration-mitigation device can be used to reduce demand (on the left-hand side of equations 11.5-1, 11.5.1-1, 11.9.3-1 and C.3-1) as an alternative to modifying the structural details to provide increased resistance (on the right-hand side of equations 11.5-1, 11.5.1-1, 11.9.3-1 and C.3-1) in cases where the fatigue demand exceeds the fatigue resistance.

When a vibration-mitigation device approved for design of new structures by the owner is present, the response modification factor, R, shall be determined by the designer for truck gust (TrG), natural wind gust (NWG), combined wind on high-mast towers (HMT), and galloping induced vibration (GVW) in a proposed equation 11.8.2-1 in the AASHTO LRFD SLTS Specifications:

$$R = \begin{cases} \gamma_R \frac{\zeta_c}{\zeta_u} & for\ R > \Psi_R \\ 1 & otherwise \end{cases} \qquad \text{(11.8.2-1, } \textit{AASHTO LRFD SLTS Specifications}\text{)}$$

where: γ_R is a multiplier to account for the uncertainty in the prediction of the vibration-mitigation device performance, ζ_c is the damping ratio of the structure including the vibration-mitigation device determined as described in the product documentation identified in the test procedure for evaluating the effectiveness of vibration-mitigation devices; and ζ_u is the damping ratio of the structure without the vibration-mitigation device (equal to 0.2% unless published experimentally determined values for the specific structure type being examined are available). The minimum required value Ψ_R accounts for further uncertainty in the process. For each device, testing is required that either directly provides ζ_c values for a range of properties of the intended structural system or provides an analytical model which the designer can utilize to determine ζ_c for their specific structure. When R, in equation 11.8.2-1 of the AASHTO LRFD SLTS Specifications, falls below Ψ_R, a value of 1.0 shall be used for R instead. If no vibration-mitigation device is utilized a value of 1.0 shall be used for R. As a result of this research, the multiplier γ_R is set to $\gamma_R = 0.6$, and the minimum required value Ψ_R is set to $\Psi_R = 3.0$. These values are determined based on engineering judgment of the team, considering the variability of data, and the need for a non-marginal effect of the mitigation device. It should be noted that since the structure's dynamic response is directly proportional to the stress range, requiring a minimum response modification factor of 3.0 is equivalent to requiring the resulting stress range be reduced to less than 0.33 (1/3.0) for the vibration mitigation device to be considered for that wind load.

The design process for a vibration-mitigation device is illustrated in Figure 3.29.

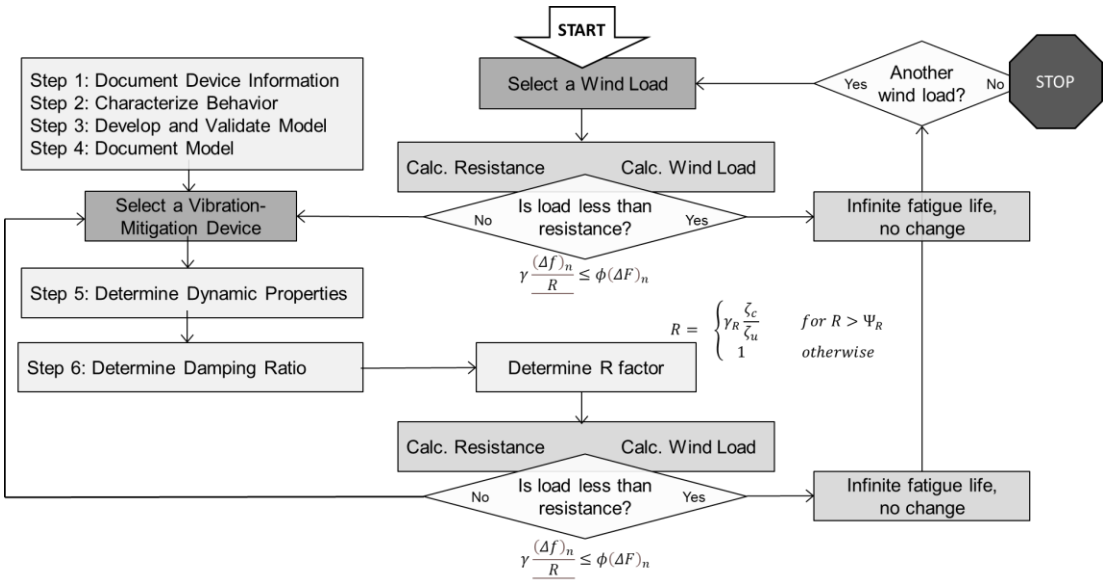

Figure 3.29. Schematic of the design process.

CONCLUSIONS AND SUGGESTED RESEARCH

The current AASHTO LRFD Specifications for Structural Supports for Signs, Luminaries, and Traffic Signals (AASHTO LRFD SLTS Specifications) addresses potential failure due to wind vibrations by requiring members and connections to have nominal strengths in excess of the expected loadings by a sufficient margin to reduce risk of failure to an acceptable amount (AASHTO, 2013). The AASHTO LRFD SLTS Specifications indicate that in lieu of designing to resist periodic galloping forces, effective vibration-mitigation devices can be implemented. This research identified test methods and procedures for evaluating the effectiveness of vibration-mitigation devices for structural supports of signs, luminaires, and traffic signals and propose a procedure for considering the effectiveness of these devices in the design process of the structural supports. The evaluation of effectiveness of vibration mitigation devices is primarily intended to reduce fatigue loads specified in AASHTO LRFD SLTS Specifications but can also be applied for excessive vertical deflections resulting from galloping wind loads. These procedures are appropriate for potential incorporation into the AASHTO LRFD SLTS Specifications.

3.5 General Conclusions

An effective vibration-mitigation device can be accounted for in the design process by reducing the fatigue demand through use of a response modification factor (R, or R-factor). Additionally, excessive vertical deflections resulting from galloping wind loads can also be accounted for through the use of a response modification factor. In this way, the complex behaviors of the interaction between the structure and the vibration-mitigation device can be accounted for in a simple manner when designing sign, luminaire, and traffic signal structures.

The use of an R-factor to reduce fatigue demands in Section 11 of the AASHTO LRFD SLTS Specifications requires that suitable testing and modeling of the device has been performed and documented by the device manufacturer (or other entity). The generalized steps required to apply the “R-factor” method are described below. It is the responsibility of the entity performing the testing and developing the model to ensure that the testing and modeling are sufficient to suitably capture the effect of the vibration-mitigation device on structures, indicate the range of properties of structures to which the device and developed model are applicable, and provide the required information to the owner to account for device influence on behavior as utilized. Additionally, owner approval is required for the use of these devices in accordance with Section 11 of the AASHTO LRFD SLTS Specifications.

Because of the complexities associated with the behavior of the vibration-mitigation device and potential difficulties in generating models which are fully consistent with the actual behavior, two approaches are available to develop the R-factors: 1) use of a validated model or 2) direct use of test data. The selected approach may influence the number of test data points required. The first approach involves validating a model and using that for development of the R-factors over the range of structure input parameters. Damping values between test data points can be found using interpolation provided that the test points are spaced sufficiently close such that linear interpolation is an appropriate, or at least conservative, estimate of actual behavior. It is the responsibility of the entity performing the testing and documenting the results to indicate the range over which the use the provided data is applicable, and to ensure the provided data adequately captures the behavior over that range.

This research has developed a test procedure for evaluating the effectiveness of mechanical vibration-mitigation devices for structural supports of signs, luminaires, and traffic signals. The

six-step process should be carried out and documented by the device manufacturer (or other entity) and the design structure designer. These steps include documenting the vibration-mitigation device general information; characterizing the dynamic response reduction behavior of the device; developing and validating models of the device; documenting the vibration-mitigation device model; and then as part of the design process, determine that design structure's dynamic properties; and lastly to determine increased damping ratio of the structure with the applied vibration-mitigation device, for a specific wind loading.

This research also proposed a procedure, consistent with the AASHTO LRFD SLTS Specifications, for considering the effectiveness of these devices in the design process of the structural supports. This procedure for the design of new structures is a simplified analysis which accounts for the complex dynamic behaviors of the interaction of the structure and the vibration-mitigation device. The use of a mitigation device to reduce fatigue demands of new structures are included in the design, through revising equations 11.5-1, 11.5.1-1, 11.9.3-1 and C.3-1 in the AASHTO LRFD SLTS Specifications to include a response modification factor, R, to reduce demand (on the left-hand side of the equations) as an alternative to modifying the structural details to provide increased resistance (on the right-hand side of the equations) in cases where the fatigue demand exceeds the fatigue resistance. Excessive vertical deflections of cantilevered single-arm sign supports and traffic signal arms and non-cantilevered supports resulting from galloping wind loads may be reduced through the use of a mitigation device and use of the response modification factor, R.

When a vibration-mitigation device approved for design of new structures by the owner is present, the response modification factor, R, shall be determined by the designer for Galloping, Natural Wind Gust, Truck-Induced Gust, and High-Mast Wind-Induced Vibrations in a proposed equation in the AASHTO LRFD SLTS Specifications and applied to the design in a similar manner as done currently.

3.6 Suggested Research

This final report provides a test procedure to evaluate performance and a corresponding design procedure for mechanical vibration-mitigation devices. Future research is suggested to identify methods to evaluate aerodynamic vibration-mitigation devices. An aerodynamic flat-plate damper was studied extensively as part of this research, conducting field and wind tunnel testing. This findings of the NCHRP 12-111 project were only able to provide damping results for this aerodynamic damper for vortex induced vibration. It should be noted that vortex induced vibration is not included in the current specifications and so the results from this project have no applicability to the current AASHTO LRFD SLTS Specifications as they currently exist. The field tests conducted in this study observed only vortex induced vibration with no galloping observed (for both the uncontrolled and controlled traffic signal support structures on multiple length mast arms). In fact, vortex induced vibration was only observed in some cases as well, not present even without the mitigation device installed. The wind tunnel tests were ultimately only able to be conducted at small amplitudes, at amplitudes indicative of vortex induced vibration. The results of this research do not provide insight for galloping, natural wind or truck gust wind loads. A method to evaluate aeroelastic damping was proposed and demonstrated in the NCHRP 12-111 research and the aeroelastic damper damping is shown to be a function of mast arm configuration, wind direction and speed. However, no conclusions can be drawn from the research to propose a test method or design procedure for aeroelastic dampers for galloping, natural wind or truck gust wind loads. It is recommended that a research project be conducted to identify methods to evaluate aerodynamic vibration-mitigation devices.

As related, further exploration of the role of vortex induced vibration (VIV) versus galloping wind loading should be conducted. The vortex induced vibration was observed in this project, however, it is not an identified wind loading in the current AASHTO LRFD STS Specifications.

Research is suggested to focus on better understanding and quantifying the uncertainty in the process to quantify vibration-mitigation device performance and the resulting design process. Currently the predicted dynamic properties of the support structure are considered to have errors of 10%-20%, response modification factor is reduced by a multiplier of 0.6; and the minimum response factor is set to 3.0. These are all based on the engineering judgement of the project team and the findings in the various examples examined over the course of the project. The conservativeness of these factors can be verified and/or reduced pending further directed research to examine uncertainty, including device performance over the life of the structure; predicting effectiveness of the vibration-mitigation device; and assumptions and accuracy of dynamic modeling of structural supports for signs, luminaries, and traffic signals.

Further exploration on advanced testing methods, such as the proposed real-time hybrid substructuring also known as real-time hybrid simulation (RTHS) (Saouma and Sivaselvan, 2008) examined in this research should be further explored. RTHS is a cyber-physical method of testing that provides the capability to isolate and physically test the critical components of a mechanical system, similar to the blocked component level test, while including the full dynamic interaction with a numerical representation of the support structure. RTHS shows promise to accurately represent the dynamics of multiple support structures in an efficient and timely manner. The results of RTHS were validated only for a single light pole test in this project and stability and accuracy issues need to be fully explored for luminaire, sign and signal support structures.

Finally, the archetypes in this study are determined based on State responses using various versions of the specifications. This provides a reasonable broad range, however, as States transition to using AASHTO LRFD SLTS, these dynamic properties should be updated accordingly.

REFERENCES

AASHTO (2015) “LRFD Specifications for Structural Supports for Highway Signs, Luminaires, and Traffic Signals”, First Edition 2015, LRFDLTS-1.

AASHTO (2015b) “Standard Specifications for Structural Supports for Highway Signs, Luminaires, and Traffic Signals, 6th Edition, with 2015 Interim Revisions

AASHTO (2013) “Standard Specifications for Structural Supports for Highway Signs, Luminaires, and Traffic Signals, 6th Edition, 2013

AASHTO (2011) “Standard Specifications for Structural Supports of Highway Signs, Luminaires, and Traffic Signals, 5th Edition, 2010/2011

AASHTO (2006) “Standard Specifications for Structural Supports for Highway Signs, Luminaires and Traffic Signals, 4th Edition, 2002/2003/2006

AASHTO (1994) “Standard Specifications for Structural Supports for Highway Signs, Luminaires and Traffic Signals, 3rd Edition, 1994

ASCE (2010) “Minimum Design Loads for Buildings and Other Structures”, ASCE/SEI Standard 7-10.

Bendat, J. S., Piersol, A. G. (2010) “Random Data: Analysis and Measurement Procedures”. Fourth edition. John Wiley & Sons.

Caracoglia, L. and Jones, N. (2007) “Numerical and experimental study of vibration-mitigation for highway light poles” Engineering Structures, 29, 821-831.

Chopra, A.K. (2017) “Dynamics of Structures, Theory and Applications to Earthquake Engineering, 5th Edition”, Prentice Hall, Englewood Cliffs, New Jersey.

Christenson, R. (2011) “Reducing Fatigue in Wind-Excited Traffic Signal Support Structures using Smart Damping Technologies”, NCHRP-IDEA Program Project Final Report

Connor, R.J., Collicott, S.H., DeSchepper, A.M., Sherman, R.J., Ocampo, J.A., 2012. NCHRP Report 718: Fatigue loading and design methodology for high-mast lighting towers. Transportation Research Board of the National Research Academies, Washington, D.C.

Cook, R.A., Bloomquist, D., Richard, D.S. and Kalajian, M.A. (2001), “Damping of Cantilevered Traffic Signal Structures”, Journal Structural Engineering, 127(12), 1476-1483.

Cook, R.A., Bloomquist, D., Richard, D.S., Kalajian, M.A., Cannon, V.A., Arnold, D.P., and Ansley, M.H. (2000), “Design, Testing, and Specification of a Mechanical Damping Device for Mast Arm Traffic Signal Structures”, Final Project Report, UF PProject No. 4910 45 04 680 12, Structures and Materials Research Report No. BC-050.

CSI. (2021). “SAP2000 Integrated Software for Structural Analysis and Design”. Computers & Structures Inc., Berkeley, California.

Dexter, R.J. and Ricker, M.J. (2002) “NCHRP Report 469: Fatigue-Resistant Design of Cantilevered Signal, Sign and Light Supports”, Transportation Research Board, National Research Council, Washington D.C.

Dubbs, N.C. (2018) “Comparison of Modal Testing Approaches for a Light Pole Exhibiting Fatigue Failure due to Vortex Shedding”, IMAC Conference Proceedings, Orlando, FL, February 2018.

FEMA. 2009. Quantification of Building Seismic Performance Factors. FEMA P-695.

FEMA. 2015. QNEHRP Recommended Seismic Provisions for New Buildings and Other Structures. FEMA P-1050-1.

Fernandez, R., Abolmaali, A., Kamangar, F. and Le, T. (2009) “Analysis and Development of a Passive Mechanical Vibration Abatement Device for Traffic Monitoring Cameras”, Journal of Transportation Engineering, 135(5), 270-278.

Foutch, D.A., Rice, J. A., LaFave, J. M., Valdovinos, S., Kim, T. W. (2006). “Evaluation of Aluminum Highway Sign Truss Designs and Standards for Wind and Truck Gust Loadings”. Report No. FHWA/IL/PRR 153. University of Illinois at Urbana-Champaign; Bureau of materials and Physical Research, Illinois Department of Transportation.

Hamilton, H.R, G.S. Riggs, and J.A. Puckett. Increased Damping in Cantilevered Traffic Signal Structures. Journal Structural Engineering, Vol. 126, Issue 4, April 2000, pp. 530-537

Hoque, S., and R. E. Christenson (2011) “Reducing Fatigue in Wind–Excited Traffic Signal Support Structures Using an Innovative Vibration Absorber”, Transportation Research Record: Journal of the Transportation Research Board, No. 2251, Transportation Research Board of the National Academies, Washington, D.C., 2011, pp. 16-23.

Jo, I., Kaneko, T., Nagatsu, S., Takahashi, C. and Kimura, M. (1989) “Development of highway light pole with resistance to wind vortex-induced oscillations”, Technical Report 21, Kawasaki Steel Corporation.

Lengel, J.S. and Sharp, M.L. (1969). “Vibration and damping of aluminum overhead sign structures”, Highway Research Record, Issue Number: 259, 51-60.

Li, L., Song, G., Singla, M. and Mo, Y.-L. (2015) “Vibration control of a traffic signal pole using a pounding tuned mass damper with viscoelastic materials (II): experimental verification”, Journal of Vibration and Control, Vol. 21(4), 670-675.

Marra, A. M., Mannini, C., Bartoli, G. “Measurements and improved model of vortex-induced vibration for an elongated rectangular cylinder”. Journal of Wind Engineering and Industrial Aerodynamics. https://doi.org/10.1016/j.jweia.2015.08.007

McDonald, J.R., Mehta, K.C., Oler, W. and Pulipaka, N. (1995), “Wind Load Effects on Signs, Luminaires, and Traffic Signal Structures”, Report 1303-F, Prepared for Texas Department of Transportation.

McManus, P.S., H.R. Hamilton, and J.A. Puckett. Damping in Cantilevered Traffic Signal Structures under Forced Vibration. ASCE Journal of Structural Engineering, Vol. 129, No. 3, March 2003, pp. 373-382.

Premount, A., Seto, K. (2008). “Active Control of Structures”. John Wiley & Sons. ISBN: 978-0-470-03393-7

Puckett, J.A., Garlich, M.G., Nowak, A.A., Barker, M. (2014). “Development and Calibration of AASHTO LRFD Specifications for Structural Supports for Highway Signs, Luminaires, and Traffic Signals”.

Pulipaka, N., Sarkar, P.P. and McDonald, J.R. “On galloping vibration of a traffic signal structures”, Journal of Wind Engineering and Industrial Aerodynamics, 77&78 (1998), 327-336.

Rice, J.A. and Foutch, D.A. (2006) “Passive damping strategies for highway sign structures”, Proc. Fourth World Conference on Structural Control and Monitoring, San Diego, CA.

APPENDIX I: Examples

This appendix provides examples of the six-step process to evaluate the effectiveness of a mechanical vibration-mitigation device and use the results to design a traffic signal support structure with a vibration-mitigation device. The examples include three mechanical vibration-mitigation devices, denoted Damper A, Damper B and Damper C.

The Damper A is shown as an example for Steps 1-3. This example shows that forced vibration is time consuming and may not be accurate measures of performance if the excitation is not within a small tolerance of the frequency. This example also describes a highly nonlinear physics/energy based numerical model of a vibration-mitigation device. The numerical model is observed in Step 3 to have modeling errors greater than 20%.

The Damper B is shown as an example for Steps 1-2. The damper behavior was characterized in the frequency domain. This proved problematic as the amplitude dependence rendered any models inaccurate. This example demonstrated the challenge of a FRF to characterize damper performance and behavior. Consistent with the findings of prior researchers, some devices may not lend themselves to be characterized and modeled. This example led to an exemption whereby in lieu of a model, device manufactures can use actual test results, over an extensive range and with sufficient resolution in test points.

The third example, Damper C, provided a good example for Steps 1-6. This example shows how free vibration testing can be used effectively to measure the improved damping ratio of the structural support with vibration-mitigation device. This section also outlines the development of a physics-based model that can accurately capture performance. The section determines an R-factor and completes a design of a traffic signal support structure.

Step 1 – Document Device Information:

Damper A

Device Description. The Damper A is described in the United States Patent 6,234,286 B1 (Date of Patent May 22, 2001). A picture of the unit along with drawings from the patent are provided in Figure A.1.

(a) *(b)*

Figure A.1: Damper A images: (a) picture of damper tested at UConn; and (b) patent drawings for United States Patent 6,234,286 B1.

The Damper A vibration-mitigation device is classified as a vibration absorber. The device has an aluminum cylindrical housing that contains a solid steel rod that moves inside the housing when the pole vibrates. The housing is aluminum and is 14 inches in length with a 3 inch inside diameter. The steel bar is 10 inches in length with a 1-inch diameter. The entire unit weights 7 lbs. The energy dissipation mechanism is through impact, when the solid steel bar impacts the wall of the cylindrical housing. The mass of the steel bar that impacts is 0.0146 lbs-sec^2/in (5.65 lbs). Rubber caps are placed on each end of the rod and serve to dissipate energy during impact of the rod against the housing. The cylindrical housing is bolted to the inside of the pole structure, or onto the outside of the pole structure.

Intended Applications. The original intended application of this vibration-mitigation device is to reduce second mode vibration in luminaire structures, typically 10-30 feet in height. For the purpose of this study, the device will be applied to larger high mast pole structures. The combined wind loading is considered to be: Natural Wind Gust; Galloping; and Vortex Shedding. It is noted that this device is intended to be used for light poles under 50 feet in height and not for application to a high mast light pole.

Design Requirements. The device considered is commercially available. (Note, that while commercially available for second mode light pole damping, this example applies the damper to first mode vibration-mitigation.)

Device Test Data. Device test data is not available for Damper A.

Damper B

Device Description. Damper B is also commercially available. The manufacturer of Damper B states that the damper offers the most practical and economical solution for vibration problems normally encountered in highway sign trusses. The damper, weighing 31 lbs. (14.06 kg), is 22.5 in. in length and contains two 4.12 in diameter weights attached to the end of a wire rope strand. The specific Damper B used is the size most commonly used for highway truss applications.

A picture of the unit installed on a bridge-type sign structure provided in Figure A.2.

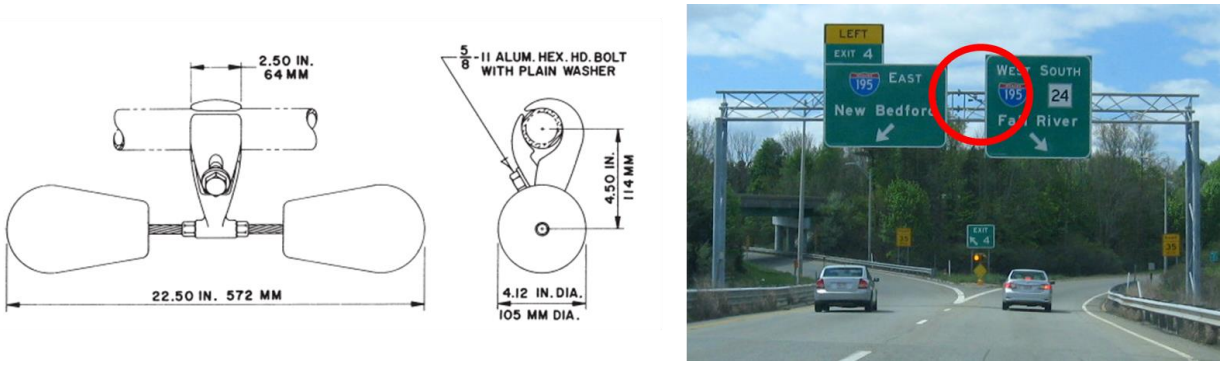

(a) *(b)*

Figure A.2: Damper B images: (a) schematic of damper from the manufacturer; (b) picture of a Damper B-type damper installed on a highway sign structure.

The Damper B vibration-mitigation device is classified as a vibration absorber. The device has two weights that are suspended by a steel wire rope that provides stiffness in both the in-plane and out-of-plane motion when installed horizontally on a sign structure. The damper bracket is installed directly to a truss member on the sign structure.

Intended Applications. As stated by the manufacturer: A single damper located at the mid-point of the truss will provide vibration protection for lengths between 60 and 140 ft (18.3-42.7 m). Special consideration should be given to longer spans or cantilever applications.

Design Requirements. The device considered is a commercially available highway truss vibration damper.

Device Test Data. Device test data is not available for Damper B. However, literature is available on performance of the effectiveness of these dampers in mitigating excessive structural vibrations and preventing fatigue (Bridge, et., al, 2017). This publication notes that the device performance is highly dependent on the dynamic characteristics of both the damper and the structure and that the expected amplitude of vibration should be considered as the damper is both frequency and amplitude dependent.

Bridge, Jennifer & LaFave, James & Foutch, Douglas & Abdullah, A.B.M.. (2017). Passive Vibration-mitigation for Highway Sign Trusses Susceptible to Wind-Induced Vibrations. Journal of Performance of Constructed Facilities. 31. 04017091. 10.1061/(ASCE)CF.1943-5509.0001076.

Damper C

Device Description. The device considered is commercially available and intended to effectively reduce vertical mast arm vibrations caused by wind vortex shedding, galloping, and truck gusts. A picture of the unit along with drawings from the patent are provided in Figure A.3.

The Damper C is classified as a vibration absorber. The device consists of a 4.5” diameter by 43” long tube that is attached near the end of the mast arm, often hidden from view by signals or signs mounted on the mast arm, with a total weight of 35.75 lbs. The Damper C energy dissipation is through both eddy current damping and pneumatic damping. The eddy currents are circular electric currents induced within conductors by the movement of a magnet next to the conductive material. These circular currents are opposite the direction of movement creating a resistance and thus damping. The pneumatic damping occurs as the damper mass translates up and down within a sealed chamber. The exchange of air from the upper air chamber to the lower air chamber creates velocity dependent resistance.

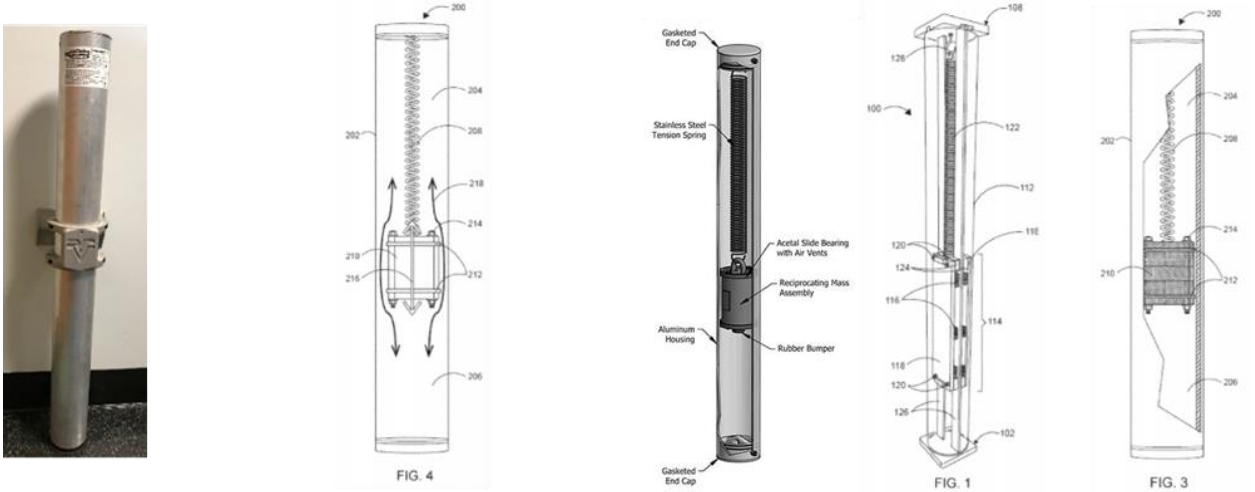

(a) *(b)* *(c)*

Figure A.3: Damper C images: (a) picture of damper; and (c) patent drawings for United States Patent 9,470,288.

Intended Applications. The intended application of this vibration-mitigation device is to reduce first mode in-plane (vertical) mast arm vibrations caused by wind vortex shedding, galloping, and truck gusts for cantilevered traffic signal support structures. The wind loading considered in the Specifications for this type of structure includes galloping and truck induced gusts.

Design Requirements. The device considered is commercially available.

Device Test Data. The Damper C device itself has been tested directly at the manufacturer for component wear and performance degradation. As noted by the manufacturer, the damper requires little to no maintenance over the life of the pole structure and has been tested to over

17.8 million large amplitude cycles, simulating extreme vertical galloping motion (58-inch peak-to-peak arm end displacement) with no observable degradation in the unit or the performance of the damper. Under normal operation conditions, the damper should surpass the design life of the traffic signal structures.

Additionally, the Damper C has been installed in the field since 2016 (June 2016 City of Omaha, NE; August 2016 State of Utah; November 2016 City of Seattle, WA) with minimal issues as reported by the manufacturer or owner. The device has been on the market as a commercial product for over seven years.

Step 2 – Characterize Behavior:

Damper A

Laboratory tests are used to test the vibration-mitigation device. A cantilevered pole structure was mounted horizontally in the laboratory at the University of Connecticut, due to height constraints in the laboratory. The pole is excited in the horizontal plane and vibrates horizontally. The Damper A is typically mounted vertically on a vertical pole. In this configuration the steel rod inside sits on the bottom end of the rod and length of the rod impacts the wall of canister. For the horizontally oriented pole in the laboratory, the impact damper was attached to the pole still oriented vertically. In such an orientation, the damping and impact mechanism remains unchanged. The luminaire support was a 20 ft round aluminum pole, 6 inches in diameter, tested in the Structures Research Laboratory at the University of Connecticut, as shown in Figure A.4.

Device Sensitivities. Device must be mounted vertically and is typically attached at approximately 2/3 the height of the pole for effectiveness in multiple modes (first and second). The device is nonlinear and amplitude dependent. At large amplitudes, the steel rod impacts both sides of the aluminum tube and dissipates energy at varying levels. At low amplitudes, the rod does not impact, and energy is not dissipated (i.e., no damping occurs). The characterization of this device included amplitude dependence.

(a) *(b)* *(c)*

Figure A.4: Experimental Light Pole Test at UConn: (a) pole mounted horizontally in Structures Research Laboratory; (b) linear mass shaker mounted at tip of pole; and (c) Damper A mounted vertically at 2/3 length of pole.

Structural Archetypes. The Damper A is typically applied to Luminaire support structures, specifically, Typical Poles with Luminaire Mounted at Pole Top.

Wind Loading. Combined loading of luminaires which can include Natural Wind Gust, Galloping, and Vortex Shedding.

Laboratory Forced Vibration Testing. The pole structure was mounted to a fixed base in the laboratory. The Damper A was placed 2/3 of the length of the pole, at a distance of 13 feet 4 inches from the base, mounted vertically. A triaxle accelerometer, PCB 356A17 triaxial accelerometer with a 10g, sensitivity of 500 mV/g and frequency range from 0.5 – 3000 Hz, was placed at the location of the damper on the pole to measure the acceleration response of the pole.

A linear shaker was used to provide a point load excitation to represent a sinusoidal combined wind excitation. The Quanser Shake Table I-40 was used as a linear actuator to conduct the forced vibration tests. The shaker unit weighs in total 13 lbs. (5.88 kg) with the moving portion in the orientation used for these tests weighing 11.46 lbs. The load sits on top of a low backlash linear guide with a total travel of ± 0.787 inch and can be accelerated up to 1 g using a high torque direct drive motor. The linear actuator utilizes a Quanser power amplifier, data acquisition card and a PC running Quarc control software to provide a desired sinusoidal amplitude and frequency.

Free vibration tests with and without an additional mass placed at the damper location are collected to identify the natural frequency, stiffness and damping ratio. The free vibration time history responses are shown in Figure A.5.

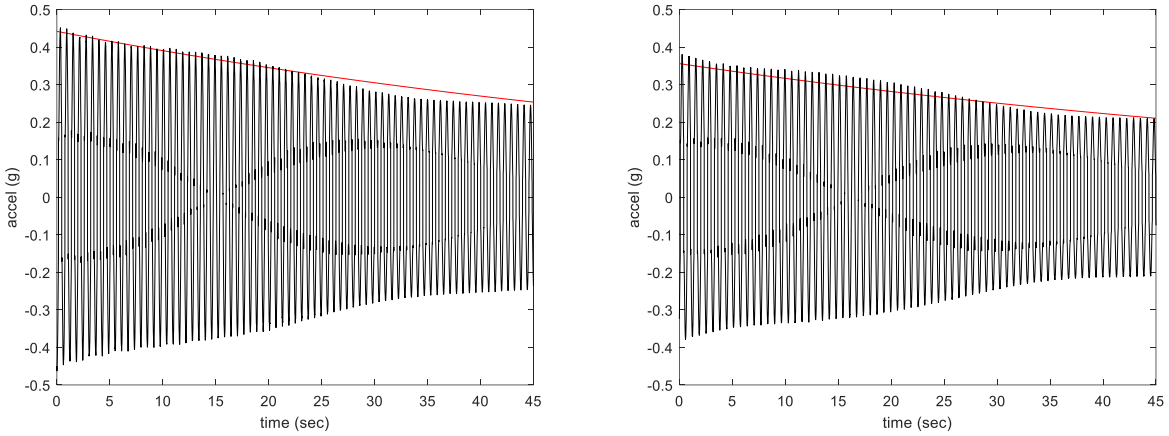

(a) (b)

Figure A.5: Free vibration time history response for: (a) original light pole; and (b) light pole with 15 lbs. added at 2/3 length of pole.

From the free vibration plots, the i^{th} natural frequency, f_i, was determined as

$$f_i = \frac{n}{T_n} \tag{A.1}$$

where n is the number of oscillations and T_n is the time for the n oscillations. The natural frequency of the light pole, f_1, was observed to be 1.64 Hz. With the addition of 15 lbs ($\Delta m = 0.0388$ lbs-sec^2/in, where g is 386.4 in/sec^2) at a length of 2/3 the length of the pole, where the impact damper was to be installed, the natural frequency, f_2, was reduce to 1.54 Hz. The circular natural frequency ($\omega_i = 2\pi f_i$) is related to the mass and stiffness as

$$\omega_1{}^2 = \frac{k}{m} \quad , \quad \omega_2{}^2 = \frac{k}{m+\Delta m} \tag{A.2}$$

The effective mass, m, of the light pole was determined by solving equation (A.2) for stiffness and setting the two equations equal to each other such that

$$k = \omega_1{}^2 m \quad , \quad k = \omega_2{}^2 (m + \Delta m) \tag{A.3}$$

where

$$\omega_1{}^2 m = \omega_2{}^2 (m + \Delta m) \quad \text{or} \quad f_1{}^2 m = f_2{}^2 (m + \Delta m) \tag{A.4}$$

and solving for mass, *m*,

$$m = \Delta m \frac{f_2{}^2}{f_1{}^2 - f_2{}^2} \,. \tag{A.5}$$

The effective mass of the light pole was experimentally determined from the laboratory testing to be 0.2895 lbs-sec^2/in (111.87 lbs). The stiffness was determined from equation (A.3) to be 30.74 lbs/in.

The damping ratio was determined from the logarithmic decrement method such that

$$\zeta = \frac{1}{2\pi n} \ln \left(\frac{a_o}{a_n} \right) \tag{A.6}$$

where a_o is the initial response and a_n is the response after *n* oscillations. The damping ratio was experimentally estimated to be 0.12% (0.0012). A plot of the exponential decay of the free vibration response is illustrated in Figure A.5 as a red exponential curve, tracking the decay of the peak of oscillations, thus visually confirming the appropriateness of a 0.12% damping ratio.

The light pole can be simplified to a single-degree-of-freedom spring-mass-damper system, fully characterized by an effective mass (a.k.a. modal mass), frequency and damping ratio. The corresponding stiffness and damping coefficient can be determined as $k = (2\pi f_1)^2 m$ and $c = 2\zeta m(2\pi f_1)$. Table A.1 provides the measured and calculated effective mass (dynamic weight), stiffness and damping coefficient for the uncontrolled light pole (pole with no damper).

Table A.1: Dynamic Properties of the Light Pole.

Mass	0.2866 lbs-sec^2/in
Weight	*110.7 lbs*
Stiffness	30.74 lbs/in
Frequency	*1.64 Hz*
Damping Coefficient	0.0072 lbs-sec/in

The pole structure was excited at sinusoidal excitation frequencies around the fundamental natural frequency of the pole at high, medium and low amplitudes of force and corresponding tip acceleration, to observe the response and response mitigation of the vibration-mitigation device. The laboratory setup has acceleration measurements available along the length of the light pole. Assuming a sinusoidal displacement response, $x(t) = a \sin(2\pi \bar{f} t)$, where a is the peak displacement and $\bar{f}$ is the forcing frequency, the measured peak acceleration, assumed to be of the form $\ddot{x}(t) = -a\,(2\pi \bar{f})^2 \sin(2\pi \bar{f} t)$, and the forcing frequency are used to calculate the peak displacement as

$$a = \frac{\ddot{x}_{peak}}{(2\pi \bar{f})^2} \tag{A.7}$$

A linear shaker was used to provide an inertial excitation force at the tip of the light pole. The sinusoidal motion of the mass of the shaker was $x_s(t) = a_s \sin(2\pi \bar{f} t)$, where a_s is the displacement of the moving mass of the shaker relative to the pole structure, m_s is the moving

mass of the shaker, measured to be 0.0297 lbs-sec^2/in (11.46 lbs), and $\ddot{x}_s(t) = -a_s\,(2\pi\bar{f})^2 \sin\,(2\pi\bar{f}t)$. The peak shaker force from the sinusoidal shaker motion was determined as

$$F_s = m_s\ddot{x}_s = -m_s a_s\,(2\pi\bar{f})^2 \sin\,(2\pi\bar{f}t) \tag{A.8}$$

where $F_s^{peak} = m_s a_s\,(2\pi\bar{f})^2$.

The procedure used in this luminaire example for testing was to first test the controlled pole (pole with damper installed) at four levels of shaker displacement, a_s. The pole was excited for 120-240 seconds at numerous forcing frequencies around the natural frequency as identified in Table 8.1, for a duration to ensure that the response has reached steady state (the peak response was no longer growing/increasing). The acceleration at the tip of the pole was measured using an accelerometer at a sampling rate of 100 Hz. The acceleration was filtered and a maximum absolute value determined for use in equation (A.7) to determine an equivalent displacement. The peak response was observed at a forcing frequency of 1.64 Hz. Four amplitudes of peak shaker displacement amplitude are considered. As such, for each test the frequency and peak shaker amplitude can be varied as the inputs. Time history plots showing the pole tip acceleration and displacement are provided in Figures A.6 and A.7, respectively. The controlled structure (i.e. structure with vibration-mitigation device applied to it) force vibration testing is summarized in Table A.2.

Table A.2: Response of Controlled Structure, Forced Vibration Testing.

Frequency (Hz)	**Peak Acceleration (g)**	**Peak Displacement (in)**	***Peak Shaker Amplitude (in)***	**Peak Shaker Force (lbs)**
1.64	10.83	0.16	*0.02*	0.04
1.64	77.43	1.13	*0.05*	0.11
1.64	160.60	2.33	*0.10*	0.21
1.64	295.29	4.29	*0.20*	0.43

Next, the uncontrolled pole was excited at the corresponding levels of force from the controlled tests. The amplitude of the shaker displacement was determined by rearranging equation (A.8) such that

$$a_s = \frac{m_s\,(2\pi\bar{f})^2}{F_s} \tag{A.9}$$

A number of frequencies near the calculated natural frequency are experimentally tested to ensure the pole was excited at resonance and the duration of the excitation was monitored to ensure the response has reached steady state. The uncontrolled forced vibration testing is summarized in Table A.3. Four amplitudes of peak shaker force are considered, correspond to those first identified in Table A.2. As such, for each test the frequency and peak shaker force can be varied as the inputs. Note that the peak shaker forces in Table A.3 correspond to those first identified in Table A.2. The resulting peak shaker displacements/forces are shown subsequently to provide an adequate range to understand the amplitude dependence of the vibration-mitigation device being tested.

Table A.3: Response of Uncontrolled Structure, Forced Vibration Testing.

Frequency (Hz)	Peak Acceleration (g)	Peak Displacement (in)	Peak Shaker Amplitude (in)	*Peak Shaker Force (lbs)*
1.64	19.02	0.26	0.02	*0.04*
1.64	134.12	1.84	0.05	*0.11*
1.64	221.68	3.04	0.09	*0.21*
1.64	325.11	4.45	0.19	*0.43*

Measured time history plots of the acceleration of the pole tip are provided in Figure A.5. The response was observed to reach steady state within the time period plotted for both controlled and uncontrolled. The uncontrolled response is shown as the black line in each plot. The red and cyan color lines are both from the controlled response, the response of the pole tip with the damper installed. The cyan line shows the measured acceleration. The red line shows the post processed acceleration. High frequency peaks in the measured acceleration are observed (cyan lines) in all four levels of excitation. These acceleration spikes correspond to the impact mass hitting the wall of the canister. It was observed from the larger amplitude higher frequency unfiltered accelerations (cyan) that even at the smallest level of excitation, (a), there was some moderate impacting, while the impacting reaches its full level from 0.11 lbs force and up. The accelerations are filtered by a 20 Hz 8-pole Butterworth low pass filter to remove the high frequency energy of the impacting, as this does not contribute significantly to the overall displacement response of the light pole found from the testing results post-processing.

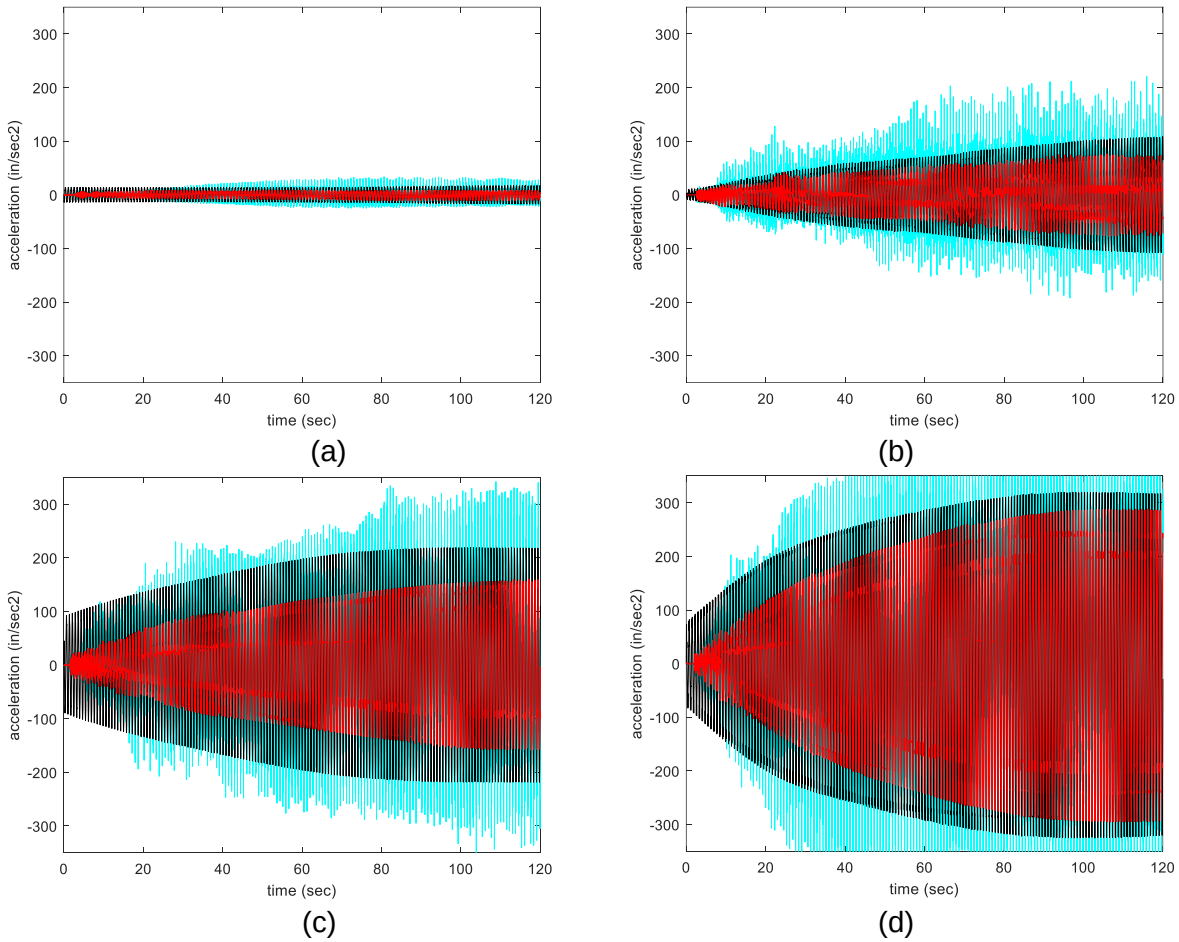

Figure A.6: Time history absolute acceleration response of light pole tip to: (a) 0.04 lbs; (b) 0.11 lbs; (c) 0.21 lbs; and (d) 0.43 lbs force at resonance. (black – uncontrolled; cyan – controlled; red – controlled with high frequency energy filtered)

Calculated time history plots of the displacement are provided in Figure A.6. One thing to note here is that the time required to reach steady state for the uncontrolled response is decreased as the excitation and displacement is increased. This was a result of an increase in the inherent damping of the pole with displacement. It was identified that in the laboratory setup of the pole, the base of the structure was providing unintended energy dissipation at large amplitudes of vibration. Further exploration of the amplitude dependence of the inherent damping from a series of free vibration tests to confirm the forced vibration test observations shows that the damping ratio at low amplitudes of vibration, 0.12%, increases to 0.45% at moderate excitations and to as much as 1% at large excitations. This behavior should be further examined for luminaires in the field but will be taken into account for the results of this example in the confidence factor for device characterization.

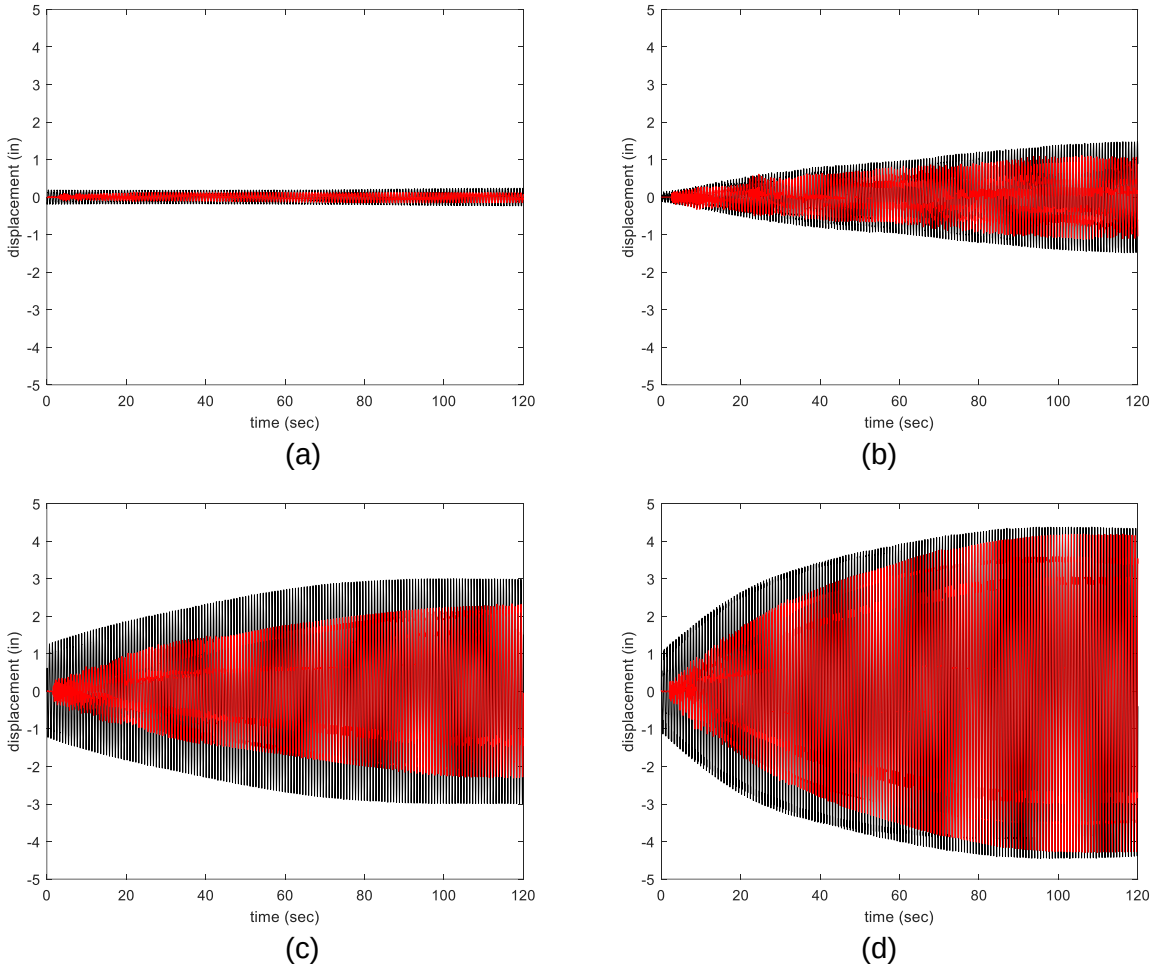

Figure A.7: Time history displacement response of light pole tip to: (a) 0.04 lbs; (b) 0.11 lbs; (c) 0.21 lbs; and (d) 0.43 lbs force at resonance. (black – uncontrolled; red – controlled with high frequency energy filtered)

The confidence in the device characterization can be considered reasonable as the device was tested in the laboratory on a single 20-foot light pole but intended to be applied to a 100-foot-high mast pole. Additional amplitude dependent damping in the pole was observed in the laboratory, which has not yet been confirmed for the field. In lieu of increasing the rigidity of the test fixture, the confidence factor is reduced. Device *characterization* confidence factor, C_c: 0.85. Again, Phase II of this project will examine more closely the appropriate ranges and determination of confidence factors and will provide further guidance on selecting the device characterization confidence factor.

Damper B

Device Sensitivities. The device is attached at mid-span for bridge-type sign structures, however, was mounted at 1/3 location on the light pole structure available for testing at UConn. The device was nonlinear and amplitude dependent. At large amplitudes, the wire steel rope changes in stiffness and damping. The characterization of this device was at a single amplitude, which proved detrimental to the efficacy of the resulting numerical model. The device is sensitive to amplitude of vibration.

(a) *(b)* *(c)*

Figure A.8: Experimental Damper B testing at UConn: (a) damper mounted onto a 6DOF shaker table to provide vertical excitation; (b) side-angle on 6DOF shaker table; and (c) damper installed at 2/3 length of pole.

Structural Archetypes. The Damper B is typically applied to Sign structures, specifically, Bridge-Type Sign Structures, as identified by manufacturer.

Wind Loading. Loading of the sign structure can include Natural Wind (NWG), Galloping (GVW), and Truck (TrG).

Laboratory Forced Vibration Testing. The damper was first tested independently on a shake table that could provide vertical excitation. Between the damper and the shake table, a PCB Piezotronics triaxial force sensor (model 261A02) is attached, to provide a measurement of damper force f_P in conjunction with an accelerometer (PBC, model 356A17) placed on the top of the shake table.

The input force of a sine excitation moving with a displacement amplitude of 0.25 inches at various natural frequencies was provided and the ratio of the peak measured output force to peak measured input acceleration was calculated, as shown in Figure A.9. This provides, at a fixed amplitude, a linear characterization of Damper B in the frequency domain.

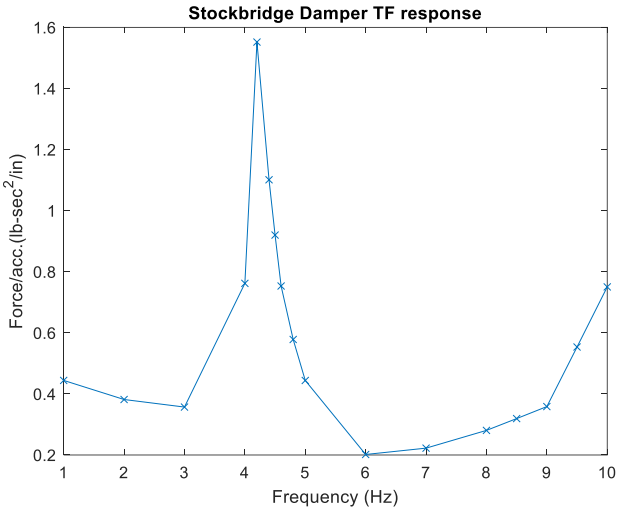

Figure A.9. Experimental response of the Damper B.

Damper C

The performance of a Damper C vibration-mitigation device to reduce the unwanted vibration is examined in this step over a range mast arm lengths intended to represent the potential structures it will be applied to. Testing was conducted at the University of Connecticut (UConn) to include both free and forced vibration testing of 4 distinct configurations of 50 foot long (50') mast arms, namely a: Higher Frequency 50' mast arm; Large Mass 50' mast arm; Smaller Mass 50' mast arm; and Low Frequency 50' mast arm.

Device Sensitivities. The Damper C must be mounted vertically and is typically attached near the end of the mast arm. The device is easily plumbed with the provided mounting hardware, however, misalignment should be considered, and tests have been conducted to verify the unit will work properly even if installed with some misalignment. The damper was purposefully misaligned by: (i) 10 degrees forward; (ii) 10 degrees Counterclockwise (CCW); and (iii) 10 degrees forward and 10 degrees Counterclockwise (CCW). Testing is conducted in the misaligned positions and performance was verified to be unaffected.

Structural Archetypes. The Damper C was applied to Traffic Signal Support Structures. A range of mast arm lengths from 15 ft to 75 ft were considered with natural frequencies from 0.69 Hz to 1.2 Hz (in-plane vibration mode) and dynamic weights from 141 lbs to 396 lbs, consistent with the archetypes identified in Table 3.5 and typical frequencies of 0.8 Hz to 1.4 Hz and dynamic weights of 300 lbs to 600 lbs. The shift in dynamic weight is necessary, due to limitations in the mast arms available for testing in the laboratory.

Wind Loading. The wind loading considered in the Specifications for Traffic Signal Support structures with in-plane (vertical) motion includes galloping and truck induced gusts.

Laboratory Free Vibration Testing. To characterize the behavior of Damper C, a series of free vibration tests were conducted on four (4) traffic signal support structure configurations set up in the Structures Research Laboratory at the University of Connecticut (UConn). An eccentric

mass shaker was used to provide a force to excite the first vertical mode of the mast arm structure at resonance. The excitation was stopped, and free vibration of the system observed. Each mast arm configuration was tested with and without the damper installed near the tip of the mast arm. The response of the mast arm was measured with a strain sensor attached to the underside of the mast arm 5" from the connection with the pole and with an accelerometer attached at the tip of the mast arm.

The four (4) traffic signal support structure configurations were realized by testing two different mast arms with and without added mass. Both mast arms were attached to the same shortened pole that was bolted to the strong floor. The steel pole had a height of 4.5 ft. with a 13.2" outside diameter (OD) at the base, a 12.5" OD at the tip, and a wall thickness of 0.2391". Mast Arm 1 (Large 50' Mast arm) was 50 ft. long with a 12.5" outside diameter (OD) at the base, a 5.5" OD at the tip, and a wall thickness of 0.2391". Mast Arm 2 (Slender 50' Mast arm) was 50 ft. long with a 10" outside diameter (OD) at the base, a 3" OD at the tip, and a wall thickness of 0.1793". Configuration "a" was without any added weight to the mast arm. In configuration "b", weights totaling 125 lbs were placed near the tip of each mast arm (at 48 ft) to provide for a different dynamic configuration and to assist in the system identification of the mast arm structures.

The forcing frequency was adjusted such that the resonance of the structure was matched with the excitation and the steady state response to this forced vibration was measured. The eccentric mass shaker was then turned off such that the mass no longer was rotating, and the free vibration response was measured. This was done for each configuration for the mast arm with and without Damper C installed. Acceleration and strain time history response was measured for each test. In this section, the four mast arm configurations were tested without any vibration-mitigation device to characterize the dynamic properties (natural frequency, dynamic weight, and damping ratio) of the traffic signal support structures. The time history acceleration and strain responses of the free vibration tests without any added damping device are shown in Figure A.10.

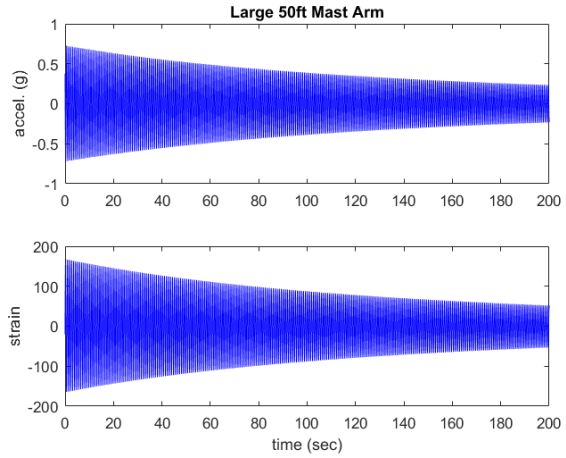

Mast Arm 1a

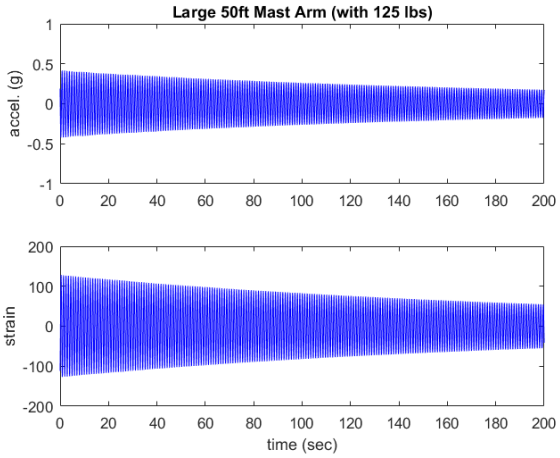

Mast Arm 1b

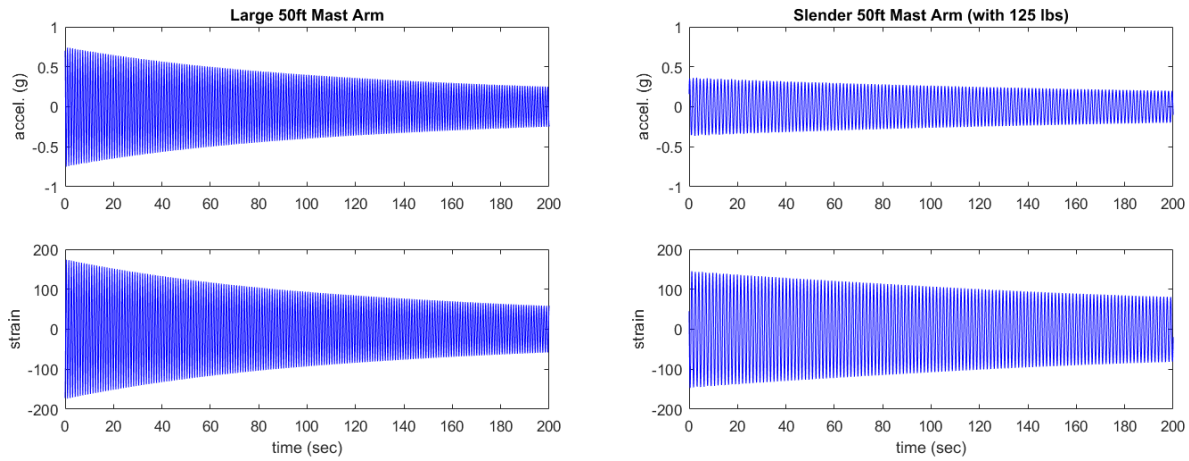

Mast Arm 2a Mast Arm 2b

Figure A.10: Free Vibration Testing of the traffic signal support structures.

From the free vibration plots, the natural frequency, f_{ij}, was determined as:

$$f_{ij} = \frac{n}{T_n} \tag{A.10}$$

where *n* was the number of oscillations and T_n is the time for the n oscillations for the i^{th} mast arm with j^{th} weight configuration.

The damping ratio was determined from the logarithmic decrement method such that:

$$\zeta_{ij} = \frac{1}{2\pi n} \ln\left(\frac{a_o}{a_n}\right) \tag{A.11}$$

where a_o was the initial response and a_n was the response after *n* oscillations for the i^{th} mast arm with j^{th} weight configuration.

The natural frequency and damping ratio for each mast arm configuration was determined from the time histories shown in Figure A.10 and calculated using equations (A.10) and (A.11), respectively. These experimentally determined natural frequencies and damping ratios are given in Table A.4.

Table A.4: Dynamic Properties of the Traffic Signal Support Structures tested at UConn.

	Mast Arm 1a	Mast Arm 1b	Mast Arm 2a	Mast Arm 2b
Frequency (Hz)	*1.20*	*0.99*	*0.95*	*0.69*
Damping Ratio (%)	0.09%	0.07%	0.08%	0.07%

The four traffic signal support structure configurations consist of two different mast arms with the additional weight (125 lbs) added to the tip of the mast arm, where Damper C will be installed. As such, for the Mast Arm 1b and 2b configurations a new frequency for an added mass ($\Delta m = 125/g$ lbs-sec^2/in) was measured. Each mast arm has a fixed stiffness, regardless of the amount

of weight added to the pole. This fact, along with the added mass, can be used to determine the effective dynamic mass of each pole (for the frequency being measured). The circular natural frequency ($\omega_i = 2\pi f_i$) is related to the mass and stiffness as:

$$\omega_1{}^2 = \frac{k}{m} \quad , \quad \omega_2{}^2 = \frac{k}{m+\Delta m} \tag{A.12}$$

The effective mass, *m*, of the traffic signal support structure was determined by solving (A.12) for stiffness and setting the two equations equal to each other such that:

$$k_i = \omega_{ia}{}^2 m_i \quad , \quad k_i = \omega_{ib}{}^2 (m_i + \Delta m) \tag{A.13}$$

where:

$$\omega_{ia}{}^2 m_i = \omega_{ib}{}^2 (m_i + \Delta m) \quad \text{or} \quad f_1{}^2 m_i = f_2{}^2 (m_i + \Delta m) \tag{A.14}$$

and solving for mass, m_i:

$$m_i = \Delta m \frac{f_{ib}{}^2}{f_{ia}{}^2 - f_{ib}{}^2} \, . \tag{A.15}$$

The effective mass for each traffic signal support was determined from the laboratory testing results using equation (A.15), as shown in Table A.5. The stiffness was determined from (A.13) and is also provided in Table A.5. For completeness, Table A.5 provides the experimentally measured effective mass (and corresponding dynamic weight, which is the product of mass and gravity; and is equivalent to the dynamic mass calculated from the numerical model in Eq. 3.8), stiffness and damping coefficient for the uncontrolled traffic signal support structures tested in the laboratory (with no damper installed) that can be used to model the traffic signal support structure as a single degree-of-freedom mass-spring system with damping.

Table A.5: Dynamic Properties of the Traffic Signal Support Structures tested at UConn.

	Mast Arm 1a	Mast Arm 1b	Mast Arm 2a	Mast Arm 2b
Mass (lbs-sec^2/in)	0.70	1.02	0.36	0.69
Dynamic Weight (lbs)	*271*	*396*	*141*	*266*
Stiffness (lbs/in)	39.87	39.65	13.00	12.94
Damping Coefficient (lbs-sec/in)	0.0095	0.0089	0.0035	0.0042

As part of Step 2, Characterizing Behavior, the Damper C device was installed near the mast arm tip of each of these traffic signal support structures and free vibration tests were conducted. The results are provided below.

Damper C Performance on Mast Arm 1a (Higher Frequency 50' Mast Arm). The first mast arm traffic signal support structure was determined to have a natural frequency of 1.20 Hz and a dynamic weight (product of modal mass and gravity) of 271 lbs. The frequency of 1.20 Hz represents a traffic signal structure in the higher frequency range. A photo of the mast arm and the free vibration measurements are shown in Figure A.11, with the Damper C performance compared to the uncontrolled (no damping device) response. The damping was determined using equation (A.11). The free vibration analysis shows an increase in damping from 0.09% to 2.7%.

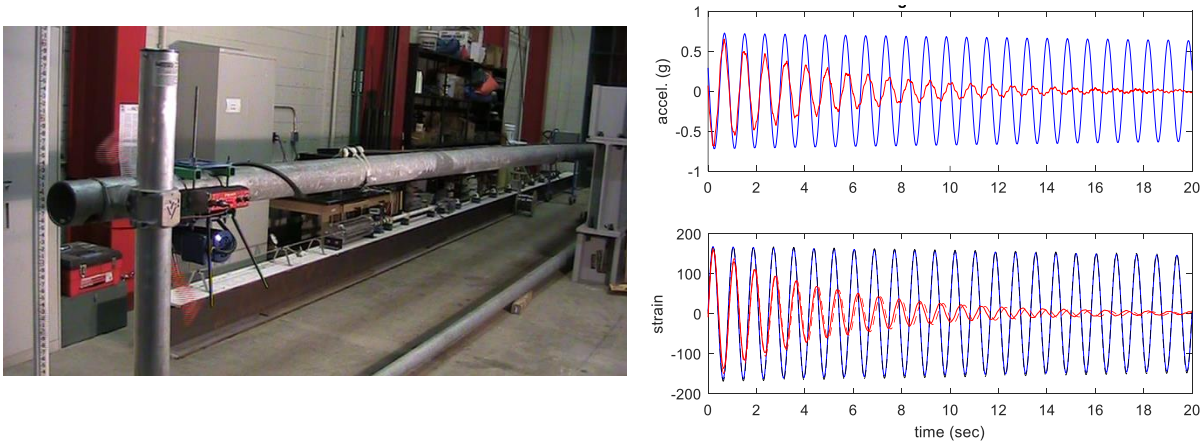

(a) (b)

Figure A.11: Mast Arm 1a (High Frequency 50' Traffic Signal Mast Arm): (a) Picture; and (b) Free Vibration Testing (uncontrolled – blue; Damper C – red).

Damper C Performance on Mast Arm 1b (Large Mass 50' Mast Arm). The second mast arm traffic signal support structure tested used the same pole and mast arm as the first test, with an additional 125 lbs rigidly mounted near the tip of the mast arm. This mast arm structure was determined to have a natural frequency of 0.99 Hz and a dynamic weight of 396 lbs. The dynamic weight of 396 lbs represents a traffic signal structure in the higher mass range. A photo of the mast arm and the free vibration measurements are shown in Figure A.12, with the Damper C performance compared to the uncontrolled (no damping device) response. The damping was again determined using equation (A.11). The free vibration analysis shows an increase in damping from 0.07% to 3.2%.

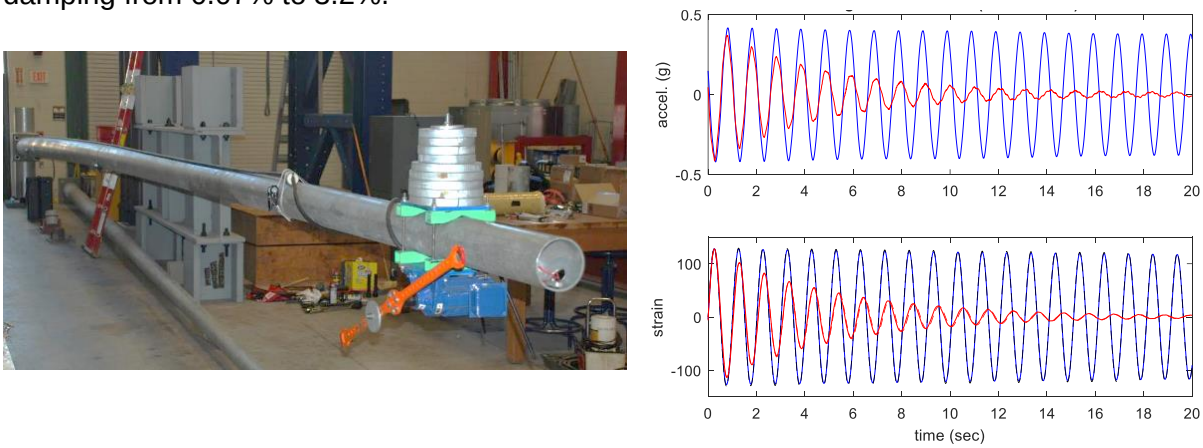

(a) (b)

Figure A.12: Mast Arm 1b (Large Mass 50' Traffic Signal Mast Arm): (a) Picture; and (b) Free Vibration Testing (uncontrolled – blue; Damper C – red).

Damper C Performance on Mast Arm 2a (Smaller Mass 50' Mast Arm). The third mast arm traffic signal support structure tested used the smaller diameter mast arm. This mast arm structure was determined to have a natural frequency of 0.95 Hz and a dynamic weight of 141 lbs. The dynamic weight of 141 lbs. represents a traffic signal structure in the smaller dynamic mass range. A photo of the mast arm and the free vibration measurements are shown in Figure A.13, with the Damper C performance compared to the uncontrolled (no damping

device) response. The damping was again determined using equation (A.11). The free vibration analysis shows an increase in damping from 0.08% to 9.5%.

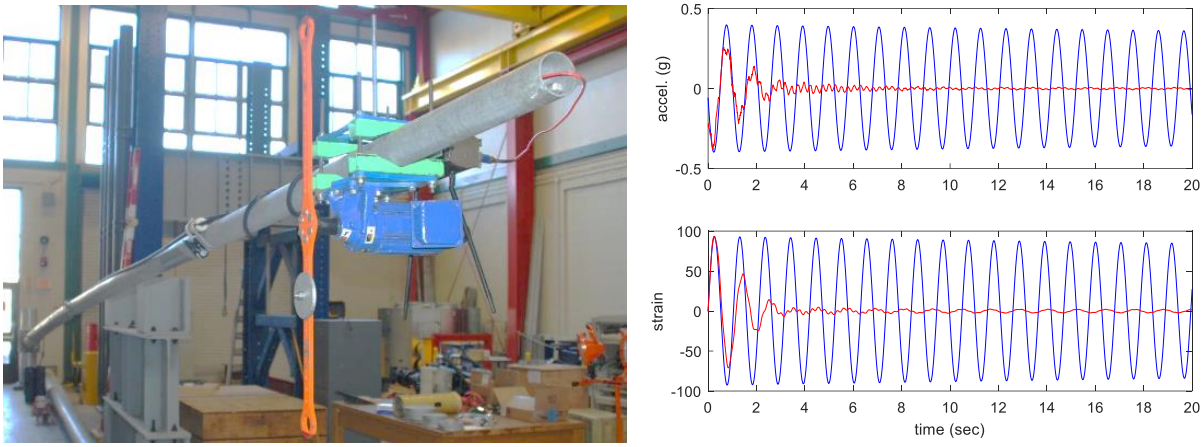

(a) (b)

Figure A.13: Mast Arm 2a (Smaller Mass 50' Traffic Signal Mast Arm): (a) Picture; and (b) Free Vibration Testing (uncontrolled – blue; Damper C – red).

Damper C Performance on Mast Arm 2b (Low Frequency 50' Mast Arm). The fourth mast arm traffic signal support structure used the same pole and mast arm as the third test, with an additional 125 lbs rigidly mounted near the tip of the mast arm. The mast arm system was determined to have a natural frequency of 0.69 Hz and a dynamic weight of 266 lbs. The frequency of 0.69 Hz represents a traffic signal structure in the lower frequency range. A photo of the mast arm and the free vibration measurements are shown in Figure A.14, with the Damper C performance compared to the uncontrolled (no damping device) response. The damping was again determined using equation (A.11). The free vibration analysis shows an increase in damping from 0.07% to 2.5%.

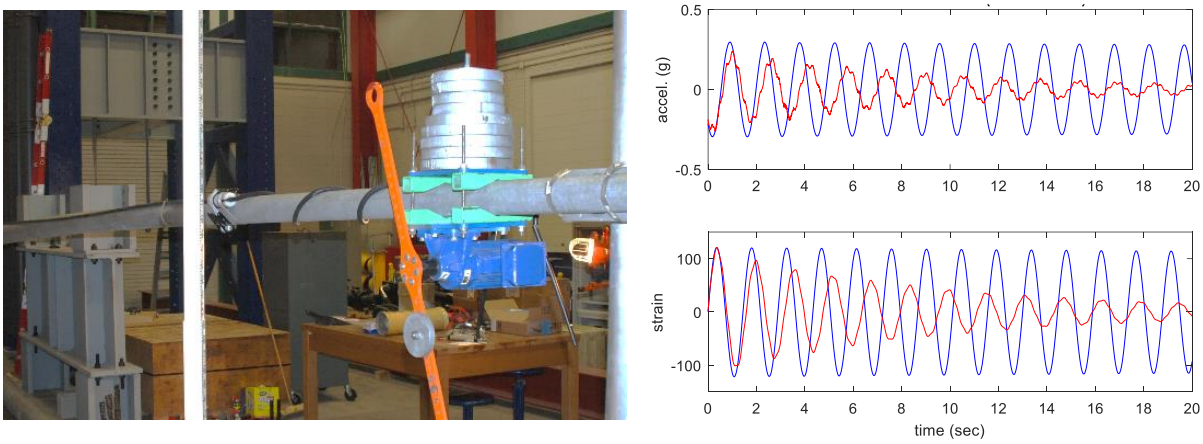

(a) (b)

Figure A.14: Mast Arm 2b (Low Frequency 50' Traffic Signal Mast Arm): (a) Picture; and (b) Free Vibration Testing (uncontrolled – blue; Damper C – red).

The results of these tests, rounded to the nearest tenth of a percent, are provided in Table A.6.

Table A.6: Measured Damping Ratio (%), Free Vibration Testing

	Mast Arm 1a	Mast Arm 1b	Mast Arm 2a	Mast Arm 2b
Uncontrolled	0.09%	0.07%	0.08%	0.07%
Damped	2.3%	3.2%	9.3%	3.2%

Step 3 – Develop and Validate Model:

Damper A

A numerical nonlinear model based on energy conservation was developed for Damper A applied to the light pole in the laboratory. An idealized impact damper applied to a simplified undamped single degree-of-freedom light pole, where the mass and stiffness of the light pole, *m* and *k*, have an impact damper mass, m_d, in a housing with gap *d*.

To develop a model of this system, assume a forced sinusoidal motion of the light pole, such that the displacement and velocity of the light pole are:

$$x(t) = asin\varpi t \tag{A.16}$$

$$\dot{x}(t) = a\varpi cos\varpi t \tag{A.17}$$

where $x(t)$ is the light pole displacement as a function of time *t*, *a* is the amplitude of displacement and ϖ is the forcing frequency in rad/sec ($\varpi = 2\pi\bar{f}$), where $\bar{f}$ is the forcing frequency in Hz).

The energy present in this system can be represented completely by strain energy at maximum displacement (zero velocity)

$$E_o = \frac{1}{2}ka_o^2 \tag{A.18}$$

where a_o is the amplitude of the displacement without impacting.

During an impacting event, the damper mass leaves the wall of the housing when the velocity is maximum (zero displacement, $x(t) = 0$) and begins to travel across the canister. The damper mass will impact the other side of the canister after some time t_i, where

$$\dot{x}_{max}t_i = asin\varpi t + d \tag{A.19}$$

From (A.17) $\dot{x}_{max} = a\varpi$ at $t = 0$ or $t = \frac{\pi}{\varpi}$.

$$a\varpi t_i = asin\varpi t_i + d \tag{A.20}$$

which can be written as

$$\varpi t_i = sin\varpi t_i + \frac{d}{a} \tag{A.21}$$

and

$$\frac{sin\varpi t_i + \frac{d}{a}}{\varpi t_i} = 1 \tag{A.22}$$

The time t_i is determined numerically as the solution to

$$sin\varpi t_i + \frac{d}{a} - \varpi t_i = 0 \tag{A.23}$$

but t_i is no larger than $\frac{\pi}{\varpi}$ as that is the end of a half period and it means that the impact mass has not reached the opposite wall during that half cycle.

Assuming that upon impact with the opposite canister wall the damper mass dissipates energy to become fixed to the far wall, until such a time that light pole passes back through zero displacement, and that the second impact on the return oscillation dissipates approximately the same energy as the first impact, the energy of the system after one oscillation including the impact is

$$E = \frac{1}{2}ka^2 + 2\left(\frac{1}{2}m_a a^2\varpi^2 - \frac{1}{2}m_a(a\varpi cos\varpi t_i)^2\right) \tag{A.24}$$

where m_a is the moving mass of the impact damper and equation (A.24) can be simplified to

$$E = \frac{1}{2}ka^2 + m_a a^2\varpi^2(1 - cos^2\varpi t_i) \tag{A.25}$$

The reduction in the light pole displacement amplitude over a single oscillation can be determined by setting the initial energy in the system (A.18) to the energy after two impacts (A.25), such that

$$\frac{1}{2}ka_o^2 = \frac{1}{2}ka^2 + m_a a^2\varpi^2(1 - cos^2\varpi t_i) \tag{A.26}$$

where the reduced amplitude is solved for as

$$a_o^2 = a^2\left(1 + 2\frac{m_a}{k}\varpi^2(1 - cos^2\varpi t_i)\right) \tag{A.27}$$

The ratio of the original displacement amplitude to amplitude after one cycle can then be determined, where the mass ratio is defined as the mass of the impact damper over the mass of the main structure, $\mu = m_a/m$ or $m_a = \mu m$, as

$$\frac{a^2}{a_o^2} = \frac{1}{1+2\mu\frac{\varpi^2}{\omega^2}(1-cos^2\varpi t_i)} \tag{A.28}$$

such that

$$\frac{a}{a_o} = \frac{1}{\sqrt{1+2\mu\left(\frac{\varpi}{\omega}\right)^2(1-cos^2\varpi t_i)}} \tag{A.29}$$

Assuming an equivalent system with viscous damping, the response is attenuated as

$$a = a_o e^{-\zeta \omega t} \tag{A.30}$$

where after one cycle of the forced vibration, $t = \frac{2\pi}{\varpi}$ such that

$$a = a_o e^{-2\pi\zeta\frac{\varpi}{\omega}} \tag{A.31}$$

For the equivalent system with viscous damping, the ratio of the original displacement amplitude to amplitude after one cycle can then be determined as

$$\frac{a}{a_o} = e^{-2\pi\zeta\frac{\varpi}{\omega}} \tag{A.32}$$

The equivalent viscous damping ratio is then found to be

$$\zeta = -\frac{1}{2\pi}\frac{\varpi}{\omega} ln\left(\frac{a}{a_o}\right) \tag{A.33}$$

where $\frac{a}{a_o}$ is determined in (8.23) and t_i found from the numerical solution of (A.23).

To understand the variation in damping due to the amplitude of vibration, consider a plot of damping versus the normalized amplitude of vibration $\frac{a}{d}$, normalized by the damper gap, as shown in Figure A.15. Assume the excitation is at the resonant frequency, $\varpi = \omega$, and a mass ratio of 0.05 (5%). It is observed that at amplitudes below $a = 0.32d$ the damper does not work (the impact mass does not make contact with the damper housing and thus no energy is dissipated). Further, at amplitude $a = 1.75d$ the impact damper has an optimal performance. It should be noted that at larger amplitudes of vibration the equivalent viscous damping (the energy dissipation) of an impact damper decreases.

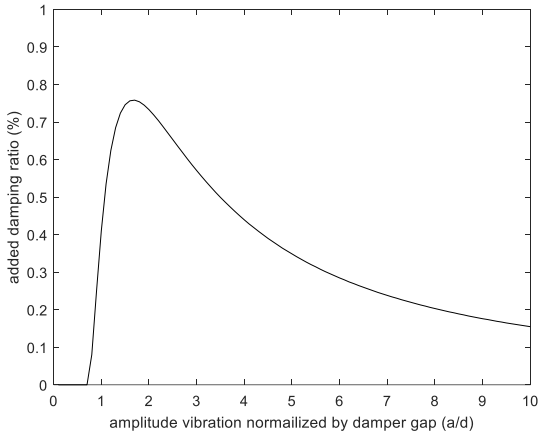

Figure A.15: Added damping as a function of amplitude of vibration for Damper A.

For first mode vibration-mitigation, the Damper A performs in a different manner than during the higher frequency (larger horizontal acceleration) second mode vibration-mitigation. It is observed that the inertial force of the impact rod for many of the first mode frequency and amplitude of vibration combination considered is not sufficient to overcome the friction at the bottom of the canister. As such the rod does not translate back and forth, but instead pivots about a fixed bottom end. This behavior reduces the energy dissipated. Consider the work done by the rod as it moves within the canister for sinusoidal motion at ϖ, such that $\ddot{x} = -\varpi^2 x$

$$W = Fx = \int_0^L (\rho\ddot{x})x dy = -\rho\varpi^2 \int_0^L x^2 dy \tag{A.34}$$

where the mass density, ρ, is defined as the mass per unit length $\rho = m/L$, or alternatively, $m = \rho L$. For the rod translating vertically within the canister *x* is not a function *y*, but is simply *d*. The work can then be evaluated as

$$W_T = -\rho\varpi^2 \int_0^L d^2 dy = -\rho\varpi^2 d^2 \int_0^L dy = -\rho\varpi^2 d^2 L = -m\varpi^2 d^2 \tag{A.35}$$

For the case of the impact rod rocking about the base, the displacement of the rod varies over the height of the rod as $x = \frac{d}{L}y$.

$$W_R = -\rho\varpi^2 \int_0^L \left(\frac{d}{L}y\right)^2 dy = -\rho\varpi^2 \frac{d^2}{L^2}\int_0^L y^2 dy = -\rho\varpi^2 \frac{d^2}{L^2}\frac{L^3}{3} = -\frac{1}{3}m\varpi^2 d^2 \tag{A.36}$$

Comparing (A.35) and (A.36) it is observed that the work done by the rocking damper is 1/3 of the translating damper. As such, an equivalent mass can be adopted for the rocking mode of operation that is equivalent to 1/3 the mass of the rod. As such the mass of the rod used for this mode of operation is 0.0049 lbs-sec^2/in (1.88 lbs). This corresponds to a mass ratio for the pole in the laboratory of 0.017 (1.7%).

Interpreting Experimental Results. The model is validated with the experimental tests to characterize behavior. As the Damper A model provides an equivalent viscous damping ratio added to the system, the equivalent added damping ratio from the experimental tests is determined to allow for a comparison of the model and experiment.

The amplitude of the response of a steady state response excited at the natural frequency is related to the damping ratio (Chopra, 2017) as

$$a_u = \frac{1}{2\zeta_u} \tag{A.37a}$$

$$a_c = \frac{1}{2\zeta_c} \tag{A.37b}$$

Using the displacements from Table A.3 and the measured damping of the uncontrolled system from Table A.1, equation (A.37) can be rearranged to solve for the controlled damping ratio as

$$\zeta_c = \zeta_u \frac{a_u}{a_c} \tag{A.38}$$

Of interest is the amount of increased damping due to the damping device, $\zeta_c - \zeta_u$, which can be determined as

$$\zeta_I = \zeta_u \left(\frac{a_u}{a_c} - 1 \right) \tag{A.39}$$

Using equation (A.39), the increased damping at the different amplitudes is then calculated and provided in Table A.7. The experimentally measured results are then compared to the predicted increased damping from the energy-based model of Damper A. The results are provided in Table A.7 and shown in Figure A.16.

Table A.7: Increased Damping Ratio due to Damper A.

Damper Displ. (in)	Added Damping Lab Test (%)	Added Damping Model (%)
0.16	0.079	0
1.13	0.284	0.265
2.33	0.135	0.163
4.29	0.037	0.084

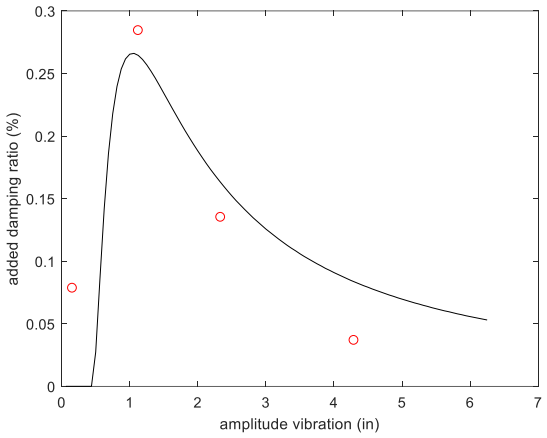

Figure A.16: Added damping as a function of amplitude of vibration for Damper A.

The Damper A model is an idealization of the behavior. From Figure A.6(a), the low amplitude vibrations are observed to have wall impacting, as seen by the high frequency larger amplitude accelerations in the measured accelerations. The model would predict that the impact rod did not hit either wall. The model does capture the optimal performance around 1 inch and the loss of performance for higher amplitudes. Including as average of the inherent damping of 0.08%, the error in the predicted increase in damping ratio of the model can be determined, as shown in Table A.8. While the general trend of increased damping is captured, the error in the model predicted damping has measured errors of as little as 5.2%, but two additional points with errors of 40-50%.

Table A.8: Error in Predicted Damping Ratio with Damper A Model.

Damper Displ. (in)	Added Damping Lab Test (%)	Added Damping Model (%)	Error in Model (%)
0.16	0.159	0.080	49.7%
1.13	0.364	0.345	5.2%
2.33	0.215	0.243	13.0%
4.29	0.117	0.164	40.2%

.

Damper B

A simplified numerical model of Damper B was used to estimate the performance of the vibration-mitigation device applied to sign structures. The transfer function of Figure A.5 is fit with numerator and denominator polynomials representing second order systems of a 4.3 Hz and a 10.5 Hz system with 5% damping. The results of the transfer function of the model amplitude comparison is presented in Figure A.17. This transfer function is a linear model of Damper B well understood to be nonlinear in nature. This is presented here as a simplified model and ultimately results in significant error in the prediction of the damper performance. The damper model results in errors from 25% to 150% in a series of 18 tested conducted. As an alternative, it is proposed that a damper such as this could be physically tested on a series of different sign structures and the test results used directly, using interpolation between data points where it is clear that the interpolation provides a reasonable estimate.

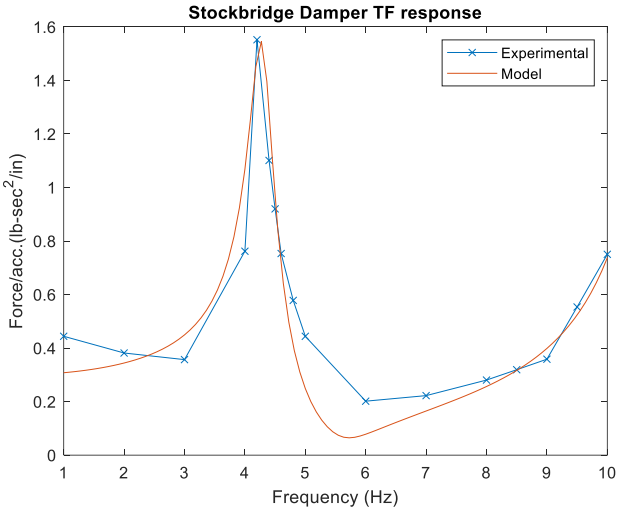

Figure A.17. Experimental response of Damper B and numerical model

Damper C

The Damper C was modeled as single-degree-of-freedom oscillator with mass, *m*, stiffness, *k*, and damping from both an eddy current effect, c_e, (which was assumed to be purely viscous damping) and a pneumatic effect, c_p, (which was assumed to be velocity squared), such that the equations of motion for the proposed dampers are:

$$m\ddot{x}_a + c_e\dot{x}_a + c_p\dot{x}_a^2 + kx_a = -m\ddot{x}_s \quad \text{(A.40)}$$

where x_a is the relative displacement of the damper mass (relative to the support structure), $[\cdot]$ represents a derivative with respect to time, and $\ddot{x}_s$ is the support acceleration.

Nonlinear time history analysis is conducted in MATLAB/Simulink for the damper model applied to a single degree-of-freedom traffic signal support structure model.

Interpreting Experimental Results. The analytical calculation of the dynamic properties of each of the traffic mast arm configurations was determined and was presented in Table A.9 compared to the experimentally determined values. For the four cases considered, the natural frequency was numerically calculated to have less than a 5% error from the measured natural frequency. The calculated dynamic weight was observed to have an error less than 20%.

Table A.9: Measured versus Calculated Dynamic Properties of Traffic Signal Supports

	Mast Arm 1a	Mast Arm 1b	Mast Arm 2a	Mast Arm 2b
Natural Frequency (Hz)				
Measured	*1.20*	*0.99*	*0.95*	*0.69*
Calculated (error)	*1.26 (5%)*	*1.02 (3%)*	*0.96 (1%)*	*0.71 (3%)*
Dynamic Weight (lbs)				
Measured	271	396	141	266
Calculated (error)	218 (19%)	332 (16%)	134 (5%)	249 (6%)

The predicted damping ratio from the numerical model was validated with the experimental tests to characterize behavior. The damping ratio for both the experiment and the model are provided in Table A.10. The predicted damping ratio error was less than 10%.

Table A.10: Damping Ratio with Damper C.

	Mast Arm 1a	Mast Arm 1b	Mast Arm 2a	Mast Arm 2b
Experiment	2.3%	3.2%	9.3%	3.2%
Model	2.4%	3.2%	9.0%	3.5%
Model Error	4.3%	0	3.2%	9.4%

The error in the model prediction of the damping ratio was less that 10%. Due to the small levels of damping, this error is reasonable. Note that a 0.3% error in the prediction of damping results in a 9.4% error.

Step 4 – Document Model:

Damper C

The device manufacturer has a sufficiently accurate damper model and corresponding Excel spreadsheet lookup table for the damping, given the natural frequency and dynamic weight of the design structure.

Step 5 – Determine Dynamic Properties of Design Structure:

The dynamic properties can be determined using a commercial finite element package. This is demonstrated in Section 3.4 of this report. As an example, the following describes how the dynamics of a cantilever structure (e.g., luminaire or in-plane behavior of a traffic signal support structure) can be modeled.

Given the physical characteristics of an existing structure, the fundamental natural frequency in Hz (cycles per second), given as f_n, can be estimated by determining the mass and stiffness of the traffic-signal support structure. The mass can be determined as:

$$m = \int_0^L \bar{m}(x)\Phi(x)\Phi(x)\,dx + \sum_{i=1}^{n} M_i\Phi(L_i) \tag{A.41}$$

where the mass per unit length was given as: $\bar{m}(x)=\rho A(x)$, where ρ is the mass density (mass per unit volume) and A is the cross-sectional area which is given as: $A(x)=\pi/4(D_o(x) - D_i(x))$, where D_o and D_i are the outer and inner diameters of the pole and mast arm, as functions of length, and where Mi is the mass of the nth discrete signal or sign located at length L_i from the base, and where $\Phi(L_i)$ is a shape function of the assumed deflected shape, where an effective shape function has been shown here to be:

$$\Phi(x) = [\sin\beta L - \sinh\beta L]\left[\sin\frac{\beta L}{L}x - \sinh\frac{\beta L}{L}x\right] - [\cos\beta L - \cosh\beta L]\left[\cos\frac{\beta L}{L}x - \cosh\frac{\beta L}{L}x\right] \tag{A.42}$$

where βL=1.8751 (Chopra, 2017). The stiffness can be determined as:

$$k = \int_0^L EI(x)\Phi''(x)\Phi''(x)\,dx \tag{A.43}$$

where the E is the modulus of elasticity, I is the moment of inertia calculated as:

$$I(x) = \pi/4 \left[\left(\frac{D_o(x)}{2} \right)^4 - \left(\frac{D_i(x)}{2} \right)^4 \right] \quad \text{(A.44)}$$

and Φ" is the second derivative of the shape function, Φ(L_i), with respect to length *x*.

The natural frequency is then determined as:

$$\omega_n = \sqrt{k/m}$$
$$f_n = \omega_n / 2\pi \quad \text{(A.45)}$$

Typically, the structure dynamic properties needed are the frequency and dynamic weight (note: dynamic weight is different, and less, than the total weight of the structure). These properties are developed for the in-plane and/or out-of-plane behavior depending on the fatigue wind load being mitigated against.

Step 6 – Determine Damping Ratio:

This is determined in the context of the following design example.

Structural Design Example: 50 ft. Mast Arm Traffic Signal Support Structure with Damper C

The structure to be considered in this example is a traffic signal support structure with a 50 ft mast arm. The pole of the structure is 20 ft tall, round in shape, made of S220 steel with a yield strength of 50 ksi, and a full-penetration base weld type. The base outside diameter is 17.00 in. and the top outside diameter is 14.20 in., with a wall thickness of 0.3125 in and a taper of 0.14 in/ft. The mast arm of the structure is 50 ft long, round in shape, made of S220 steel with a yield strength of 50 ksi. The base outside diameter of the mast arm is 14.00 in with a wall thickness of 0.3125 in and a taper of 0.14 in/ft. The mast arm is loaded with signals and signs with attributes as given in Tables A.11 and A.12. A schematic of the traffic signal support structure is shown in Figure A.18.

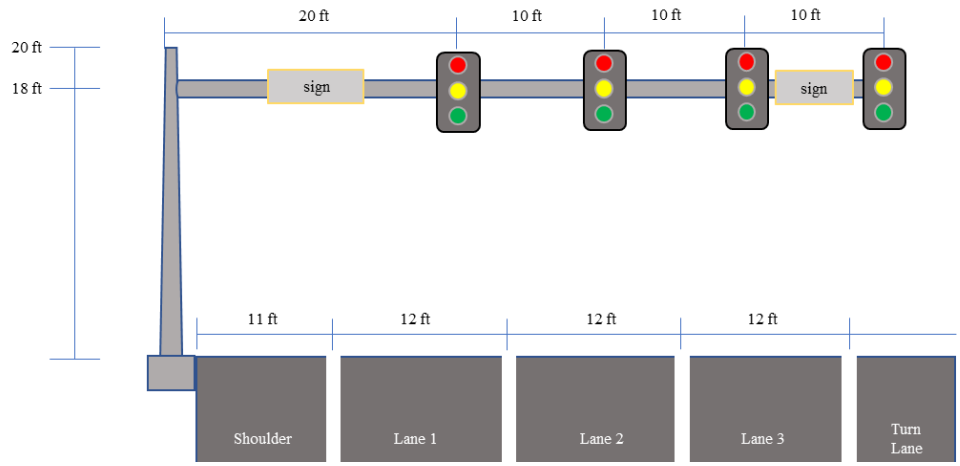

Figure A.18: Schematic of the traffic signal support structure in the example.

Table A.11: Description of Signal Loading.

Mounting height (ft)	Centroid height (ft)	Distance to center from pole (ft)	Signal weight (lbs)	Signal vertical plane (ft^2)	Projected area horizontal plane (ft^2)
18.00	18.00	50.00	105	13.72	2.56
18.00	18.00	40.00	65	8.62	1.18
18.00	18.00	30.00	65	8.62	1.18
18.00	18.00	20.00	65	8.62	1.18

Table A.12: Description of Sign Loading.

Mounting height (ft)	Centroid height (ft)	Distance to center from pole (ft)	Sign weight (lbs)	Sign width (ft)	Sign height (ft)	Sign depth (ft)	Sign drag coeff. C_d
18.00	18.00	47.00	25	2.50	3.00	0.00	1.19
18.00	18.00	10.00	100	8.00	1.50	0.00	1.23

The design philosophy incorporating the use of vibration-mitigation devices is based on the Load and Resistance Factor Design (LRFD) with appropriate load and resistance factors utilized. In such a manner, support structures shall be designed for fatigue to resist wind-induced stresses, as provided in a modified version of Equation 11.9.3-1:

$$\frac{1}{R}\gamma(\Delta f)_n \leq \varphi(\Delta F)_{TH} \qquad \text{(Equation 11.9.3-1)}$$

where γ is the load factor defined in Table 3.4-1 (AASHTO, 2015) and is equal to 1.0, $(\Delta f)_n$ is the wind-induced nominal stress range defined in Article 11.9.2 and determined subsequently, $(\Delta F)_{TH}$ is the CAFT fatigue resistance as specified Article 11.9.3 also determined subsequently, φ is the resistance factor and is equal to 1.0 for fatigue loading, and R is the response modification factor as being suggested in this project.

Load and Resistance Factors. The load and resistance factors, γ and φ, respectively, provided in AASHTO LTS were calibrated to provide a reliability index of approximately 3.0 for 300-year Mean Recurrence Interval (MRI), 3.0 to 3.5 for 700-year MRI, and 3.5-4.0 for 1700-year MRI for main members (Puckett, et al., 2014). The AASHTO LTS Design section uses the infinite life approach for fatigue design. The load and resistance factors, γ and φ, for fatigue are identified to be 1.0 in Table 3.4-1 of the AASHTO LRFD SLTS Specifications for fatigue loads, including truck gust (TrG), natural wind gust (NWG), vortex-induced vibration (VVW), combined wind on high-level towers, and galloping induced vibration (GVW). Load factor $\gamma = 1$. Resistance factor $\varphi = 1$.

The proposed modifications to the LRFD Specifications for Structural Supports for Highway Signs, Luminaires, and Traffic Signals incorporates a response modification factor, R, which accounts for the reduction in response due to the vibration-mitigation device. When there is no effective vibration-mitigation device used, R is equal to 1.0.

Wind-Induced Nominal Stress Range. The structure is assumed to be in Fatigue Category I. As the specifications indicate, structures without mitigation devices may be classified as Category I if any of the following apply: cantilevered sign structures with a span in excess of 50 ft or high-mast towers in excess of 100 ft; large sign structures, both cantilevered and non-cantilevered, including changeable message signs; and structures located in an area that is known to have wind conditions that are conducive to vibration. Prior to installing any mitigation device, if we assume this structure is located in an area known to have wind conditions that are conducive to vibration, the Importance Category I rating is justified. The fatigue importance factor is determined from Table 11.6-1 for a cantilevered traffic signal structure to have a fatigue importance factor, I_F, for galloping, natural wind gusts and truck-induced gusts of $I_F = 1.0$.

For traffic signal structures, section 11.7.1 is used to determine the equivalent static pressures to identify the loading due to galloping, natural wind gusts and truck-induced gusts. These loads are used to calculate nominal stress ranges near fatigue-sensitive connection details described in Article 11.5 Equation (17), and deflections for service limits described in Article 11.8. In general, the fatigue-sensitive connection details would include: the pole at the base (0 ft elevation); the hand hole opening; the mast arm tube at the base; the mast arm simplex bolts; and the anchor bolts. Assuming appropriately sized plates and details, this example will focus on the stress of the mast arm at the base (connection of the mast arm to the pole – on the mast arm). All fatigue-sensitive details should be checked in an actual full design.

11.7.1.1 – Galloping. The overhead traffic signal support structure is designed for galloping-induced cyclic loads by applying an equivalent vertical static shear pressure determined from (11.7.1.1-1) as:

$$P_G = 21 I_F = 21(1) = 21 \text{ psf} \tag{A.46}$$

where P_G is the equivalent vertical static shear pressure. The galloping loads are determined by applying the equivalent static shear pressure in equation (A.46) "vertically to the surface area, as viewed in normal elevation, to all sign panels and/or traffic signal heads and back plates rigidly mounted to the cantilevered horizontal support".

The moment and shear at the base of the mast arm are determined to be 40,620 lb-ft and 1,241 lbs, respectively. The corresponding normal (bending) stress is 10.84 ksi and shear stress is 0.18 ksi. The wind-induced nominal stress range from galloping is determined to be $(\Delta f)_n = 10.84$ ksi.

11.7.1.2 – Natural Wind Gust. While Damper C does not protect against the out-of-plane motion of natural wind gusts, this fatigue case is considered here for illustrative purposes. The overhead traffic signal support structure is designed for natural wind gust loads by applying an equivalent horizontal static gust pressure determined from (11.7.1.2-1) as

$$P_{NW} = 5.2 C_d I_F = 5.2(1)(1) = 5.2 \text{ psf} \tag{A.47}$$

where P_{NW} is the equivalent static natural wind gust pressure, and C_d, is the drag coefficient, determined from Table 3.8.7-1. When the effective projected area (EPA) of attachments is not provided, the drag coefficient is taken as 1.0. From the specification the "natural wind gust pressure range shall be applied in the horizontal direction to the exposed area of all support structure members, signs, traffic signals, and/or miscellaneous attachments."

The moment and shear at the base of the mast arm are determined to be 17,358 lb-ft and 580 lbs, respectively. The corresponding normal (bending) stress is 4.63 ksi and shear stress is 0.09 ksi. The wind-induced nominal stress range from natural wind gust is determined to be $(\Delta f)_n = 4.63$ ksi.

11.7.1.1 – Truck-Induced Gust. The overhead traffic signal support structure is designed for truck gust loads by applying an equivalent vertical static shear pressure determined from (11.7.1.3-1) as:

$$P_{TG} = 18.8 C_d I_F = 21 \text{ psf} \tag{A.48}$$

where P_{TG} is the equivalent vertical static shear pressure and the drag coefficient, C_d, remains 1.0. The truck-induced gust loads are determined by applying the equivalent static shear pressure

in the “vertical direction to the horizontal support as well as the area of all signs, attachments, walkways, and/or lighting fixtures projected on a horizontal plane”. The pressure range is applied along any 12-ft length located directly above a traffic lane to create the maximum stress range.

The moment and shear at the base of the mast arm are determined to be 7,254 lb-ft and 177 lbs, respectively. The corresponding normal (bending) stress is 1.94 ksi and shear stress is 0.03 ksi. The wind-induced nominal stress range from galloping is determined to be $(\Delta f)_n = 1.94$ ksi.

CAFT fatigue resistance. The fatigue design is conducted here using the nominal stress-based classifications of typical connection details as provided in Article 11.9.1 and Table 11.9.3.1-1. The traffic signal structure is to be designed such that the wind-induced stress is below the constant amplitude fatigue threshold (CAFT) providing infinite life. For this example, it is assumed that the mast-arm-to-flange-plate socket connection is a full penetration groove-welded tube-to-transverse plate connection (Table 11.9.3.1-1, 4.6). Table C11.9.3.1-2 provides the K_F equation for the full penetration groove-welded tube-to-transverse plate connections welded from both sides with back gouging (without backing ring), using section type (11.9.3.1-2), determined with the outermost bolt circle diameter of 28.64 in, a diameter of concentric opening in the transverse plate of 9.25”, and a mast arm flange thickness of 3.0 in. The value of K_F is calculated to be 1.9. The fatigue stress concentration factor, K_I, is calculated from (11.9.3.1-2) for a groove-welded tube-to-transverse plate connection to be 4.0. As a result, the CAFT fatigue resistance is determined to be $(\Delta F)_{TH} = 7.0$ ksi. Table A.13 shows the calculated stress range and fatigue resistance for galloping, natural wind gust, and truck-induces gust.

Table A.13: Uncontrolled Stress Range versus Fatigue Resistance.

	Stress Range (ksi)	Fatigue Resistance (ksi)
Galloping	10.84	7.0
Natural Wind Gust	4.63	7.0
Truck-Induced Gust	1.94	7.0

Is load less than resistance? Considering Equation 11.9.3-1, the inequality for galloping, natural wind gust, and truck-induced gust loads are determined as:

$$\begin{aligned} \tfrac{1}{1}(1)(10.84) \le 1(7.0)\ \text{ksi} \quad & 10.84 \not\le 7.0 \quad \text{Galloping} \\ \tfrac{1}{1}(1)(4.63) \le 1(7.0)\ \text{ksi} \quad & 4.63 \le 7.0 \quad \text{Natural Wind} \\ \tfrac{1}{1}(1)(1.94) \le 1(2.6)\ \text{ksi} \quad & 1.94 \le 7.0 \quad \text{Truck-Induced} \end{aligned} \qquad \text{(A.49)}$$

Using the traffic signal support structure initial design, the load for the galloping is not less than the resistance. This would prompt the designer to either redesign the support structure or select a vibration-mitigation device and identify the location of the device on the structure. Assume here

that the designer selected Damper C as a vibration-mitigation device. The location of the device is selected at the tip of the mast arm.

Calculate frequency, mass and deformation. The frequency and mass are determined in this example as described previously and a SDOF system is identified in a similar method as for the laboratory pole. The 18 lb non-moving portion of the Damper C is included in the calculation. The frequency of the first mode is determined to be 0.92 Hz. The effective mass is 1.48 lbs-sec^2/in (571 lbs). The damping ratio for this structure is predicted from the numerical model developed and validated to be 2.84%.

The designer must consider 9 different structural combinations of frequency +-10% and dynamic weight +-20%. The results are provided in Table A.14.

Table A.14: Damping over Range of Frequency and Dynamic Weight.

	456 lbs	571 lbs	685 lbs
0.83 Hz	4.18%	3.36%	2.89%
0.92 Hz	3.54%	2.84%	2.44%
1.01 Hz	2.46%	2.01%	1.75%

The controlled damping ratio is the minimum value over this range, or 1.75%. Considering the default (and conservative) undamped damping ratio of 0.2%. The R-factor, from equation 2.10, written here for convenience, is

$$R = \begin{cases} 0.6\frac{\zeta_c}{\zeta_u} = 0.6\frac{1.75}{0.20} = 5.25 & for\ R > 3 \\ 1 & otherwise \end{cases} \qquad (2.10)$$

For this particular structure and vibration-mitigation device, R = 5.25.

Check if now satisfied. The R-factor for the Damper C is used to effectively modify the wind load for the 50 ft traffic structure examined here. With the R = 11.62, the inequality in equation (A.49) is reevaluated and found to be satisfied for galloping and an infinite fatigue life is satisfied.

$$\frac{1}{5.25}(1)(10.84) \leq 1(7.0)\ \text{ksi} \qquad 2.06 \leq 7.0 \qquad \text{Galloping} \qquad (10.50)$$

The other wind conditions for fatigue were previously satisfied. The design is complete and the proposed traffic signal support structure with Damper C meets the Specifications.